Convergent finite element approximations for problems of near-incompressible and near-inextensible transversely isotropic linear elasticity

presented by

Faraniaina Rasolofoson

Department of Mathematics and Applied Mathematics,

Centre for Research in Computational and Applied Mechanics

Supervisor: Prof. B.D. Reddy

Department of Mathematics and Applied Mathematics,

Centre for Research in Computational and Applied Mechanics

Thesis is submitted in fulfillment of the requirements

for the award of the degree of Doctor of Philosophy

February 2019

Abstract

This work comprises a detailed theoretical and computational study of the boundary value problem for transversely isotropic linear elastic bodies. The main objective is the development and implementation of low-order finite element methods that are uniformly convergent in the incompressible and inextensible limits. The first step in the investigation is a study of the constitutive relation for transversely isotropic elasticity, and establishment of conditions on the five material parameters under which the relation is pointwise stable. This forms the basis for a study of well-posedness of the weak displacement-based formulation.

Conforming finite element approximations are studied. The error estimate indicates the possibility of extensional locking; on the other hand, anisotropy, measured as the ratio of Young's moduli in the fibre and transverse directions, plays a role in minimizing or even eliminating volumetric locking behaviour. Extensional locking is circumvented with the use of selective under-integration, in the context of low-order quadrilateral elements. Its equivalence with mixed and perturbed Lagrangian methods are shown. A series of numerical results illustrates the various features of the formulations considered.

In a second approach, interior penalty or discontinuous Galerkin (DG) formulations of the problem are considered. Low-order approximations on triangles are adopted, with the use of three interior penalty discontinuous Galerkin methods, viz. nonsymmetric, symmetric and incomplete. It is known that these methods are uniformly convergent in the incompressible limit for the case of isotropy. This property carries over to the transversely isotropic case for moderate anisotropy. An error estimate suggests the possibility of extensional locking, and under-integration of the extensional edge terms is proposed as a remedy. This modification is shown to lead to an error estimate that is consistent with locking-free behaviour. Numerical tests confirm the uniformly convergent behaviour, at an optimal rate, of the under-integrated scheme.

Acknowledgements

First and foremost, I would like to express my sincere gratitude to my supervisor, Prof. Daya Reddy, for his unlimited help, support and guidance throughout this research. He has never stopped to believe in me and has encouraged me especially during my lowest moments. He has provided me with helpful remarks, has cultivated my interest in this field. He has taught me to be independent and responsible. Without his guidance, this work would not have been possible.

I am highly in debt to Dr. Beverley Grieshaber for being a wonderful mentor. She has never complained about all my unfinished questions. She has been a great help especially in the computing aspect of the research. Her comments and works had a profound influence on my research.

I greatly appreciate the financial support to this project from the National Research Foundation through the South African Research Chair in Computational Mechanics.

Particular thanks goes to all my friends at CERECAM, especially to Ms Natalie Bent for her encouragement and assistance with any paper work and material problems.

Special thanks goes to Dr. Mika Rafieferantsoa for all his love, time and support, especially for helping me with python coding. I thank my dear friends Dr. Andry Rasoanaivo and Manankasina Ramanantoanina, who have been closely alongside me throughout this journey. I really thank you guys for being there when I needed you the most.

Finally, my deepest thanks to my parents and family. “Misaotra indrindra Dada sy Neny tamin’ny fanohanana sy fampirisihana tamin’ny lafiny rehetra ka nahatrarako izao tanjona izao.”

Table of Contents

Chapter 1

Introduction

A vast range of natural phenomena and technological innovations can be modelled successfully through systems of differential equations. These may be ordinary or partial differential equations (PDEs), and either linear or nonlinear. While techniques exist for finding closed-form solutions of PDEs in some cases, this is not generally possible. For this reason the development of approximate solution methods and their computational solution are of great importance in the context of modelling.

The three most widely used methods for the numerical solution of systems of PDEs are the finite element method, the finite difference method, and the finite volume method. For each of these approaches there are varieties of special approaches: for example, for the finite element method, in addition to standard approaches, mixed formulations are popular [9]. Likewise, p- and hp- finite element methods differ from standard approaches in seeking convergent approximations by progressively increasing the polynomial order p, or combining the latter with mesh refinement (see for example [5, 7]). More recently, popular variants of the finite element method include isogeometric formulations [12] and the virtual element method [14].

Many significant developments of the finite element method have taken place in the context of solid mechanics, with the earliest formulations being developed for problems of linear elasticity. The focus has traditionally been on problems of isotropic elasticity. Anisotropic materials, however, arise in a variety of natural and engineering situations, and are worthy of attention. For example, anisotropy is a feature of composite materials, used in the aerospace, automotive, and other industries. It also occurs naturally in crystalline structures, geotechnical materials, and in the mechanical properties of biological media such as muscles, tendons, or bones (see for example [1, 17, 27, 32, 35, 39]). Transverse isotropy is a form of anisotropy characterized by isotropic behaviour in a plane defined by a given normal vector or fibre direction. Fibrous or fibre-reinforced structures are generally modelled as transversely isotropic materials. Important early contributions to the mechanics of fibre-reinforced materials include the works [22, 33, 40]. The monograph [42] gives a detailed presentation of the mechanics of anisotropic materials. This thesis will focus on finite element formulations for boundary value problems of linear transversely isotropic elasticity.

There have been various contributions aimed at deriving general forms for the constitutive equations of transversely isotropic elasticity. Some examples include the work [30], which uses the representation theorems in [41] to obtain the elasticity tensor and its inverse, the compliance tensor. In [17], the compliance matrix is given in terms of engineering constants such as Young's moduli, Poisson's ratios, and shear moduli relative to the fibre direction and plane of isotropy. Conditions for positive-definiteness of the compliance matrix, and hence for pointwise stability, are derived. Corresponding results for various types of anisotropic materials, that is, monoclinic, orthotropic, and transversely isotropic, are presented in [28].

In the context of hyperelasticity there has been extensive work aimed at deriving general conditions for constructing strain energy functions for transversely isotropic material models. The work [36] develops a form for the strain energy function in terms of the invariants, such that the strain energy function is polyconvex, a key criterion for well-posedness of the boundary value problem. The work of [37] presents mathematical foundations of the derivation of the constitutive relations for transversely isotropic bodies at large strain: materially stable transversely isotropic energies for soft tissues that satisfy the Legendre-Hadamard condition are constructed. The development of stable finite element approximations for transversely isotropic hyperelastic has also received attention, an important early work being [44].

Early work on well-posedness for anisotropic materials has generally taken the form of studies of pointwise stability and uniqueness of the boundary value problem for linear elasticity. These features are explored in [23, 24] for materials with the constraint of inextensibility.

There has been little work on the well-posedness of boundary value problems for materials with internal constraints such as inextensibility, in contrast to the many treatments of incompressibility. The investigation [3] approaches the problem via a mixed formulation of Hellinger-Reissner type, and establishes conditions on the elastic constants for the problem to be well-posed for inextensible materials, and also for the case of orthotropy. Corresponding abstract results have been presented in [15] for the case of non-homogeneous materials.

In the context of elasticity problems, low-order finite element numerical approximations often lead to locking for small values of a parameter. Locking refers to a parameter-dependent inability of the finite element approximation to converge to the exact solution. Some examples are volumetric locking in the incompressible limit, extensional locking for near-inextensibility, and shear locking when the relevant parameter is the thickness [26]. The work [6] analyses the strength of locking and robustness of various h-version schemes. It is known that p- and hp-versions are free from locking when the polynomial degree $p \geq 4$ on triangular meshes (see also [38, 43]).

The use of higher-order approximations generally avoids locking. Alternative approaches that circumvent locking behaviour include the use of nonconforming methods [18]. A range of mixed methods have been shown to be uniformly convergent for near-incompressibility (see for example [9] and the references therein), while the works [16, 29] provide a unified treatment of uniformly convergent formulations using two- or three-field approximations, and low-order (quadrilateral) approximations.

Discontinuous Galerkin (DG) finite element methods provide a further powerful example of a class of approaches to overcome locking behaviour. Important contributions include the works [20, 25]. With the use of low-order triangles, the DG method for isotropic elasticity is uniformly convergent in the incompressible limit [20, 45]. For conventional conforming bi- or trilinear approximations on quadrilaterals and hexahedra, however, it is known [19] that locking occurs; this may be circumvented with the use of under-integration of the edge terms in the formulation.

Near-inextensibility is studied computationally in the work [4], using Lagrange multiplier, perturbed Lagrangian, and penalty approaches. There have also been a number of computational investigations of transversely isotropic and inextensible behaviour for large-displacement problems [46, 47, 48, 49].

There have not however been systematic analyses and corresponding computational studies of locking-free behaviour for near-inextensible materials. This topic constitutes the main aim of this thesis: namely, to investigate stable, locking-free approximations for problems of transversely isotropic linear elasticity. The emphasis will be on low-order elements, and on conditions for uniformly convergent behaviour in the incompressible and inextensible limits.

Related work has recently been reported in [34], on a virtual element formulation for transverse isotropy: this formulation is shown computationally to be robust and locking-free in the inextensible limit, for both constant and variable fibre directions.

After presenting the background material, the constitutive relations for transversely isotropic elastic materials are formulated and investigated. In particular, conditions for pointwise stability are derived; these play an important role in determining conditions for well-posedness of the displacement-based weak formulation.

With regard to finite element formulations, two avenues are explored. The first concerns low-order conforming finite element approximations. The discrete form of the displacement problem is formulated. The error estimate reveals that anisotropy can play a role in minimizing or even eliminating locking behaviour, for moderate values of the ratio of Young's moduli in the fibre and transverse directions. In addition to the standard conforming approximation, an alternative formulation, involving under-integration of the volumetric and extensional terms in the weak formulation, is considered. The latter is equivalent to either a mixed or a perturbed Lagrangian formulation, analogously to the well-known situation for the volumetric term. A set of numerical examples confirms the locking-free behaviour in the near-incompressible limit of the standard formulation with moderate anisotropy, with locking behaviour being clearly evident in the case of near-inextensibility. On the other hand, under-integration of the extensional term leads to extensional locking-free behaviour.

The second approach concerns low-order DG approximations. Low-order approximations on triangles are adopted, with the use of three interior penalty DG methods, viz. nonsymmetric, symmetric and incomplete. It is known that these methods are uniformly convergent in the incompressible limit. This work focuses on the behaviour in the inextensible limit. An error estimate suggests the possibility of extensional locking, a feature that is confirmed by numerical experiments. Under-integration of the extensional edge terms is proposed as a remedy. This modification is shown to lead to an error estimate that is consistent with the locking-free behaviour. Numerical tests confirm the uniformly convergent behaviour, at an optimal rate, of the under-integrated scheme.

The rest of the thesis is organised as follows. In Chapter 2, the constitutive equations for linear transversely isotropic materials are presented. These are expressed in terms of a set of five primary material parameters, and alternatively in terms of a corresponding set of physically meaningful constants. Conditions for pointwise stability and strong ellipticity are presented. The weak form of the boundary value problem is formulated in Chapter 3, and conditions for the existence of unique solutions established. Conforming finite element approximations are analysed, and the potential for locking behaviour noted. Under-integration is introduced as a remedy and its equivalence to perturbed Lagrangian and mixed formulations established. Numerical results that illustrate the conforming and under-integrated formulations are presented in Chapter 4; these verify the extensional locking of the standard formulation and the locking-free behaviour of the under-integrated formulation. Volumetric locking is shown to be absent for anisotropic materials, with the usual locking behaviour observed in the isotropic limit. In Chapter 5, corresponding discontinuous Galerkin formulations for the three interior penality methods are presented, and conditions for well-posedness established. The a priori error estimate suggests the existence of extensional locking at the inextensible limit. Under-integration of the extensional edge term is introduced as a remedy, and the new error estimate suggests a convergent behaviour. A set of numerical examples to illustrate the theory on discontinuous Galerkin formulations are presented in Chapter 6. Chapter 7 concludes the work.

Two publications are based on the work presented in this thesis. The article

- F. Rasolofoson, B.J. Grieshaber, B.D. Reddy, Finite element approximations for near-incompressible and near-inextensible transversely isotropic bodies. International Journal for Numerical Methods in Engineering, 117(6):693-712, 2018.

is based largely on the material in Chapters 2, 3 and 4, while the manuscript

- B.J. Grieshaber, F. Rasolofoson, B.D. Reddy, Discontinuous Galerkin approximations for near-incompressible and near-inextensible transversely isotropic bodies. In review, available at arXiv:1810.13267.

is based on the material in Chapters 5 and 6.

1.1 General notation

Notation for scalars, vectors and tensors

We make use of a combination of direct (coordinate-free) and indicial notation for vectorial and tensorial quantities.

Throughout this work, we denote:

Scalars (including, for example, material parameters) with lightface Roman or Greek letters $(a, b, \ldots, A, B, \ldots, \alpha, \beta, \ldots)$

Vectors with boldface letters $(\boldsymbol{a}, \boldsymbol{b}, \boldsymbol{c}, \ldots)$

Second-order tensors with boldface uppercase Roman or lowercase Greek letters $(\boldsymbol{A}, \boldsymbol{B}, \ldots, \boldsymbol{\sigma}, \boldsymbol{\varepsilon}, \ldots)$

Fourth-order tensors with blackboard bold typeface: $\mathbb{A}, \mathbb{B}, \mathbb{C}, \ldots$

Function spaces with calligraphic typeface: $\mathcal{A}, \mathcal{B}, \mathcal{C}, \ldots$

Subscripts t and l indicate that the parameter is defined in the transverse and longitudinal or fibre direction respectively.

We also make use of a number of well-established symbols and conventions, for any second order tensor $\boldsymbol{A}$, such as the transpose $\boldsymbol{A}^T$, the inverse $\boldsymbol{A}^{-1}$, the trace $\operatorname{tr}\boldsymbol{A}$, and the determinant $\det \boldsymbol{A}$.

Index notation

We make use of a cartesian coordinate system with associated orthonormal basis $\mathbf{e}_i$ $(i = 1, 2, 3)$ and coordinates x_i $(i = 1, 2, 3)$ of a point $\boldsymbol{x}$.

The Kronecker delta is defined as follows:

$$\delta_{ij} = \begin{cases} 1 & \text{if } i = j, \\ 0 & \text{otherwise.} \end{cases}$$

We adopt the Einstein summation on repeated indices: that is, we write $a_i b_i$ for $\sum_i a_i b_i$.

For any vectors $\boldsymbol{a}$ and $\boldsymbol{b}$, and any second order tensors $\boldsymbol{A}$ and $\boldsymbol{B}$, the scalar products are given by

$$\boldsymbol{a} \cdot \boldsymbol{b} = a_i b_i,$$
$$\boldsymbol{A} : \boldsymbol{B} = A_{ij} B_{ij},$$

and the tensor products by

$$\boldsymbol{a} \otimes \boldsymbol{b} = a_i b_j \boldsymbol{e}_i \otimes \boldsymbol{e}_j,$$
$$\boldsymbol{A} \otimes \boldsymbol{B} = A_{ij} B_{kl} \boldsymbol{e}_i \otimes \boldsymbol{e}_j \otimes \boldsymbol{e}_k \otimes \boldsymbol{e}_l.$$

For any fourth order tensor $\mathbb{A}$ and any second order tensor $\boldsymbol{T}$, we have

$$\mathbb{A}\boldsymbol{T} = \mathbb{A}_{ijkl} T_{kl} \boldsymbol{e}_i \otimes \boldsymbol{e}_j.$$

The gradient of a scalar function $u(x_1, \ldots, x_d)$ is defined by

$$\nabla u = \frac{\partial u}{\partial x_i} \boldsymbol{e}_i,$$

the gradient of a vector $\boldsymbol{u}$ by

$$\nabla \boldsymbol{u} = \frac{\partial u_i}{\partial x_j} \boldsymbol{e}_i \otimes \boldsymbol{e}_j,$$

and the divergence of a vector $\boldsymbol{u}$ by

$$\operatorname{div} \boldsymbol{u} = \nabla \cdot \boldsymbol{u} = \frac{\partial u_i}{\partial x_i}.$$

Function spaces

Let Ω be an open subset of $\mathbb{R}^d$, with $d \in \{1, 2, 3\}$ the space dimension, with smooth boundary $\partial\Omega$.

We denote by $\mathcal{L}^2(\Omega)$ the set of all real-valued functions defined on Ω such that

$$\int_\Omega |u(x)|^2 \, dx < \infty.$$

This is a Hilbert space when equipped with the inner product

$$(u, v)_{\mathcal{L}^2(\Omega)} := \int_\Omega u(x) v(x) \, dx, \tag{1.1}$$

and corresponding norm

$$\begin{aligned} ||u||_{\mathcal{L}^2(\Omega)} &:= (u, u)_{\mathcal{L}^2(\Omega)} \\ &= \left(\int_\Omega |u(x)|^2 \, dx \right)^{1/2}. \end{aligned} \tag{1.2}$$

We define the Sobolev space

$$\mathcal{H}^1(\Omega) := \left\{ u \in \mathcal{L}^2(\Omega) : \frac{\partial u}{\partial x_j} \in \mathcal{L}^2(\Omega),\ j = 1, \dots, d \right\}, \tag{1.3}$$

which is a Hilbert space when equipped with the inner product

$$(u, v)_{\mathcal{H}^1(\Omega)} := (u, v)_{\mathcal{L}^2(\Omega)} + \int_\Omega \sum_{i=1}^{d} \frac{\partial u}{\partial x_i} \frac{\partial v}{\partial x_i}\, dx, \tag{1.4}$$

and the corresponding norm

$$\begin{aligned} ||u||_{\mathcal{H}^1(\Omega)} &:= (u, u)_{\mathcal{H}^1(\Omega)} \\ &= \left(||u||^2_{\mathcal{L}^2(\Omega)} + ||\nabla u||^2_{\mathcal{L}^2(\Omega)} \right)^{1/2}. \end{aligned} \tag{1.5}$$

Here and henceforth norms of vector- and tensor-valued quantities are evaluated componentwise: that is,

$$||\nabla u||^2_{\mathcal{L}^2(\Omega)} = \sum_{i=1}^{d} \int_\Omega \left| \frac{\partial u}{\partial x_i} \right|^2 dx.$$

We also define the $\mathcal{H}^1$-seminorm by

$$|u|_{\mathcal{H}^1(\Omega)} := ||\nabla u||_{\mathcal{L}^2(\Omega)}. \tag{1.6}$$

We define the Sobolev space

$$\mathcal{H}^2(\Omega) := \left\{ u \in \mathcal{L}^2(\Omega) : \frac{\partial u}{\partial x_j} \in \mathcal{L}^2(\Omega), \frac{\partial^2 u}{\partial x_i \partial x_j} \in \mathcal{L}^2(\Omega),\ i, j = 1, \cdots, d \right\}, \tag{1.7}$$

equipped with the inner product

$$(u, v)_{\mathcal{H}^2(\Omega)} := (u, v)_{\mathcal{L}^2(\Omega)} + (u, v)_{\mathcal{H}^1(\Omega)} + \int_\Omega \sum_{i,j=1}^{d} \frac{\partial^2 u}{\partial x_i \partial x_j} \frac{\partial^2 v}{\partial x_i \partial x_j}\, dx, \tag{1.8}$$

and the corresponding norm

$$\begin{aligned} \|u\|_{\mathcal{H}^2(\Omega)} &:= (u, v)_{\mathcal{H}^2(\Omega)} \\ &= \left(||u||^2_{\mathcal{H}^1(\Omega)} + \sum_{i,j=1}^{d} || \frac{\partial^2 u}{\partial x_i \partial x_j} ||^2_{\mathcal{L}^2(\Omega)} \right)^{1/2}, \end{aligned} \tag{1.9}$$

and seminorm

$$|u|_{\mathcal{H}^2(\Omega)} := \left(\sum_{i,j=1}^{d} || \frac{\partial^2 u}{\partial x_i \partial x_j} ||^2_{\mathcal{L}^2(\Omega)} \right)^{1/2}. \tag{1.10}$$

We define the subspace

$$\mathcal{H}_0^1(\Omega) := \left\{ u \in \mathcal{H}^1(\Omega) : u = 0 \text{ on } \partial\Omega \right\}. \tag{1.11}$$

The seminorm $|\cdot|_{\mathcal{H}^1(\Omega)}$ is a norm on $\mathcal{H}_0^1(\Omega)$, equivalent to the standard $\mathcal{H}^1$-norm.

Throughout this work, the following notations are adopted:

$$\|\cdot\|_{0,*} = \|\cdot\|_{[\mathcal{L}^2(*)]^d}, \quad \|\cdot\|_{1,*} = \|\cdot\|_{[\mathcal{H}^1(*)]^d}, \quad \text{and} \quad \|\cdot\|_{2,*} = |\cdot|_{[\mathcal{H}^2(*)]^d}, \tag{1.12a}$$

$$|\cdot|_{1,*} = |\cdot|_{[\mathcal{H}^1(*)]^d}, \quad \text{and} \quad |\cdot|_{2,*} = |\cdot|_{[\mathcal{H}^2(*)]^d}. \tag{1.12b}$$

We use the same notation for vector- and tensor-valued functions whose components are members of $\mathcal{L}^2(*)$ or $\mathcal{H}^m(*)$, with inner products and norms all defined componentwise.

Chapter 2

Transversely isotropic elasticity

In this chapter, we present the constitutive relations for transversely isotropic elastic materials, and analyse conditions on the material parameters that are required for the corresponding boundary value problems to be well-posed.

The structure of this chapter is as follows. In Section 2.1, the elasticity tensor for transversely isotropic linear elastic materials is derived from the strain energy function for the general large deformation case. The corresponding compliance tensor is then derived in Section 2.2. Expressions for the primary material parameters are given in terms of physically meaningful alternatives in Section 2.3. Section 2.4 establishes conditions on the material constants for pointwise stability. Finally, conditions for strong ellipticity of the material constants are given in Section 2.5.

2.1 The elasticity tensor

Transversely isotropic (TI) materials are characterized by the existence of a single plane of isotropy and a single axis of rotational symmetry, the normal to the isotropy plane. Let the unit vector $\boldsymbol{a}$ denote the direction of the axis of rotational symmetry, and set $\boldsymbol{M} := \boldsymbol{a} \otimes \boldsymbol{a}$.

The elasticity tensor for a linearly elastic transversely isotropic material may be derived by linearization of the general expression for finite deformations.

Let us consider a body in a motion occupying a domain $\Omega \subset \mathbb{R}^d$ $(d = 2, 3)$ in its reference configuration. The current configuration Ω_t of the body is given by the motion

$$\boldsymbol{x} = \boldsymbol{\varphi}(\boldsymbol{X}, t) = \boldsymbol{X} + \boldsymbol{u}(\boldsymbol{X}, t),$$

where $\boldsymbol{x}$ and $\boldsymbol{X}$ parametrize the current and the reference configurations, respectively, and $\boldsymbol{u}$ is the displacement vector (Figure 2.1). The deformation gradient is defined by

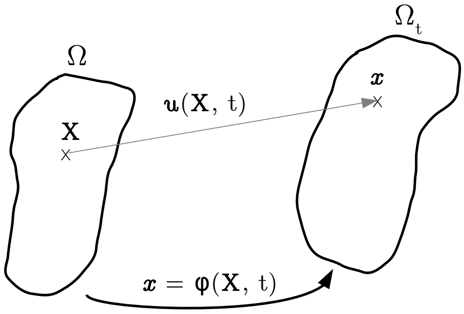

Figure 2.1: Motion of a body from the reference configuration to the current configuration

$$\boldsymbol{F} := \boldsymbol{I} + \nabla \boldsymbol{u},$$

with $\boldsymbol{I}$ the second-order identity tensor, and the right Cauchy-Green tensor by

$$\boldsymbol{C} := \boldsymbol{F}^T \boldsymbol{F}.$$

To derive the elasticity tensor for transversely isotropic materials, we start with the hyperelastic formulation, following Schröder et al. [36]. The strain energy function ψ for a transversely isotropic material is most generally given as a function of five invariants; that is,

$$\psi = \hat{\psi}(I_1, \ldots, I_5), \tag{2.1}$$

where

$$I_1 = \operatorname{tr} \boldsymbol{C}, \quad I_2 = \frac{1}{2}\left((\operatorname{tr} \boldsymbol{C})^2 - \operatorname{tr} \boldsymbol{C}^2\right), \quad I_3 = \det \boldsymbol{C}, \quad I_4 = \operatorname{tr}(\boldsymbol{C}\boldsymbol{M}), \quad \text{and} \quad I_5 = \operatorname{tr}(\boldsymbol{C}^2\boldsymbol{M}). \tag{2.2}$$

The derivatives of the invariants with respect to the right Cauchy-Green tensor $\boldsymbol{C}$ are

$$\frac{\partial I_1}{\partial \boldsymbol{C}} = \boldsymbol{I}, \qquad \frac{\partial I_2}{\partial \boldsymbol{C}} = I_1 \boldsymbol{I} - \boldsymbol{C},$$

$$\frac{\partial I_3}{\partial \boldsymbol{C}} = I_2 \boldsymbol{I} - I_1 \boldsymbol{C} + \boldsymbol{C}^2, \qquad \frac{\partial I_4}{\partial \boldsymbol{C}} = \boldsymbol{M},$$

$$\frac{\partial I_5}{\partial \boldsymbol{C}} = \boldsymbol{C}\boldsymbol{M} + \boldsymbol{M}\boldsymbol{C}.$$

The second Piola-Kirchhoff stress $\boldsymbol{S}$ is given by

$$\boldsymbol{S} := 2\frac{\partial\hat{\psi}}{\partial\boldsymbol{C}}.$$

We introduce the notation

$$\psi_i := \frac{\partial\psi}{\partial I_i} \qquad \text{and} \qquad \psi_{ij} := \frac{\partial^2\psi}{\partial I_i \partial I_j} = \psi_{ji},$$

so that

$$\begin{aligned}\boldsymbol{S} &= 2\sum_{i=1}^{5}\frac{\partial\psi}{\partial I_i}\frac{\partial I_i}{\partial\boldsymbol{C}}\\ &= 2\Big((\psi_1 + I_1\psi_2 + I_2\psi_3)\boldsymbol{I} - (\psi_2 + I_1\psi_3)\boldsymbol{C} + \psi_3\boldsymbol{C}^2 + \psi_4\boldsymbol{M} + \psi_5(\boldsymbol{CM}+\boldsymbol{MC})\Big).\end{aligned}$$

The material tangent modulus or elasticity tensor is defined by

$$\mathbb{C} := 2\frac{\partial\boldsymbol{S}}{\partial\boldsymbol{C}}; \tag{2.3}$$

therefore,

$$\begin{aligned}\mathbb{C} =4\Bigg(&\frac{\partial\psi_1}{\partial\boldsymbol{C}}\otimes\boldsymbol{I} + (\psi_2 + I_1\psi_3)\boldsymbol{I}\otimes\boldsymbol{I} + I_1\frac{\partial\psi_2}{\partial\boldsymbol{C}}\otimes\boldsymbol{I} + I_2\frac{\partial\psi_3}{\partial\boldsymbol{C}}\otimes\boldsymbol{I}\\ &-\frac{\partial\psi_2}{\partial\boldsymbol{C}}\otimes\boldsymbol{C} - \psi_3\boldsymbol{I}\otimes\boldsymbol{C} - I_1\frac{\partial\psi_3}{\partial\boldsymbol{C}}\otimes\boldsymbol{C} - (\psi_2 + I_1\psi_3)\frac{\partial\boldsymbol{C}}{\partial\boldsymbol{C}} + \frac{\partial\psi_3}{\partial\boldsymbol{C}}\otimes\boldsymbol{C}^2\\ &+\psi_3\frac{\partial\boldsymbol{C}^2}{\partial\boldsymbol{C}} + \frac{\partial\psi_4}{\partial\boldsymbol{C}}\otimes\boldsymbol{M} + \frac{\partial\psi_5}{\partial\boldsymbol{C}}\otimes(\boldsymbol{CM}+\boldsymbol{MC}) + \psi_5\frac{\partial}{\partial\boldsymbol{C}}(\boldsymbol{CM}+\boldsymbol{MC})\Bigg).\end{aligned}$$

The derivative of ψ_i with respect to the right Cauchy-Green tensor $\boldsymbol{C}$ is:

$$\begin{aligned}\frac{\partial\psi_i}{\partial\boldsymbol{C}} &= \psi_{i1}\frac{\partial I_1}{\partial\boldsymbol{C}} + \psi_{i2}\frac{\partial I_2}{\partial\boldsymbol{C}} + \psi_{i3}\frac{\partial I_3}{\partial\boldsymbol{C}} + \psi_{i4}\frac{\partial I_4}{\partial\boldsymbol{C}} + \psi_{i5}\frac{\partial I_5}{\partial\boldsymbol{C}}\\ &= (\psi_{i1} + I_1\psi_{i2} + I_2\psi_{i3})\boldsymbol{I} - (\psi_{i2} + I_1\psi_{i3})\boldsymbol{C} + \psi_{i3}\boldsymbol{C}^2 + \psi_{i4}\boldsymbol{M} + \psi_{i5}(\boldsymbol{CM}+\boldsymbol{MC}).\end{aligned}$$

In index notation, we have the following derivatives with respect to the right Cauchy-Green tensor $\boldsymbol{C}$:

$$\begin{aligned}&\frac{\partial C_{ij}}{\partial C_{kl}} = \delta_{ik}\delta_{jl},\\ &\frac{\partial C_{ip}C_{pj}}{\partial C_{kl}} = \delta_{ik}C_{jl} + C_{ik}\delta_{jl},\\ &\frac{\partial}{\partial C_{kl}}(C_{ip}M_{pj} + M_{ip}C_{pj}) = \delta_{ik}M_{jl} + M_{ik}\delta_{jl}.\end{aligned} \tag{2.4}$$

Noting that the fourth-order identity tensor is defined by

$$\mathbb{I} = \delta_{ik}\delta_{jl}\boldsymbol{e}_i \otimes \boldsymbol{e}_j \otimes \boldsymbol{e}_k \otimes \boldsymbol{e}_l,$$

and two other fourth-order tensors $\mathbb{M}$ and $\mathbb{P}$ are defined by

$$\begin{aligned}\mathbb{M} &= (\delta_{ik}M_{jl} + M_{ik}\delta_{jl})\boldsymbol{e}_i \otimes \boldsymbol{e}_j \otimes \boldsymbol{e}_k \otimes \boldsymbol{e}_l,\\ \mathbb{P} &= (\delta_{ik}C_{jl} + C_{ik}\delta_{jl})\boldsymbol{e}_i \otimes \boldsymbol{e}_j \otimes \boldsymbol{e}_k \otimes \boldsymbol{e}_l,\end{aligned}$$

we can write the derivatives given by (2.4) in tensor notation as follows:

$$\frac{\partial \boldsymbol{C}}{\partial \boldsymbol{C}} = \mathbb{I}, \quad \frac{\partial \boldsymbol{C}^2}{\partial \boldsymbol{C}} = \mathbb{P} \quad \text{and} \quad \frac{\partial}{\partial \boldsymbol{C}}(\boldsymbol{CM} + \boldsymbol{MC}) = \mathbb{M}. \tag{2.5}$$

We then have

$$\begin{aligned}\mathbb{C} =4\Big(&(\psi_{11} + 2I_1\psi_{12} + 2I_2\psi_{13} + \psi_2 + I_1\psi_3 + I_1^2\psi_{22} + 2I_1I_2\psi_{23} + I_2^2\psi_{33})\boldsymbol{I} \otimes \boldsymbol{I}\\ &- (\psi_{12} + I_1\psi_{13} + I_1\psi_{22} + (I_1^2 + I_2)\psi_{23} + I_1I_2\psi_{33})(\boldsymbol{C} \otimes \boldsymbol{I} + \boldsymbol{I} \otimes \boldsymbol{C}) - \psi_3\boldsymbol{I} \otimes \boldsymbol{C}\\ &+ (\psi_{13} + I_1\psi_{23} + I_2\psi_{33})(\boldsymbol{C}^2 \otimes \boldsymbol{I} + \boldsymbol{I} \otimes \boldsymbol{C}^2) + (\psi_{14} + I_1\psi_{24} + I_2\psi_{34})(\boldsymbol{M} \otimes \boldsymbol{I} + \boldsymbol{I} \otimes \boldsymbol{M})\\ &+ (\psi_{15} + I_1\psi_{25} + I_2\psi_{35})\big((\boldsymbol{CM} + \boldsymbol{MC}) \otimes \boldsymbol{I} + \boldsymbol{I} \otimes (\boldsymbol{CM} + \boldsymbol{MC})\big) + (\psi_{22} + 2I_1\psi_{23} + I_1^2\psi_{33})\boldsymbol{C} \otimes \boldsymbol{C}\\ &- (\psi_{23} + I_1\psi_{33})(\boldsymbol{C}^2 \otimes \boldsymbol{C} + \boldsymbol{C} \otimes \boldsymbol{C}^2) - (\psi_{24} + I_1\psi_{34})(\boldsymbol{M} \otimes \boldsymbol{C} + \boldsymbol{C} \otimes \boldsymbol{M}) - (\psi_2 + I_1\psi_3)\mathbb{I}\\ &- (\psi_{25} + I_1\psi_{35})\big((\boldsymbol{CM} + \boldsymbol{MC}) \otimes \boldsymbol{C} + \boldsymbol{C} \otimes (\boldsymbol{CM} + \boldsymbol{MC})\big) + \psi_{33}\boldsymbol{C}^2 \otimes \boldsymbol{C}^2 + \psi_{34}(\boldsymbol{M} \otimes \boldsymbol{C}^2 + \boldsymbol{C}^2 \otimes \boldsymbol{M})\\ &+ \psi_{35}\big((\boldsymbol{CM} + \boldsymbol{MC}) \otimes \boldsymbol{C}^2 + \boldsymbol{C}^2 \otimes (\boldsymbol{CM} + \boldsymbol{MC})\big) + \psi_3\mathbb{P} + \psi_{44}\boldsymbol{M} \otimes \boldsymbol{M}\\ &+ \psi_{45}\big((\boldsymbol{CM} + \boldsymbol{MC}) \otimes \boldsymbol{M} + \boldsymbol{M} \otimes (\boldsymbol{CM} + \boldsymbol{MC})\big) + \psi_{55}\big((\boldsymbol{CM} + \boldsymbol{MC}) \otimes (\boldsymbol{CM} + \boldsymbol{MC})\big) + \psi_5\mathbb{M}\Big).\end{aligned}$$

We linearize about $\boldsymbol{C} = \boldsymbol{I}$ to obtain

$$\begin{aligned}\mathbb{C} = 4\Big(&(\psi_{11} + 4\psi_{12} + \psi_2 + 4\psi_{22} + 2\psi_{13} + 4\psi_{23} + \psi_{33} + 2\psi_3)\boldsymbol{I} \otimes \boldsymbol{I} - (\psi_2 + 2\psi_3)\mathbb{I}\\ &+ (\psi_{14} + 2\psi_{24} + 2\psi_{15} + 4\psi_{25} + \psi_{34} + 2\psi_{35})(\boldsymbol{I} \otimes \boldsymbol{M} + \boldsymbol{M} \otimes \boldsymbol{I})\\ &+ (4\psi_{45} + 4\psi_{55} + \psi_{44})\boldsymbol{M} \otimes \boldsymbol{M} + \psi_5\mathbb{M}\Big).\end{aligned} \tag{2.6}$$

In index notation,

$$\mathbb{C}_{ijkl} = c_1\delta_{ij}\delta_{kl} + c_2\delta_{ik}\delta_{jl} + c_3(\delta_{ij}M_{kl} + M_{ij}\delta_{kl}) + c_4M_{ij}M_{kl} + c_5(\delta_{ik}M_{jl} + M_{ik}\delta_{jl}), \tag{2.7}$$

where

$$\begin{aligned}
c_1 &= 4(\psi_{11} + 4\psi_{12} + \psi_2 + 4\psi_{22} + 2\psi_{13} + 4\psi_{23} + \psi_{33} + 2\psi_3), \\
c_2 &= -4(\psi_2 + 2\psi_3), \\
c_3 &= 4(\psi_{14} + 2\psi_{24} + 2\psi_{15} + 4\psi_{25} + \psi_{34} + 2\psi_{35}), \\
c_4 &= 4(4\psi_{45} + 4\psi_{55} + \psi_{44}), \\
c_5 &= 4\psi_5.
\end{aligned}$$

We define an alternative set of five material constants λ, μ_t, μ_l, α and β according to

$$c_1 = \lambda,\ c_2 = -2\mu_t,\ c_3 = \alpha,\ c_4 = \beta,\ \text{and}\ c_5 = \gamma := 2(\mu_l - \mu_t).$$

Then for a transversely isotropic linearly elastic material with fibre direction given by the unit vector $\boldsymbol{a}$, the elasticity tensor is given by [30, 41]

$$\mathbb{C} = \lambda \boldsymbol{I} \otimes \boldsymbol{I} + 2\mu_t \mathbb{I} + \alpha(\boldsymbol{I} \otimes \boldsymbol{M} + \boldsymbol{M} \otimes \boldsymbol{I}) + \beta \boldsymbol{M} \otimes \boldsymbol{M} + \gamma \mathbb{M}\,. \tag{2.8}$$

Here λ denotes the first Lamé parameter, the shear modulus in the plane of isotropy is μ_t, μ_l is the shear modulus along the fibre direction. The further material constants α and β do not have a direct interpretation, though it will be seen that β becomes unbounded in the inextensible limit.

The corresponding linear stress-strain relation for small deformations is then

$$\begin{aligned}
\boldsymbol{\sigma} &= \mathbb{C}\boldsymbol{\varepsilon} \\
&= \lambda(\operatorname{tr}\boldsymbol{\varepsilon})\boldsymbol{I} + 2\mu_t\boldsymbol{\varepsilon} + \alpha\big((\boldsymbol{M}:\boldsymbol{\varepsilon})\boldsymbol{I} + (\operatorname{tr}\boldsymbol{\varepsilon})\boldsymbol{M}\big) + \beta(\boldsymbol{M}:\boldsymbol{\varepsilon})\boldsymbol{M} + \gamma(\boldsymbol{\varepsilon}\boldsymbol{M} + \boldsymbol{M}\boldsymbol{\varepsilon}),
\end{aligned} \tag{2.9}$$

in which $\boldsymbol{\sigma}$ and $\boldsymbol{\varepsilon}$ denote the stress and the infinitesimal strain tensors; $\operatorname{tr}\boldsymbol{\varepsilon}$ denotes the trace of $\boldsymbol{\varepsilon}$, and $\boldsymbol{M}:\boldsymbol{\varepsilon} = \boldsymbol{\varepsilon}\boldsymbol{a}\cdot\boldsymbol{a}$, obtained from the definition of $\boldsymbol{M}$, gives the strain in the direction of $\boldsymbol{a}$.

The special case of an isotropic material is recovered by setting $\alpha = \beta = 0$ and $\mu_l = \mu_t$.

For the particular case in which $\boldsymbol{a} = \boldsymbol{e}_3$, the stress-strain relationship can be written in matrix form as

$$\begin{pmatrix} \sigma_{11} \\ \sigma_{22} \\ \sigma_{33} \\ \sigma_{23} \\ \sigma_{13} \\ \sigma_{12} \end{pmatrix} = \begin{pmatrix} \lambda + 2\mu_t & \lambda & \lambda + \alpha & 0 & 0 & 0 \\ \lambda & \lambda + 2\mu_t & \lambda + \alpha & 0 & 0 & 0 \\ \lambda + \alpha & \lambda + \alpha & \lambda + 2\mu_t + 2\alpha + \beta + 2\gamma & 0 & 0 & 0 \\ 0 & 0 & 0 & \mu_l & 0 & 0 \\ 0 & 0 & 0 & 0 & \mu_l & 0 \\ 0 & 0 & 0 & 0 & 0 & \mu_t \end{pmatrix} \begin{pmatrix} \varepsilon_{11} \\ \varepsilon_{22} \\ \varepsilon_{33} \\ 2\varepsilon_{23} \\ 2\varepsilon_{13} \\ 2\varepsilon_{12} \end{pmatrix}. \tag{2.10}$$

2.2 The compliance tensor

It is also useful to have available the inverse of (2.9), and to find the compliance tensor $\mathbb{S}$ corresponding to $\mathbb{C}$; that is,

$$\boldsymbol{\varepsilon} = \mathbb{S}\boldsymbol{\sigma}. \tag{2.11}$$

We derive here an explicit form for $\mathbb{S}$, using an approach that is more direct than that in [30]. First, from (2.9) we have

$$2\mu_t\boldsymbol{\varepsilon} = \boldsymbol{\sigma} - (\lambda\boldsymbol{I} + \alpha\boldsymbol{M})(\operatorname{tr}\boldsymbol{\varepsilon}) - (\alpha\boldsymbol{I} + \beta\boldsymbol{M})(\boldsymbol{M} : \boldsymbol{\varepsilon}) - \gamma(\boldsymbol{\varepsilon}\boldsymbol{M} + \boldsymbol{M}\boldsymbol{\varepsilon}), \tag{2.12}$$

$$\begin{aligned} \operatorname{tr}\boldsymbol{\sigma} &= \lambda(\operatorname{tr}\boldsymbol{\varepsilon})(\operatorname{tr}\boldsymbol{I}) + 2\mu_t(\operatorname{tr}\boldsymbol{\varepsilon}) + \alpha\big((\boldsymbol{M} : \boldsymbol{\varepsilon})(\operatorname{tr}\boldsymbol{I}) + (\operatorname{tr}\boldsymbol{\varepsilon})(\operatorname{tr}\boldsymbol{M})\big) + \beta(\boldsymbol{M} : \boldsymbol{\varepsilon})(\operatorname{tr}\boldsymbol{M}) + \gamma\big(\operatorname{tr}(\boldsymbol{\varepsilon}\boldsymbol{M}) + \operatorname{tr}(\boldsymbol{M}\boldsymbol{\varepsilon})\big) \\ &= 3\lambda(\operatorname{tr}\boldsymbol{\varepsilon}) + 2\mu_t(\operatorname{tr}\boldsymbol{\varepsilon}) + \alpha\big(3(\boldsymbol{M} : \boldsymbol{\varepsilon}) + (\operatorname{tr}\boldsymbol{\varepsilon})\big) + \beta(\boldsymbol{M} : \boldsymbol{\varepsilon}) + 2\gamma(\boldsymbol{M} : \boldsymbol{\varepsilon}) \\ &= (3\lambda + 2\mu_t + \alpha)\operatorname{tr}\boldsymbol{\varepsilon} + (3\alpha + \beta + 2\gamma)(\boldsymbol{M} : \boldsymbol{\varepsilon}), \end{aligned} \tag{2.13}$$

and

$$\begin{aligned} \boldsymbol{M} : \boldsymbol{\sigma} =& \lambda(\operatorname{tr}\boldsymbol{\varepsilon})(\boldsymbol{M} : \boldsymbol{I}) + 2\mu_t(\boldsymbol{M} : \boldsymbol{\varepsilon}) + \alpha\big((\boldsymbol{M} : \boldsymbol{\varepsilon})(\boldsymbol{M} : \boldsymbol{I}) + (\operatorname{tr}\boldsymbol{\varepsilon})(\boldsymbol{M} : \boldsymbol{M})\big) + \beta(\boldsymbol{M} : \boldsymbol{\varepsilon})(\boldsymbol{M} : \boldsymbol{M}) \\ &+ \gamma(\boldsymbol{M} : \boldsymbol{\varepsilon}\boldsymbol{M} + \boldsymbol{M} : \boldsymbol{M}\boldsymbol{\varepsilon}) \\ =& \lambda(\operatorname{tr}\boldsymbol{\varepsilon}) + 2\mu_t(\boldsymbol{M} : \boldsymbol{\varepsilon}) + \alpha\big((\boldsymbol{M} : \boldsymbol{\varepsilon}) + (\operatorname{tr}\boldsymbol{\varepsilon})\big) + \beta(\boldsymbol{M} : \boldsymbol{\varepsilon}) + 2\gamma(\boldsymbol{M} : \boldsymbol{\varepsilon}) \\ =& (\lambda + \alpha)\operatorname{tr}\boldsymbol{\varepsilon} + (2\mu_t + \alpha + \beta + 2\gamma)(\boldsymbol{M} : \boldsymbol{\varepsilon}). \end{aligned} \tag{2.14}$$

We also have

$$\begin{aligned} \boldsymbol{M}\boldsymbol{\sigma} =& \lambda(\operatorname{tr}\boldsymbol{\varepsilon})\boldsymbol{M} + 2\mu_t\boldsymbol{M}\boldsymbol{\varepsilon} + \alpha\big((\boldsymbol{M} : \boldsymbol{\varepsilon})\boldsymbol{M} + (\operatorname{tr}\boldsymbol{\varepsilon})\boldsymbol{M}^2\big) + \beta(\boldsymbol{M} : \boldsymbol{\varepsilon})\boldsymbol{M}^2 + \gamma\big(\boldsymbol{M}\boldsymbol{\varepsilon}\boldsymbol{M} + \boldsymbol{M}\boldsymbol{M}\boldsymbol{\varepsilon}\big) \\ =& \lambda(\operatorname{tr}\boldsymbol{\varepsilon})\boldsymbol{M} + 2\mu_t\boldsymbol{M}\boldsymbol{\varepsilon} + \alpha\big((\boldsymbol{M} : \boldsymbol{\varepsilon})\boldsymbol{M} + (\operatorname{tr}\boldsymbol{\varepsilon})\boldsymbol{M}\big) + \beta(\boldsymbol{M} : \boldsymbol{\varepsilon})\boldsymbol{M} + \gamma\big((\boldsymbol{M} : \boldsymbol{\varepsilon})\boldsymbol{M} + \boldsymbol{M}\boldsymbol{\varepsilon}\big) \\ =& (\lambda + \alpha)(\operatorname{tr}\boldsymbol{\varepsilon})\boldsymbol{M} + (2\mu_t + \gamma)\boldsymbol{M}\boldsymbol{\varepsilon} + (\alpha + \beta + \gamma)(\boldsymbol{M} : \boldsymbol{\varepsilon})\boldsymbol{M} \end{aligned} \tag{2.15}$$

and

$$\begin{aligned}\boldsymbol{\sigma M} =&\lambda(\operatorname{tr}\boldsymbol{\varepsilon})\boldsymbol{M} + 2\mu_t\boldsymbol{\varepsilon M} + \alpha\big((\boldsymbol{M}:\boldsymbol{\varepsilon})\boldsymbol{M} + (\operatorname{tr}\boldsymbol{\varepsilon})\boldsymbol{M}^2\big) + \beta(\boldsymbol{M}:\boldsymbol{\varepsilon})\boldsymbol{M}^2 + \gamma\big(\boldsymbol{\varepsilon MM} + \boldsymbol{M\varepsilon M}\big)\\ =&\lambda(\operatorname{tr}\boldsymbol{\varepsilon})\boldsymbol{M} + 2\mu_t\boldsymbol{\varepsilon M} + \alpha\big((\boldsymbol{M}:\boldsymbol{\varepsilon})\boldsymbol{M} + (\operatorname{tr}\boldsymbol{\varepsilon})\boldsymbol{M}\big) + \beta(\boldsymbol{M}:\boldsymbol{\varepsilon})\boldsymbol{M} + \gamma\big(\boldsymbol{\varepsilon M} + (\boldsymbol{M}:\boldsymbol{\varepsilon})\boldsymbol{M}\big)\\ =&(\lambda+\alpha)(\operatorname{tr}\boldsymbol{\varepsilon})\boldsymbol{M} + (2\mu_t+\gamma)\boldsymbol{\varepsilon M} + (\alpha+\beta+\gamma)(\boldsymbol{M}:\boldsymbol{\varepsilon})\boldsymbol{M}.\end{aligned} \tag{2.16}$$

Using (2.13) and (2.14), we obtain

$$\begin{pmatrix}\operatorname{tr}\boldsymbol{\sigma}\\ \boldsymbol{M}:\boldsymbol{\sigma}\end{pmatrix} = \begin{pmatrix}3\lambda+2\mu_t+\alpha & 3\alpha+\beta+2\gamma\\ \lambda+\alpha & 2\mu_t+\alpha+\beta+2\gamma\end{pmatrix}\begin{pmatrix}\operatorname{tr}\boldsymbol{\varepsilon}\\ \boldsymbol{M}:\boldsymbol{\varepsilon}\end{pmatrix}$$

and its inverse

$$\begin{pmatrix}\operatorname{tr}\boldsymbol{\varepsilon}\\ \boldsymbol{M}:\boldsymbol{\varepsilon}\end{pmatrix} = \frac{1}{\mathcal{K}}\begin{pmatrix}2\mu_t+\alpha+\beta+2\gamma & -3\alpha-\beta-2\gamma\\ -\lambda-\alpha & 3\lambda+2\mu_t+\alpha\end{pmatrix}\begin{pmatrix}\operatorname{tr}\boldsymbol{\sigma}\\ \boldsymbol{M}:\boldsymbol{\sigma}\end{pmatrix}, \tag{2.17}$$

where

$$\mathcal{K} = 2(\lambda+\alpha)(\mu_t-\alpha) + 2(\lambda+\mu_t)(2\mu_t+\alpha+\beta+2\gamma). \tag{2.18}$$

Adopting the notations

$$A = \frac{2\mu_t+\alpha+\beta+2\gamma}{\mathcal{K}},\qquad B = -\frac{3\alpha+\beta+2\gamma}{\mathcal{K}},\qquad C = -\frac{\lambda+\alpha}{\mathcal{K}}\quad\text{and}\quad D = \frac{3\lambda+2\mu_t+\alpha}{\mathcal{K}}, \tag{2.19}$$

we substitute into (2.12) the expressions for $\operatorname{tr}\boldsymbol{\varepsilon}$ and $\boldsymbol{M}:\boldsymbol{\varepsilon}$ from (2.17):

$$2\mu_t\boldsymbol{\varepsilon} = \boldsymbol{\sigma} - \big((A\lambda+C\alpha)\boldsymbol{I} + (A\alpha+C\beta)\boldsymbol{M}\big)\operatorname{tr}\boldsymbol{\sigma} - \big((B\lambda+D\alpha)\boldsymbol{I} + (B\alpha+D\beta)\boldsymbol{M}\big)(\boldsymbol{M}:\boldsymbol{\sigma}) - \gamma(\boldsymbol{\varepsilon M} + \boldsymbol{M\varepsilon}). \tag{2.20}$$

From (2.15) and (2.16), we have

$$\begin{aligned}\boldsymbol{\sigma M} + \boldsymbol{M\sigma} =&2\big((\lambda+\alpha)A + (\alpha+\beta+\gamma)C\big)(\operatorname{tr}\boldsymbol{\sigma})\boldsymbol{M} + 2\big((\lambda+\alpha)B + (\alpha+\beta+\gamma)D\big)(\boldsymbol{M}:\boldsymbol{\sigma})\boldsymbol{M}\\ &+ (2\mu_t+\gamma)(\boldsymbol{\varepsilon M} + \boldsymbol{M\varepsilon})\\ =&2(\lambda+\alpha)(2\mu_t+\gamma)(\operatorname{tr}\boldsymbol{\sigma})\boldsymbol{M} + 2\big((\lambda+\alpha)B + (\alpha+\beta+\gamma)D\big)(\boldsymbol{M}:\boldsymbol{\sigma})\boldsymbol{M} + (2\mu_t+\gamma)(\boldsymbol{\varepsilon M} + \boldsymbol{M\varepsilon}).\end{aligned}$$

Assuming that $2\mu_t + \gamma = 2\mu_l \neq 0$, that is,

$$\mu_l \neq 0, \tag{2.21}$$

we obtain

$$\boldsymbol{\varepsilon M} + \boldsymbol{M\varepsilon} = \frac{1}{2\mu_t+\gamma}\Big((\boldsymbol{\sigma M} + \boldsymbol{M\sigma}) - 2(\lambda+\alpha)(2\mu_t+\gamma)(\operatorname{tr}\boldsymbol{\sigma})\boldsymbol{M} - 2\big((\lambda+\alpha)B + (\alpha+\beta+\gamma)D\big)(\boldsymbol{M}:\boldsymbol{\sigma})\boldsymbol{M}\Big).$$

Inserting into (2.20), we obtain

$$\begin{aligned}2\mu_t\boldsymbol{\varepsilon} =& \boldsymbol{\sigma} - (A\lambda + C\alpha)(\operatorname{tr}\boldsymbol{\sigma})\boldsymbol{I} + \big(2\gamma(\lambda+\alpha) - (A\alpha + C\beta)\big)(\operatorname{tr}\boldsymbol{\sigma})\boldsymbol{M} - (B\lambda + D\alpha)(\boldsymbol{M}:\boldsymbol{\sigma})\boldsymbol{I} \\ &+ \left(\frac{2\gamma}{2\mu_t+\gamma}\big((\lambda+\alpha)B + (\alpha+\beta+\gamma)D\big) - (B\alpha + D\beta)\right)(\boldsymbol{M}:\boldsymbol{\sigma})\boldsymbol{M} \\ &- \frac{\gamma}{2\mu_t+\gamma}(\boldsymbol{\sigma}\boldsymbol{M} + \boldsymbol{M}\boldsymbol{\sigma});\end{aligned}$$

assuming

$$\mu_t \neq 0, \tag{2.22}$$

we obtain the following strain-stress relation:

$$\begin{aligned}\boldsymbol{\varepsilon} =& \frac{1}{2\mu_t}\Bigg(\boldsymbol{\sigma} - (A\lambda + C\alpha)(\operatorname{tr}\boldsymbol{\sigma})\boldsymbol{I} - (B\lambda + D\alpha)\Big((\boldsymbol{M}:\boldsymbol{\sigma})\boldsymbol{I} + (\operatorname{tr}\boldsymbol{\sigma})\boldsymbol{M}\Big) \\ &+ \left(\frac{2\gamma}{2\mu_t+\gamma}\big((\lambda+\alpha)B + (\alpha+\beta+\gamma)D\big) - (B\alpha + D\beta)\right)(\boldsymbol{M}:\boldsymbol{\sigma})\boldsymbol{M} - \frac{\gamma}{2\mu_t+\gamma}(\boldsymbol{\sigma}\boldsymbol{M} + \boldsymbol{M}\boldsymbol{\sigma})\Bigg).\end{aligned} \tag{2.23}$$

In simpler form, we can write this expression as

$$\boldsymbol{\varepsilon} = s_1(\operatorname{tr}\boldsymbol{\sigma})\,\boldsymbol{I} + s_2\boldsymbol{\sigma} + s_3\Big((\boldsymbol{M}:\boldsymbol{\sigma})\boldsymbol{I} + (\operatorname{tr}\boldsymbol{\sigma})\,\boldsymbol{M}\Big) + s_4(\boldsymbol{M}:\boldsymbol{\sigma})\boldsymbol{M} + s_5(\boldsymbol{\sigma}\boldsymbol{M} + \boldsymbol{M}\boldsymbol{\sigma}). \tag{2.24}$$

Here

$$\begin{aligned} s_1 &= -\frac{A\lambda + C\alpha}{2\mu_t}, & s_2 &= \frac{1}{2\mu_t}, \\ s_3 &= -\frac{B\lambda + D\alpha}{2\mu_t}, & s_4 &= \frac{2\gamma}{2\mu_t+\gamma}\big((\lambda+\alpha)B + (\alpha+\beta+\gamma)D\big) - (B\alpha + D\beta), \\ s_5 &= -\frac{\gamma}{2\mu_t(2\mu_t+\gamma)}. \end{aligned} \tag{2.25}$$

From (2.11) and (2.24), we have

$$\mathbb{S} = s_1\boldsymbol{I}\otimes\boldsymbol{I} + s_2\mathbb{I} + s_3(\boldsymbol{I}\otimes\boldsymbol{M} + \boldsymbol{M}\otimes\boldsymbol{I}) + s_4\boldsymbol{M}\otimes\boldsymbol{M} + s_5\mathbb{M}\,. \tag{2.26}$$

2.3 Material parameters

In this section, we express the five material parameters given in (2.9) in terms of the five independent physically meaningful constants, E_t: Young's modulus in the transverse direction; E_l: Young's modulus in the fibre direction; ν_t and ν_l: respectively Poisson's ratios for the transverse strain with respect to the fibre direction and the plane normal to it; and the longitudinal shear modulus μ_l. One may further define the transversal shear modulus μ_t by

$$\mu_t = \frac{E_t}{2(1+\nu_t)}. \tag{2.27}$$

Choosing the fibre direction to coincide with the basis vector $\boldsymbol{e}_3$, the compliance relation has the alternate form [17]

$$\begin{pmatrix} \varepsilon_{11} \\ \varepsilon_{22} \\ \varepsilon_{33} \\ 2\varepsilon_{23} \\ 2\varepsilon_{13} \\ 2\varepsilon_{12} \end{pmatrix} = \begin{pmatrix} \frac{1}{E_t} & -\frac{\nu_t}{E_t} & -\frac{\nu_l}{E_l} & 0 & 0 & 0 \\ -\frac{\nu_t}{E_t} & \frac{1}{E_t} & -\frac{\nu_l}{E_l} & 0 & 0 & 0 \\ -\frac{\nu_l}{E_l} & -\frac{\nu_l}{E_l} & \frac{1}{E_l} & 0 & 0 & 0 \\ 0 & 0 & 0 & \frac{1}{\mu_l} & 0 & 0 \\ 0 & 0 & 0 & 0 & \frac{1}{\mu_l} & 0 \\ 0 & 0 & 0 & 0 & 0 & \frac{1}{\mu_t} \end{pmatrix} \begin{pmatrix} \sigma_{11} \\ \sigma_{22} \\ \sigma_{33} \\ \sigma_{23} \\ \sigma_{13} \\ \sigma_{12} \end{pmatrix}. \tag{2.28}$$

The nature of the Poisson's ratios may be determined by considering some simple loading cases. For the case of uniaxial stress in the x_3-direction, with $\boldsymbol{a} = \boldsymbol{e}_3$, the strains are given by

$$\varepsilon_{11} = -\frac{\nu_l}{E_l}\sigma_{33}, \quad \varepsilon_{22} = -\frac{\nu_l}{E_l}\sigma_{33} \quad \text{and} \quad \varepsilon_{33} = \frac{\sigma_{33}}{E_l}. \tag{2.29}$$

Thus

$$\varepsilon_{11} = \varepsilon_{22} = -\nu_l \varepsilon_{33}, \tag{2.30}$$

so that ν_l determines the lateral contraction in the plane of isotropy, as a result of strain in the longitudinal or fibre direction.

Similarly, considering the case of uniaxial stress in the (transverse) x_1-direction, we have

$$\varepsilon_{11} = \frac{\sigma_{11}}{E_t}, \quad \varepsilon_{22} = -\frac{\nu_t}{E_t}\sigma_{11}, \quad \text{and} \quad \varepsilon_{33} = -\frac{\nu_l}{E_l}\sigma_{11}, \tag{2.31}$$

so that

$$\varepsilon_{33} = -\nu_l \frac{E_t}{E_l}\varepsilon_{11}. \tag{2.32}$$

Thus, lateral contraction in the fibre direction depends directly on the ratio of Young's moduli in the fibre and transverse directions. In the inextensible limit, when $E_l/E_t \to \infty$, there is no lateral contraction in the fibre direction.

Returning to the strain-stress relation given by (2.23), for the particular case of $\boldsymbol{a} = \boldsymbol{e}_3$, we have

$$\begin{pmatrix} \varepsilon_{11} \\ \varepsilon_{22} \\ \varepsilon_{33} \\ 2\varepsilon_{23} \\ 2\varepsilon_{13} \\ 2\varepsilon_{12} \end{pmatrix} = \begin{pmatrix} \dfrac{1-A\lambda-C\alpha}{2\mu_t} & -\dfrac{A\lambda+C\alpha}{2\mu_t} & -\dfrac{\lambda+\alpha}{\mathcal{K}} & 0 & 0 & 0 \\ -\dfrac{A\lambda+C\alpha}{2\mu_t} & \dfrac{1-A\lambda-C\alpha}{2\mu_t} & -\dfrac{\lambda+\alpha}{\mathcal{K}} & 0 & 0 & 0 \\ -\dfrac{\lambda+\alpha}{\mathcal{K}} & -\dfrac{\lambda+\alpha}{\mathcal{K}} & \dfrac{2(\lambda+\mu_t)}{\mathcal{K}} & 0 & 0 & 0 \\ 0 & 0 & 0 & \dfrac{1}{\mu_l} & 0 & 0 \\ 0 & 0 & 0 & 0 & \dfrac{1}{\mu_l} & 0 \\ 0 & 0 & 0 & 0 & 0 & \dfrac{1}{\mu_t} \end{pmatrix} \begin{pmatrix} \sigma_{11} \\ \sigma_{22} \\ \sigma_{33} \\ \sigma_{23} \\ \sigma_{13} \\ \sigma_{12} \end{pmatrix}. \tag{2.33}$$

Comparing (2.33) with (2.28), the expressions of the engineering constants are given in terms of the material parameters by

$$\begin{aligned} E_t &= \frac{2\mu_t}{1-A\lambda-C\alpha}, & E_l &= \frac{\mathcal{K}}{2(\lambda+\mu_t)}, \\ \nu_t &= \frac{A\lambda+C\alpha}{1-A\lambda-C\alpha}, & \nu_l &= \frac{\lambda+\alpha}{2(\lambda+\mu_t)}. \end{aligned} \tag{2.34}$$

From (2.10), we have

$$\begin{cases} C_{1111} &= \lambda + 2\mu_t, \\ C_{1122} &= \lambda \\ C_{1133} &= \lambda + \alpha, \\ C_{3333} &= \lambda - 2\mu_t + 2\alpha + \beta + 4\mu_l, \\ C_{3131} &= \mu_l. \end{cases} \tag{2.35}$$

By inverting (2.28), we have

$$\begin{cases} C_{1111} &= \dfrac{(E_l - \nu_l^2 E_t)E_t}{(1+\nu_t)((1-\nu_t)E_l - 2\nu_l^2 E_t)}, \\ C_{1122} &= \dfrac{(\nu_l^2 E_t + \nu_t E_l)E_t}{(1+\nu_t)((1-\nu_t)E_l - 2\nu_l^2 E_t)}, \\ C_{1133} &= \dfrac{\nu_l(1+\nu_t)E_l E_t}{(1+\nu_t)((1-\nu_t)E_l - 2\nu_l^2 E_t)}, \\ C_{3333} &= \dfrac{(1-\nu_t^2)E_l^2}{(1+\nu_t)((1-\nu_t)E_l - 2\nu_l^2 E_t)}, \\ C_{3131} &= \mu_l. \end{cases} \tag{2.36}$$

By comparing (2.35) with (2.36), the material parameters λ, α and β can be written in terms of the engineering constants as

$$\begin{aligned}
\mu_l &= \mu_l, \\
\lambda &= \frac{(\nu_l^2 E_t + \nu_t E_l)E_t}{(1+\nu_t)((1-\nu_t)E_l - 2\nu_l^2 E_t)}, \\
\alpha &= \frac{\left(E_l\nu_l(1+\nu_t) - \nu_l^2 E_t - \nu_t E_l\right)E_t}{(1+\nu_t)((1-\nu_t)E_l - 2\nu_l^2 E_t)}, \\
\beta &= \frac{E_l^2(1-\nu_t^2) - E_t^2\nu_l^2 + E_t E_l(1-2\nu_t\nu_l - 2\nu_l)}{(1+\nu_t)((1-\nu_t)E_l - 2\nu_l^2 E_t)} - 4\mu_l.
\end{aligned} \tag{2.37}$$

Henceforth, we set

$$E_l = pE_t \quad \text{and} \quad \mu_l = q\mu_t\,. \tag{2.38}$$

Thus p measures the stiffness in the fibre direction relative to that in the plane of isotropy, and q is the ratio of the two shear moduli. Using (2.38) the expressions (2.37) become

$$\frac{\mu_l}{E_t} = \frac{q}{2(1+\nu_t)}, \tag{2.39a}$$

$$\frac{\lambda}{E_t} = \frac{\nu_t p + \nu_l^2}{(1+\nu_t)\big((1-\nu_t)p - 2\nu_l^2\big)}, \tag{2.39b}$$

$$\frac{\alpha}{E_t} = \frac{(\nu_l - \nu_t + \nu_t\nu_l)p - \nu_l^2}{(1+\nu_t)\big((1-\nu_t)p - 2\nu_l^2\big)}, \tag{2.39c}$$

$$\frac{\beta}{E_t} = \frac{(1-\nu_t^2)p^2 + (-2\nu_t\nu_l + 2q\nu_t - 2\nu_l + 1 - 2q)p - (1-4q)\nu_l^2}{(1+\nu_t)\big((1-\nu_t)p - 2\nu_l^2\big)}. \tag{2.39d}$$

Later, we will consider the special case in which

$$\nu_l = \nu_t = \nu \quad \text{and} \quad \mu_l = \mu_t, \quad \text{that is} \quad q = 1. \tag{2.40}$$

In this way, we will focus on behaviour in relation to three independent parameters, viz. (λ, α, β) or (E_t, E_l, ν), rather than the full set of five parameters. The expressions given by equations (2.39) then become

$$\frac{\mu_l}{E_t} = \frac{1}{2(1+\nu)}, \tag{2.41a}$$

$$\frac{\lambda}{E_t} = \frac{\nu(p+\nu)}{(1+\nu)\big((1-\nu)p - 2\nu^2\big)}, \tag{2.41b}$$

$$\frac{\alpha}{E_t} = \frac{\nu^2(p-1)}{(1+\nu)\big((1-\nu)p - 2\nu^2\big)}, \tag{2.41c}$$

$$\frac{\beta}{E_t} = \frac{(p-1)\big((1-\nu^2)p - 3\nu^2\big)}{(1+\nu)\big((1-\nu)p - 2\nu^2\big)}. \tag{2.41d}$$

Throughout this work, our interest is in the behaviour of the material at near-incompressibility and at near-inextensibility. Clearly, inextensibility corresponds to the case $p \to \infty$, or equivalently $\beta \to \infty$. Note that λ and α are bounded in the limit $p \to \infty$.

We now consider the case of incompressibility, that is, values of the material parameters for which $\operatorname{tr} \boldsymbol{\varepsilon} = 0$. With the assumption (2.40), from (2.28), we have

$$\operatorname{tr} \boldsymbol{\varepsilon} = \frac{1}{E_t}\left(1 - \nu - \frac{\nu}{p}\right)\sigma_{11} + \frac{1}{E_t}\left(1 - \nu - \frac{\nu}{p}\right)\sigma_{22} + \frac{1}{pE_t}(1 - 2\nu)\sigma_{33}.$$

Assuming $\sigma_{11}, \sigma_{22}, \sigma_{33} \neq 0$, we have $\operatorname{tr} \boldsymbol{\varepsilon} = 0$ if and only if

$$\begin{cases} \nu = \dfrac{p}{p+1} \\ \nu = \dfrac{1}{2} \end{cases} \quad \Leftrightarrow \quad p = 1 \quad \text{and} \quad \nu = \frac{1}{2}. \tag{2.42}$$

Thus, incompressible behaviour is possible only for the isotropic case, and corresponds to Poisson's ratio $\nu = 1/2$.

The same applies if $\sigma_{11} = 0$ or $\sigma_{22} = 0$. On the other hand, if $\sigma_{11} = \sigma_{22} = 0$, incompressible behaviour occurs for $\nu = 1/2$, independent of p.

For the case in which $\sigma_{33} = 0$, we have $\operatorname{tr} \boldsymbol{\varepsilon} = 0$ if and only if

$$\nu = \frac{p}{p+1}. \tag{2.43}$$

Thus, for this case, incompressible behaviour occurs for any pair (ν, p) that satisfies (2.43).

Under plane strain conditions, by setting $\varepsilon_{22} = 0$ and eliminating σ_{22}, we have

$$\operatorname{tr} \boldsymbol{\varepsilon} = \frac{1}{E_t}\left(1 - \nu^2 - \frac{\nu^2}{p} - \frac{\nu}{p}\right)\sigma_{11} + \frac{1}{pE_t}\left(1 - \nu - \nu^2 - \frac{\nu^2}{p}\right)\sigma_{33}.$$

Assuming $\sigma_{11}, \sigma_{33} \neq 0$, we have

$$\operatorname{tr} \boldsymbol{\varepsilon} = 0 \quad \Leftrightarrow \quad \begin{cases} \nu = \dfrac{p}{p+1} \\ \nu = \dfrac{p}{2} \end{cases} \quad \Leftrightarrow \quad p = 1 \quad \text{and} \quad \nu = \frac{1}{2}. \tag{2.44}$$

So, as for the general case, the only possibility for incompressible behaviour is the isotropic case with Poisson's ratio $\nu = 1/2$.

Assuming $\sigma_{11} = 0$, we have

$$\operatorname{tr}\boldsymbol{\varepsilon} = 0 \quad \Leftrightarrow \quad \left(\frac{p+1}{p}\right)\nu^2 + \nu - 1 = 0 \quad \Leftrightarrow \quad p = \frac{\nu^2}{1-\nu-\nu^2}. \tag{2.45}$$

Thus, for this case, incompressible behaviour occurs for any pair (ν, p) that satisfies (2.45). If $\nu = 1/2$ then incompressibility corresponds to the case when $p = 1$.

Assuming $\sigma_{33} = 0$, we have

$$\operatorname{tr}\boldsymbol{\varepsilon} = 0 \quad \Leftrightarrow \quad \nu = \frac{p}{p+1}, \tag{2.46}$$

as for the general case (2.43).

The following table summarizes the conditions on the material parameters for incompressibility. These are of course pointwise or local conditions.

case	values for ν and p
$\sigma_{11}, \sigma_{22}, \sigma_{33} \neq 0$ $\sigma_{11} = 0$ or $\sigma_{22} = 0$ plane strain: $\sigma_{11}, \sigma_{33} \neq 0$	$\nu = \frac{1}{2}, p = 1$
$\sigma_{11} = \sigma_{22} = 0$	$\nu = \frac{1}{2}$, any p
$\sigma_{33} = 0$ plane strain: $\sigma_{33} = 0$	$\nu = \frac{p}{p+1}$
plane strain: $\sigma_{11} = 0$	$p = \frac{\nu^2}{1-\nu-\nu^2}$

Table 2.1: Conditions on ν and p for incompressibility, for various stress states

2.4 Pointwise stability

The condition of pointwise stability is equivalent to the positive definiteness of the elasticity tensor $\mathbb{C}$, that is,

$$\boldsymbol{\varepsilon} : \mathbb{C}\boldsymbol{\varepsilon} > 0 \quad \text{for any non-zero second order tensor } \boldsymbol{\varepsilon}. \tag{2.47}$$

We write (2.47) in matrix form, that is

$$\underline{\boldsymbol{\varepsilon}}^T \underline{\mathbb{C}}\, \underline{\boldsymbol{\varepsilon}} > 0,$$

in which $\underline{\varepsilon} = (\varepsilon_{11}, \varepsilon_{22}, \varepsilon_{33}, 2\varepsilon_{13}, 2\varepsilon_{23}, 2\varepsilon_{33})^T$ and $\underline{\mathbb{C}}$ is a 6×6 -matrix. Then from (2.10), we have

$$\underline{\mathbb{C}} = \begin{pmatrix} \lambda + 2\mu_t & \lambda & \lambda + \alpha & 0 & 0 & 0 \\ \lambda & \lambda + 2\mu_t & \lambda + \alpha & 0 & 0 & 0 \\ \lambda + \alpha & \lambda + \alpha & \lambda + 2\mu_t + 2\alpha + \beta + 2\gamma & 0 & 0 & 0 \\ 0 & 0 & 0 & \mu_l & 0 & 0 \\ 0 & 0 & 0 & 0 & \mu_l & 0 \\ 0 & 0 & 0 & 0 & 0 & \mu_t \end{pmatrix}.$$

A necessary and sufficient set of conditions for positive definiteness is

$$\mu_t > 0, \quad \mu_l > 0, \tag{2.48}$$

and that the $1 \times 1, 2 \times 2$ and 3×3 upper left subdeterminants are all positive [28]. That is

$$\lambda + 2\mu_t > 0, \tag{2.49a}$$

$$\begin{vmatrix} \lambda + 2\mu_t & \lambda \\ \lambda & \lambda + 2\mu_t \end{vmatrix} > 0, \tag{2.49b}$$

$$\text{and} \quad \begin{vmatrix} \lambda + 2\mu_t & \lambda & \lambda + \alpha \\ \lambda & \lambda + 2\mu_t & \lambda + \alpha \\ \lambda + \alpha & \lambda + \alpha & \lambda + 2\mu_t + 2\alpha + \beta + 2\gamma \end{vmatrix} > 0. \tag{2.49c}$$

From (2.49b),

$$(\lambda + 2\mu_t)^2 - \lambda^2 = 4\mu_t(\lambda + \mu_t) > 0.$$

From (2.49c),

$$\begin{aligned} &(\lambda + 2\mu_t)\big[(\lambda + 2\mu_t)(\lambda + 2\mu_t + 2\alpha + \beta + 2\gamma) - (\lambda + \alpha)^2\big] - \lambda\big[\lambda(\lambda + 2\mu_t + 2\alpha + \beta + 2\gamma) - (\lambda + \alpha)^2\big] \\ &+ (\lambda + \alpha)\big[\lambda(\lambda + \alpha) - (\lambda + \alpha)(\lambda + 2\mu_t)\big] \\ =&4\mu_t\big[(\lambda + \mu_t)(\lambda + 2\mu_t + 2\alpha + \beta + 2\gamma) - (\lambda + \alpha)^2\big] > 0. \end{aligned}$$

Therefore positive definiteness conditions (2.48) and (2.49) maybe rewritten as follows:

$$\mu_t > 0,\ \mu_l > 0, \tag{2.50a}$$

$$\lambda + 2\mu_t > 0, \tag{2.50b}$$

$$\lambda + \mu_t > 0, \tag{2.50c}$$

$$\text{and}\ \ (\lambda + \mu_t)(\lambda + 2\mu_t + 2\alpha + \beta + 2\gamma) - (\lambda + \alpha)^2 > 0. \tag{2.50d}$$

Using the expressions in (2.39), we now rewrite these conditions in terms of the engineering constants.

From condition $(2.50a)_1$, we have

$$\mu_t = \frac{E_t}{2(1+\nu_t)} > 0. \tag{2.51}$$

From condition (2.50d), we have

$$\begin{aligned} &(\lambda + \mu_t)(\lambda + 2\mu_t + 2\alpha + \beta + 2\gamma) - (\lambda + \alpha)^2 = \frac{p^2 E_t^2}{2\big((1-\nu_t)p - 2\nu_l^2\big)} > 0 \\ \Longleftrightarrow &(1-\nu_t)p - 2\nu_l^2 > 0. \end{aligned} \tag{2.52}$$

Condition (2.50b) gives

$$\lambda + 2\mu_t = \frac{(p-\nu_l^2)E_t}{(1+\nu_t)\big((1-\nu_t)p - 2\nu_l^2\big)} > 0.$$

Using (2.51) and (2.52) yield

$$p > \nu_l^2. \tag{2.53}$$

From condition (2.50c), we have

$$\lambda + \mu_t = \frac{pE_t}{2\big((1-\nu_t)p - 2\nu_l^2\big)} > 0 \Rightarrow E_t > 0, \tag{2.54}$$

using (2.52) and (2.53).

Conditions (2.51) and (2.54) then imply

$$\nu_t > -1. \tag{2.55}$$

Conditions (2.52) and (2.53) imply

$$\nu_t < 1. \tag{2.56}$$

We summarize as follows: conditions for pointwise stability are

$$E_t > 0,\ \mu_t > 0,\ \mu_l > 0, \tag{2.57a}$$

$$p > \nu_l^2, \tag{2.57b}$$

$$(1-\nu_t)p - 2\nu_l^2 > 0. \tag{2.57c}$$

We illustrate these conditions with some special cases.

(a) For the case of plane strain with non-zero strains $\varepsilon_{11}, \varepsilon_{33}$ and ε_{13}, we have

$$\underline{\mathbb{C}} = \begin{pmatrix} \lambda + 2\mu_t & \lambda+\alpha & 0 \\ \lambda+\alpha & \lambda + 2\mu_t + 2\alpha + \beta + 2\gamma & 0 \\ 0 & 0 & \mu_l \end{pmatrix}.$$

Therefore necessary and sufficient conditions for pointwise stability are

$$\mu_t > 0,$$

$$\lambda + 2\mu_t > 0,$$

$$\text{and} \begin{vmatrix} \lambda + 2\mu_t & \lambda+\alpha \\ \lambda+\alpha & \lambda + 2\mu_t + 2\alpha + \beta + 2\gamma \end{vmatrix} = (\lambda+2\mu_t)(\lambda+2\mu_t+2\alpha+\beta+2\gamma) - (\lambda+\alpha)^2 > 0.$$

which are (2.50a)$_1$, (2.50b) and (2.52). Hence, conditions (2.57) are valid here.

(b) If we choose $p = 1$, then equation (2.57b) is equivalent to

$$|\nu_l| < 1,$$

and (2.57c) becomes

$$1 - \nu_t > 2\nu_l^2 \iff |\nu_l| < \sqrt{\frac{1-\nu_t}{2}}.$$

Then, for example, for $\nu_t = 0.5$ we have $-0.5 < \nu_l < 0.5$.

(c) Assuming $\nu_l = \nu_t = \nu$, the zones of admissible values of p and ν corresponding to the inequalities (2.57b) and (2.57c) are shown in the cross-hatched areas in Figure 2.2.

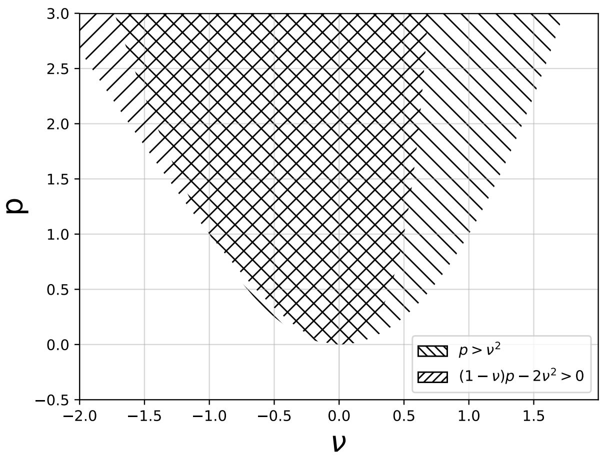

Figure 2.2: Admissible values for p and ν, according to the inequalities (2.57b) and (2.57c)

Remarks

1. From [17], positive definiteness of the compliance matrix is equivalent to

$$E_t > 0, E_l > 0, \mu_l > 0, \tag{2.59a}$$

$$\text{plane stress: } \nu_l^2 < p, \tag{2.59b}$$

$$\text{plane strain: } \nu_l^2 < \frac{1-\nu_t}{2}p. \tag{2.59c}$$

In [28], general conditions for positive definiteness of the compliance matrix are given by

$$E_t > 0, E_l > 0, \mu_t > 0, \mu_l > 0, \tag{2.60a}$$

$$-1 < \nu_t < 1, \tag{2.60b}$$

$$\nu_l^2 < p, \tag{2.60c}$$

$$1 - \frac{2\nu_l^2}{p} > \nu_t. \tag{2.60d}$$

It can be seen that these conditions are equivalent to (2.57).

2. For the special case $\nu_t = \nu_l$ and $p = 1$, we have $\beta + 2\gamma = 0$ and $\alpha = 0$, so that $\lambda + \frac{2}{3}\mu_t > 0$ and $\mu_l \geq \mu_t > 0$ would ensure pointwise stability, provided only that $\operatorname{tr}\boldsymbol{\varepsilon} \neq 0$. This includes the case of isotropy, for which $\mu_l = \mu_t$.

2.5 Strong ellipticity

From [31] the strong ellipticity condition which ensures that the governing differential equations for elastostatics problems are completely elliptic is

$$(\boldsymbol{m} \otimes \boldsymbol{r}) : \mathbb{C}(\boldsymbol{m} \otimes \boldsymbol{r}) > 0,$$

for any real non-zero vectors $\boldsymbol{m}$ and $\boldsymbol{r}$.

Strong ellipticity conditions can be derived from pointwise stability conditions as can be seen by choosing $\boldsymbol{\varepsilon} = \boldsymbol{m} \otimes \boldsymbol{r}$. Thus conditions (2.57) are sufficient conditions for strong ellipticity.

Chapter 3

Standard Galerkin finite element approximations

The conforming Galerkin method is a widely used numerical method for solving differential equations. Well developed mathematical theory, demonstrated robustness, and simplicity of implementation have made it the method of choice for many problems. For the case of linear elasticity, mostly studied for isotropic materials, the method exhibits volumetric locking behaviour when low order elements are used, whereas uniform convergence is obtained for higher order elements [26]. This chapter explores and presents a detailed study of the behaviour of transversely isotropic linear elastic bodies with the use of low order conforming finite elements.

The layout of this chapter is as follows. Conditions for well-posedness of the weak formulation are presented in Section 3.1. For conforming finite element approximations in Section 3.2, an error estimate is established. This standard error estimate reveals the role played by anisotropy in mitigating locking behaviour in the incompressible limit, and it shows the circumstances under which extensional locking may be expected for low-order elements. In Section 3.3, under-integration is proposed as a potential remedy, and its equivalence to respectively mixed and perturbed Lagrangian approaches established.

3.1 Governing equations and weak formulation

3.1.1 Governing equations

Consider a transversely isotropic elastic body occupying a bounded domain $\Omega \subset \mathbb{R}^d, d = \{2, 3\}$, with boundary $\partial\Omega$ having outward unit normal $\boldsymbol{n}$. The boundary is subdivided into a Dirichlet part Γ_D, and a Neumann part Γ_N such that

$$\partial\Omega = \Gamma_D \cup \Gamma_N, \quad \text{and} \quad \Gamma_D \cap \Gamma_N = \emptyset. \tag{3.1}$$

A displacement $\boldsymbol{g} \in [\mathcal{L}^2(\Gamma_D)]^d$ is prescribed on Γ_D, and a surface traction $\boldsymbol{h} \in [\mathcal{L}^2(\Gamma_N)]^d$ on Γ_N. The body is subject to a body force $\boldsymbol{f} \in [\mathcal{L}^2(\Omega)]^d$.

The body satisfies the following set of equations.

Equilibrium:

$$- \operatorname{div} \boldsymbol{\sigma} = \boldsymbol{f}; \tag{3.2}$$

constitutive equation for linear elasticity:

$$\boldsymbol{\sigma} = \mathbb{C}\boldsymbol{\varepsilon}, \tag{3.3}$$

where the elasticity tensor $\mathbb{C}$ is given by (2.9);

the strain-displacement relation

$$\boldsymbol{\varepsilon}(\boldsymbol{u}) := \frac{1}{2}\left(\nabla \boldsymbol{u} + \nabla^T \boldsymbol{u}\right). \tag{3.4}$$

We consider the displacement-based problem obtained by substituting (3.3) and (3.4) in (3.2), with boundary conditions

$$\boldsymbol{u} = \boldsymbol{g} \text{ on } \Gamma_D, \tag{3.5a}$$

$$\boldsymbol{\sigma n} = \boldsymbol{h} \text{ on } \Gamma_N. \tag{3.5b}$$

3.1.2 Weak formulation

We set

$$\mathcal{V} := \{\boldsymbol{u} \in \left[\mathcal{H}^1(\Omega)\right]^d;\ \boldsymbol{u} = \boldsymbol{0} \text{ on } \Gamma_D\}, \tag{3.6}$$

which is endowed with the norm

$$||\cdot||_{\mathcal{V}} = \|\cdot\|_{1,\Omega}.$$

Taking the inner product of (3.2) with a test function $\boldsymbol{v} \in \mathcal{V}$, and integrating by parts, we obtain

$$\int_\Omega \boldsymbol{\sigma}(\boldsymbol{u}) : \boldsymbol{\varepsilon}(\boldsymbol{v})\, dx = \int_{\partial\Omega} \boldsymbol{\sigma}(\boldsymbol{u})\boldsymbol{n} \cdot \boldsymbol{v}\, ds + \int_\Omega \boldsymbol{f} \cdot \boldsymbol{v}\, dx.$$

To take into account the homogeneous boundary condition (3.5a), we define the function $\boldsymbol{u}_g \in [\mathcal{H}^1(\Omega)]^d$ such that $\boldsymbol{u}_g = \boldsymbol{g}$ on Γ_D, and the bilinear form $a(\cdot,\cdot)$ and linear functional $l(\cdot)$ by

$$a : [\mathcal{H}^1(\Omega)]^d \times [\mathcal{H}^1(\Omega)]^d \to \mathbb{R}, \qquad a(\boldsymbol{u}, \boldsymbol{v}) = \int_\Omega \boldsymbol{\sigma}(\boldsymbol{u}) : \boldsymbol{\varepsilon}(\boldsymbol{v})\, dx, \tag{3.7a}$$

$$l : [\mathcal{H}^1(\Omega)]^d \to \mathbb{R}, \qquad l(\boldsymbol{v}) = \int_\Omega \boldsymbol{f} \cdot \boldsymbol{v}\, dx + \int_{\Gamma_N} \boldsymbol{h} \cdot \boldsymbol{v}\, ds - a(\boldsymbol{u}_g, \boldsymbol{v}). \tag{3.7b}$$

The weak form of the problem is then as follows: given $\boldsymbol{f} \in [\mathcal{L}^2(\Omega)]^d$ and $\boldsymbol{h} \in [\mathcal{L}^2(\Gamma_N)]^d$, find $\boldsymbol{U} \in [\mathcal{H}^1(\Omega)]^d$ such that $\boldsymbol{U} = \boldsymbol{u} + \boldsymbol{u}_g, \boldsymbol{u} \in \mathcal{V}$, and

$$a(\boldsymbol{u}, \boldsymbol{v}) = l(\boldsymbol{v}) \qquad \forall \boldsymbol{v} \in \mathcal{V}. \tag{3.8}$$

We write the bilinear form as

$$a(\boldsymbol{u}, \boldsymbol{v}) = a^{iso}(\boldsymbol{u}, \boldsymbol{v}) + a^{ti}(\boldsymbol{u}, \boldsymbol{v}),$$

where, from (2.9),

$$a^{iso}(\boldsymbol{u}, \boldsymbol{v}) = \lambda \int_\Omega (\nabla \cdot \boldsymbol{u})(\nabla \cdot \boldsymbol{v}) \, dx + 2\mu_t \int_\Omega \boldsymbol{\varepsilon}(\boldsymbol{u}) : \boldsymbol{\varepsilon}(\boldsymbol{v}) \, dx, \tag{3.9a}$$

$$\begin{aligned} a^{ti}(\boldsymbol{u}, \boldsymbol{v}) = {} & \alpha \int_\Omega \big((\boldsymbol{M} : \boldsymbol{\varepsilon}(\boldsymbol{u}))(\nabla \cdot \boldsymbol{v}) + (\nabla \cdot \boldsymbol{u})(\boldsymbol{M} : \boldsymbol{\varepsilon}(\boldsymbol{v})) \big) \, dx + \beta \int_\Omega (\boldsymbol{M} : \boldsymbol{\varepsilon}(\boldsymbol{u}))(\boldsymbol{M} : \boldsymbol{\varepsilon}(\boldsymbol{v})) \, dx \\ & + \gamma \int_\Omega \big(\boldsymbol{\varepsilon}(\boldsymbol{u})\boldsymbol{M} : \boldsymbol{\varepsilon}(\boldsymbol{v}) + \boldsymbol{M}\boldsymbol{\varepsilon}(\boldsymbol{u}) : \boldsymbol{\varepsilon}(\boldsymbol{v}) \big) \, dx. \end{aligned} \tag{3.9b}$$

Note that $a^{iso}(\cdot, \cdot)$ and $a^{ti}(\cdot, \cdot)$ are symmetric.

The well-posedness of the weak problem requires the bilinear form to be continuous and coercive, and the linear functional to be continuous.

We assume that the coefficients in the elasticity tensor $\mathbb{C}$ satisfy the conditions (2.57) for pointwise stability.

Continuity. The bilinear form $a(\cdot, \cdot)$ is uniformly continuous if there exists a constant positive C_a such that

$$|a(\boldsymbol{u}, \boldsymbol{v})| \leq C_a ||\boldsymbol{u}||_\mathcal{V} ||\boldsymbol{v}||_\mathcal{V}, \quad \forall \boldsymbol{u}, \boldsymbol{v} \in \mathcal{V}.$$

For any $\boldsymbol{u}, \boldsymbol{v} \in \mathcal{V}$, we have

$$|a(\boldsymbol{u}, \boldsymbol{v})| \leq |a^{iso}(\boldsymbol{u}, \boldsymbol{v})| + |a^{ti}(\boldsymbol{u}, \boldsymbol{v})|.$$

We start with the isotropic part:

$$|a^{iso}(\boldsymbol{u}, \boldsymbol{v})| \leq \left| \lambda \int_\Omega (\nabla \cdot \boldsymbol{u})(\nabla \cdot \boldsymbol{v}) \, dx \right| + 2 \left| \mu_t \int_\Omega \boldsymbol{\varepsilon}(\boldsymbol{u}) : \boldsymbol{\varepsilon}(\boldsymbol{v}) \, dx \right|.$$

We bound each term on the right hand side, using the Cauchy-Schwarz inequality:

$$\begin{aligned} \left| \lambda \int_\Omega (\nabla \cdot \boldsymbol{u})(\nabla \cdot \boldsymbol{v}) \, dx \right| & \leq |\lambda| \|\nabla \cdot \boldsymbol{u}\|_{0,\Omega} \|\nabla \cdot \boldsymbol{v}\|_{0,\Omega} \\ & \leq |\lambda| \|\nabla \boldsymbol{u}\|_{0,\Omega} \|\nabla \boldsymbol{v}\|_{0,\Omega} \\ & \leq |\lambda| ||\boldsymbol{u}||_\mathcal{V} ||\boldsymbol{v}||_\mathcal{V} \end{aligned}$$

and

$$\begin{aligned} 2\mu_t \left| \int_\Omega \boldsymbol{\varepsilon}(\boldsymbol{u}) : \boldsymbol{\varepsilon}(\boldsymbol{v}) \, dx \right| &\leq 2\mu_t \|\boldsymbol{\varepsilon}(\boldsymbol{u})\|_{0,\Omega} \|\boldsymbol{\varepsilon}(\boldsymbol{v})\|_{0,\Omega} \\ &\leq 2\mu_t \|\nabla \boldsymbol{u}\|_{0,\Omega} \|\nabla \boldsymbol{v}\|_{0,\Omega} \\ &\leq 2\mu_t ||\boldsymbol{u}||_{\mathcal{V}} ||\boldsymbol{v}||_{\mathcal{V}}. \end{aligned}$$

Thus

$$|a^{iso}(\boldsymbol{u}, \boldsymbol{v})| \leq \max\left(|\lambda|, 2\mu_t\right) ||\boldsymbol{u}||_{\mathcal{V}} ||\boldsymbol{v}||_{\mathcal{V}}. \tag{3.10}$$

Next, for the transversely isotropic part, we have

$$\begin{aligned} |a^{ti}(\boldsymbol{u}, \boldsymbol{v})| \leq & \left| \alpha \int_\Omega (\boldsymbol{M} : \boldsymbol{\varepsilon}(\boldsymbol{u}))(\nabla \cdot \boldsymbol{v}) \, dx \right| + \left| \alpha \int_\Omega (\nabla \cdot \boldsymbol{u})(\boldsymbol{M} : \boldsymbol{\varepsilon}(\boldsymbol{v})) \, dx \right| + \left| \beta \int_\Omega (\boldsymbol{M} : \boldsymbol{\varepsilon}(\boldsymbol{u}))(\boldsymbol{M} : \boldsymbol{\varepsilon}(\boldsymbol{v})) \, dx \right| \\ & + \left| \gamma \int_\Omega \boldsymbol{\varepsilon}(\boldsymbol{u})\boldsymbol{M} + \boldsymbol{M}\boldsymbol{\varepsilon}(\boldsymbol{u}) : \boldsymbol{\varepsilon}(\boldsymbol{v}) \, dx \right|. \end{aligned}$$

We bound each term on the right-hand side as follows:

$$\begin{aligned} \left| \alpha \int_\Omega (\boldsymbol{M} : \boldsymbol{\varepsilon}(\boldsymbol{u}))(\nabla \cdot \boldsymbol{v}) \, dx \right| &\leq |\alpha| \|\boldsymbol{M} : \boldsymbol{\varepsilon}(\boldsymbol{u})\|_{0,\Omega} \|\nabla \cdot \boldsymbol{v}\|_{0,\Omega} \\ &\leq |\alpha| C_\alpha \|\boldsymbol{\varepsilon}(\boldsymbol{u})\|_{0,\Omega} \|\nabla \cdot \boldsymbol{v}\|_{0,\Omega} \\ &\leq |\alpha| C_\alpha \|\nabla \boldsymbol{u}\|_{0,\Omega} \|\nabla \boldsymbol{v}\|_{0,\Omega} \\ &\leq |\alpha| C_\alpha ||\boldsymbol{u}||_{\mathcal{V}} ||\boldsymbol{v}||_{\mathcal{V}}. \end{aligned}$$

Similarly, we have

$$\begin{aligned} \left| \alpha \int_\Omega (\nabla \cdot \boldsymbol{u})(\boldsymbol{M} : \boldsymbol{\varepsilon}(\boldsymbol{v})) \, dx \right| &\leq |\alpha| \|\nabla \cdot \boldsymbol{u}\|_{0,\Omega} \|\boldsymbol{M} : \boldsymbol{\varepsilon}(\boldsymbol{v})\|_{0,\Omega} \\ &\leq |\alpha| C_\alpha \|\nabla \boldsymbol{u}\|_{0,\Omega} \|\nabla \boldsymbol{v}\|_{0,\Omega} \\ &\leq |\alpha| C_\alpha ||\boldsymbol{u}||_{\mathcal{V}} ||\boldsymbol{v}||_{\mathcal{V}}, \end{aligned}$$

$$\begin{aligned} \left| \beta \int_\Omega (\boldsymbol{M} : \boldsymbol{\varepsilon}(\boldsymbol{u}))(\boldsymbol{M} : \boldsymbol{\varepsilon}(\boldsymbol{v})) \, dx \right| &\leq |\beta| \|\boldsymbol{M} : \boldsymbol{\varepsilon}(\boldsymbol{u})\|_{0,\Omega} \|\boldsymbol{M} : \boldsymbol{\varepsilon}(\boldsymbol{v})\|_{0,\Omega} \\ &\leq |\beta| C_\beta \|\nabla \boldsymbol{u}\|_{0,\Omega} \|\nabla \boldsymbol{v}\|_{0,\Omega} \\ &\leq |\beta| C_\beta ||\boldsymbol{u}||_{\mathcal{V}} ||\boldsymbol{v}||_{\mathcal{V}}, \end{aligned}$$

$$\begin{aligned}\left|\gamma \int_\Omega \boldsymbol{\varepsilon}(\boldsymbol{u})\boldsymbol{M} : \boldsymbol{\varepsilon}(\boldsymbol{v})\, dx\right| &\le |\gamma| \|\boldsymbol{\varepsilon}(\boldsymbol{u})\boldsymbol{M}\|_{0,\Omega} \|\boldsymbol{\varepsilon}(\boldsymbol{v})\|_{0,\Omega} \\ &\le |\gamma| C_\gamma \|\boldsymbol{\varepsilon}(\boldsymbol{u})\|_{0,\Omega} \|\boldsymbol{\varepsilon}(\boldsymbol{v})\|_{0,\Omega} \\ &\le |\gamma| C_\gamma \|\nabla \boldsymbol{u}\|_{0,\Omega} \|\nabla \boldsymbol{v}\|_{0,\Omega} \\ &\le |\gamma| C_\gamma ||\boldsymbol{u}||_{\mathcal{V}} ||\boldsymbol{v}||_{\mathcal{V}},\end{aligned}$$

and finally

$$\left|\gamma \int_\Omega \boldsymbol{M}\boldsymbol{\varepsilon}(\boldsymbol{u}) : \boldsymbol{\varepsilon}(\boldsymbol{v})\, dx\right| \le |\gamma| C_\gamma ||\boldsymbol{u}||_{\mathcal{V}} ||\boldsymbol{v}||_{\mathcal{V}}.$$

Thus,

$$|a^{ti}(\boldsymbol{u}, \boldsymbol{v})| \le C(|\alpha| + |\beta| + |\gamma|) ||\boldsymbol{u}||_{\mathcal{V}} ||\boldsymbol{v}||_{\mathcal{V}}. \tag{3.11}$$

Therefore, from equations (3.10) and (3.11), the bilinear form a is continuous with

$$|a(\boldsymbol{u}, \boldsymbol{v})| \le C_a ||\boldsymbol{u}||_{\mathcal{V}} ||\boldsymbol{v}||_{\mathcal{V}}, \tag{3.12}$$

where

$$C_a = C(\max(|\lambda|, 2\mu_t) + |\alpha| + |\beta| + |\gamma|). \tag{3.13}$$

Next, we have, using the trace theorem,

$$\begin{aligned}|l(\boldsymbol{v})| &\le ||\boldsymbol{f}||_{0,\Omega} ||\boldsymbol{v}||_{0,\Omega} + \|\boldsymbol{h}\|_{0,\Gamma_N} ||\boldsymbol{v}||_{0,\Gamma} + C_a ||\boldsymbol{u}_g||_{\mathcal{V}} ||\boldsymbol{v}||_{\mathcal{V}}, \\ &\le ||\boldsymbol{f}||_{0,\Omega} ||\boldsymbol{v}||_{\mathcal{V}} + C_0 \|\boldsymbol{h}\|_{0,\Gamma_N} ||\boldsymbol{v}||_{\mathcal{V}} + C_a ||\boldsymbol{u}_g||_{\mathcal{V}} ||\boldsymbol{v}||_{\mathcal{V}}, \\ &\le C_l ||\boldsymbol{v}||_{\mathcal{V}}.\end{aligned} \tag{3.14}$$

Coercivity. The bilinear form $a(\cdot, \cdot)$ is coercive on $\mathcal{V}$ if there exists a constant positive K such that

$$a(\boldsymbol{v}, \boldsymbol{v}) \ge K ||\boldsymbol{v}||^2_{\mathcal{V}} \quad \forall \boldsymbol{v} \in \mathcal{V}.$$

Using the matrix notation in Section 2.4, we have

$$\boldsymbol{\sigma}(\boldsymbol{v}) : \boldsymbol{\varepsilon}(\boldsymbol{v}) = \underline{\boldsymbol{\varepsilon}}^T \underline{\mathbb{C}}\, \underline{\boldsymbol{\varepsilon}}.$$

Given that $\underline{\mathbb{C}}$ is symmetric and positive definite, it has a set of six positive eigenvalues $\Lambda_i, 1 \le i \le 6$, and a corresponding set of mutually orthogonal eigenvectors $\boldsymbol{\xi}^i, 1 \le i \le 6$. Thus, $\underline{\mathbb{C}}$ can be written as

$$\underline{\mathbb{C}} = \underline{\mathbb{Q}}^T \underline{\mathbb{D}}\, \underline{\mathbb{Q}}, \tag{3.15}$$

in which $\underline{\mathbb{D}}$ is a diagonal matrix whose diagonal components are the eigenvalues Λ_i, and $\underline{\mathbb{Q}}$ is an orthogonal matrix whose columns are the eigenvectors $\boldsymbol{\xi}^i$; that is,

$$\mathbb{D}_{ij} = \Lambda_i \delta_{ij} \quad \text{and} \quad \mathbb{Q}_{ij} = \xi^i_j. \tag{3.16}$$

For any vector $\underline{\boldsymbol{\varepsilon}}$, we define

$$\underline{\boldsymbol{\eta}} := \underline{\mathbb{Q}}\,\underline{\boldsymbol{\varepsilon}}, \tag{3.17}$$

then

$$\underline{\boldsymbol{\varepsilon}} = \underline{\mathbb{Q}}^T \underline{\boldsymbol{\eta}}. \tag{3.18}$$

Therefore,

$$\begin{aligned}
\underline{\boldsymbol{\varepsilon}}^T \underline{\mathbb{C}}\,\underline{\boldsymbol{\varepsilon}} &= \underline{\boldsymbol{\eta}}^T \underline{\mathbb{Q}}(\underline{\mathbb{Q}}^T \underline{\mathbb{D}}\,\underline{\mathbb{Q}})\underline{\mathbb{Q}}^T \underline{\boldsymbol{\eta}} \\
&= \underline{\boldsymbol{\eta}}^T \underline{\mathbb{D}} \underline{\boldsymbol{\eta}} \\
&= \eta_i \mathbb{D}_{ij} \eta_j \\
&= \sum_{i,j} \eta_i \Lambda_i \delta_{ij} \eta_j \\
&= \sum_i \eta_i^2 \Lambda_i \\
&\geq \Lambda_{min} \sum_i \eta_i^2 \\
&= \Lambda_{min} |\underline{\boldsymbol{\eta}}|^2 \\
&= \Lambda_{min} |\underline{\boldsymbol{\varepsilon}}|^2,
\end{aligned}$$

in which

$$\Lambda_{min} = \min\{\Lambda_i, 1 \leq i \leq 6\}.$$

Hence, we have

$$\begin{aligned}
a(\boldsymbol{v}, \boldsymbol{v}) &= \int_\Omega \boldsymbol{\sigma}(\boldsymbol{v}) : \boldsymbol{\varepsilon}(\boldsymbol{v})\; dx \\
&\geq \Lambda_{min} \int_\Omega |\underline{\boldsymbol{\varepsilon}}(\boldsymbol{v})|^2\; dx \\
&= \Lambda_{min} \|\boldsymbol{\varepsilon}(\boldsymbol{v})\|^2_{0,\Omega} \\
&\geq C\Lambda_{min} ||\boldsymbol{v}||^2_{\mathcal{V}} \qquad \text{(Korn's inequality)}.
\end{aligned}$$

Hence a is coercive with

$$K = C\Lambda_{min}. \tag{3.19}$$

3.1.3 Theorem. *The problem* (3.8) *has a unique solution* $\boldsymbol{u} \in \mathcal{V}$*, which satisfies*

$$||\boldsymbol{u}||_{\mathcal{V}} \leq C, \qquad \textit{where} \quad C = \frac{C_l}{K},$$

where C_l *and* K *are defined by* (3.14) *and* (3.19)*, respectively.*

3.2 Conforming finite element approximations

Suppose that Ω is polygonal (in $\mathbb{R}^2$) or polyhedral (in $\mathbb{R}^3$), and partitioned into a shape-regular mesh comprising n_e disjoint subdomains Ω_e with boundary $\partial\Omega_e$ and outward unit normal $\boldsymbol{n}_e$. Denote by $\mathcal{T}_h := \{\Omega_e\}_e$ the set of all elements.

We define the discrete space $\mathcal{V}^h \subset \mathcal{V}$ by

$$\mathcal{V}^h = \{\boldsymbol{v}_h \in \mathcal{V} \cap \mathcal{C}(\bar{\Omega}) \mid \boldsymbol{v}_h|_{\Omega_e} \in [\mathcal{R}_1(\Omega_e)]^d, \boldsymbol{v}_h = 0 \text{ on } \Gamma_D\}. \tag{3.20}$$

Here $\mathcal{R}_1(\Omega_e) = \mathcal{P}_1(\Omega_e)$ or $\mathcal{Q}_1(\Omega_e)$, where $\mathcal{P}_1(\Omega_e)$ is the space of polynomials on Ω_e of maximum total degree 1, and $\mathcal{Q}_1(\Omega_e)$ is the space of polynomials on Ω_e of degree 1 in each component.

The discrete problem corresponding to conforming approximations is as follows: find $\boldsymbol{u}_h \in \mathcal{V}^h$ that satisfies

$$a(\boldsymbol{u}_h, \boldsymbol{v}_h) = l(\boldsymbol{v}_h) \qquad \forall \boldsymbol{v}_h \in \mathcal{V}^h. \tag{3.21}$$

Since the bilinear form $a(\cdot,\cdot)$ is continuous and coercive and the linear functional $l(\cdot)$ is continuous, from standard finite element convergence theory [11] we have

$$||\boldsymbol{u} - \boldsymbol{u}_h||_{\mathcal{V}} \leq C_1 h, \tag{3.22}$$

in which, using (3.12) and (3.19), the constant C_1 is given by

$$C_1 = \frac{C(\max(|\lambda|, 2\mu_t) + |\alpha| + |\beta| + |\gamma|)}{\Lambda_{min}}. \tag{3.23}$$

For the special case of an isotropic material, with α, β and γ all equal to zero, one obtains the well-known λ-dependent bound, with $\lambda \to \infty$ in the incompressible limit.

From (2.39), all three parameters λ, α, and β have the same denominator $\mathscr{D} := (1+\nu_t)((1-\nu_t)p - 2\nu_l^2)$. Fixing $\nu_l = \nu_t = \nu$ and $q = 1$ for example, we have

$$\mathscr{D}(p, \nu) = (1+\nu)((1-\nu)p - 2\nu^2), \tag{3.24}$$

which becomes unbounded as

$$p \to \frac{2\nu^2}{1-\nu}.$$

The limit $p = 1$ corresponds to the case of isotropy, with the well-known limiting value $\nu = 1/2$, for which λ becomes unbounded, while $\alpha = \beta = 0$. For anisotropic materials, though, for which $p > 1$, it is seen from (3.23) and (3.24) that the constant C_1 in the error bound (3.22) is bounded, so that in principle one has uniform convergence. This is illustrated in Figure 3.1, which shows the behaviour of C_1 as a function of p, for near-incompressibility. This issue will be explored later numerically, in Chapter 4.

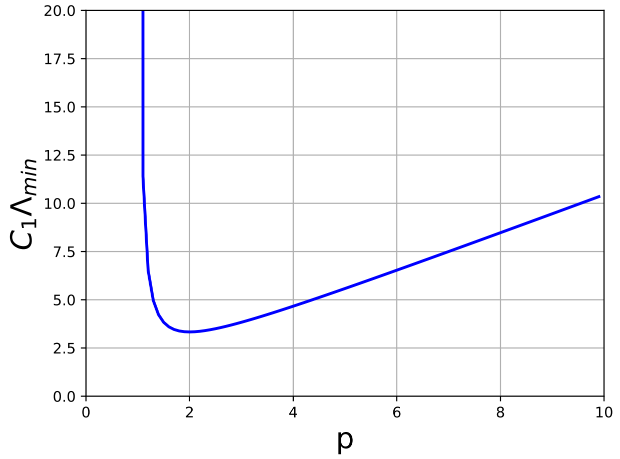

Figure 3.1: The error bound constant C_1 in (3.23) against p, with $\nu_l = \nu_t = 0.49995$ and $q = 1$

3.3 Under-integration

Anticipating locking in particular circumstances, we may address this by under-integrating (i.e. using one-point integration) the terms involving volumetric and extensional deformation. Throughout this section, we consider only the case where $\mathcal{R}_1(\Omega_e) = \mathcal{Q}_1(\Omega_e)$ in the discrete space defined by (3.20).

Let $\bar{\boldsymbol{x}}$ be the integration point and $\bar{\omega}$ the corresponding weight on element Ω_e. Here $\bar{\boldsymbol{x}}$ is the centroidal coordinate and the weight $\bar{\omega}$ is the measure $|\Omega_e|$ of the element.

Under-integration of the volumetric term

$$\lambda \int_{\Omega_e} (\nabla \cdot \boldsymbol{u}_h)(\nabla \cdot \boldsymbol{v}_h)\, dx$$

entails replacing it with

$$\lambda(\nabla \cdot \boldsymbol{u}_h(\bar{\boldsymbol{x}}))(\nabla \cdot \boldsymbol{v}_h(\bar{\boldsymbol{x}}))\bar{\omega}. \tag{3.25}$$

From (2.39), we see that α is bounded as $p \to \infty$ (the inextensional limit), while $\beta \to \infty$ as $p \to \infty$. Thus, it is likely that extensional locking may occur with $\mathcal{Q}_1$ elements. As a potential remedy, we will replace the extensional term

$$\beta \int_{\Omega_e} (\boldsymbol{M} : \boldsymbol{\varepsilon}(\boldsymbol{u}_h))(\boldsymbol{M} : \boldsymbol{\varepsilon}(\boldsymbol{v}_h))\, dx$$

with

$$\beta\Big(\boldsymbol{M} : \boldsymbol{\varepsilon}(\boldsymbol{u}_h(\bar{\boldsymbol{x}}))\Big)\Big(\boldsymbol{M} : \boldsymbol{\varepsilon}(\boldsymbol{v}_h(\bar{\boldsymbol{x}}))\Big)\bar{\omega}. \tag{3.26}$$

One can easily show that one-point integration is equivalent to projection of the integrand onto the space of constants. If we define by Π_0 the $\mathcal{L}^2$-orthogonal projection onto constants, then under-integrating the volumetric term, as in (3.25), is the same as replacing it with

$$\lambda \int_{\Omega_e} \Pi_0(\nabla \cdot \boldsymbol{u}_h)\Pi_0(\nabla \cdot \boldsymbol{v}_h)\, dx. \tag{3.27}$$

Similarly, (3.26) is equivalent to

$$\beta \int_{\Omega_e} \Pi_0(\boldsymbol{M} : \boldsymbol{\varepsilon}(\boldsymbol{u}_h))\Pi_0(\boldsymbol{M} : \boldsymbol{\varepsilon}(\boldsymbol{v}_h))\, dx = \beta\, |\Omega_e|\, \Pi_0(\boldsymbol{M} : \boldsymbol{\varepsilon}(\boldsymbol{u}_h))\Pi_0(\boldsymbol{M} : \boldsymbol{\varepsilon}(\boldsymbol{v}_h)). \tag{3.28}$$

Defining the bilinear form $\bar{a}$ by

$$\begin{aligned}
\bar{a}(\boldsymbol{u}, \boldsymbol{v}) =& \lambda \sum_{\Omega_e \in \mathcal{T}_h} \int_{\Omega_e} (\nabla \cdot \boldsymbol{u})(\nabla \cdot \boldsymbol{v})\, dx + 2\mu_t \sum_{\Omega_e \in \mathcal{T}_h} \int_{\Omega_e} \boldsymbol{\varepsilon}(\boldsymbol{u}) : \boldsymbol{\varepsilon}(\boldsymbol{v})\, dx \\
&+ \alpha \sum_{\Omega_e \in \mathcal{T}_h} \int_{\Omega_e} \big((\boldsymbol{M} : \boldsymbol{\varepsilon}(\boldsymbol{u}))(\nabla \cdot \boldsymbol{v}) + (\nabla \cdot \boldsymbol{u})(\boldsymbol{M} : \boldsymbol{\varepsilon}(\boldsymbol{v}))\big)\, dx \\
&+ \beta \sum_{\Omega_e \in \mathcal{T}_h} \Big(\boldsymbol{M} : \boldsymbol{\varepsilon}(\boldsymbol{u}_h(\bar{\boldsymbol{x}}))\Big)\Big(\boldsymbol{M} : \boldsymbol{\varepsilon}(\boldsymbol{v}_h(\bar{\boldsymbol{x}}))\Big)\bar{\omega} \\
&+ \gamma \sum_{\Omega_e \in \mathcal{T}_h} \int_{\Omega_e} \big(\boldsymbol{\varepsilon}(\boldsymbol{u})\boldsymbol{M} : \boldsymbol{\varepsilon}(\boldsymbol{v}) + \boldsymbol{M}\boldsymbol{\varepsilon}(\boldsymbol{u}) : \boldsymbol{\varepsilon}(\boldsymbol{v})\big)\, dx,
\end{aligned}$$

the formulation with under-integration of the term involving β is given by

$$\begin{aligned}
\bar{a}(\boldsymbol{u}, \boldsymbol{v}) =& \lambda \sum_{\Omega_e \in \mathcal{T}_h} \int_{\Omega_e} (\nabla \cdot \boldsymbol{u})(\nabla \cdot \boldsymbol{v})\, dx + 2\mu_t \sum_{\Omega_e \in \mathcal{T}_h} \int_{\Omega_e} \boldsymbol{\varepsilon}(\boldsymbol{u}) : \boldsymbol{\varepsilon}(\boldsymbol{v})\, dx \\
&+ \alpha \sum_{\Omega_e \in \mathcal{T}_h} \int_{\Omega_e} \big((\boldsymbol{M} : \boldsymbol{\varepsilon}(\boldsymbol{u}))(\nabla \cdot \boldsymbol{v}) + (\nabla \cdot \boldsymbol{u})(\boldsymbol{M} : \boldsymbol{\varepsilon}(\boldsymbol{v}))\big)\, dx \\
&+ \beta \sum_{\Omega_e \in \mathcal{T}_h} |\Omega_e|\, \Pi_0(\boldsymbol{M} : \boldsymbol{\varepsilon}(\boldsymbol{u}))\Pi_0(\boldsymbol{M} : \boldsymbol{\varepsilon}(\boldsymbol{v})) \\
&+ \gamma \sum_{\Omega_e \in \mathcal{T}_h} \int_{\Omega_e} \big(\boldsymbol{\varepsilon}(\boldsymbol{u})\boldsymbol{M} : \boldsymbol{\varepsilon}(\boldsymbol{v}) + \boldsymbol{M}\boldsymbol{\varepsilon}(\boldsymbol{u}) : \boldsymbol{\varepsilon}(\boldsymbol{v})\big)\, dx,
\end{aligned} \tag{3.29}$$

The under-integrated formulation will be explored numerically in Chapter 4.

3.3.1 Equivalence with perturbed Lagrangian formulation

In [4, 10], a perturbed Lagrangian formulation is proposed as a locking free method for the isotropic linear elastic problem reinforced by a single family of inextensible fibres. The approach takes as a starting point a strain energy of the form

$$W(\boldsymbol{\varepsilon}, T, \beta) = W^{\mathrm{iso}}(\boldsymbol{\varepsilon}) + W^{\mathrm{f}}(\boldsymbol{\varepsilon}, T, \rho) \tag{3.30}$$

in which the isotropic strain energy is

$$W^{\mathrm{iso}}(\boldsymbol{\varepsilon}) = \frac{1}{2}\lambda(\mathrm{tr}\,\boldsymbol{\varepsilon})^2 + \mu_t \mathrm{tr}\,(\boldsymbol{\varepsilon}^2)$$

and the strain energy corresponding to the fibres is

$$W^{\mathrm{f}}(\boldsymbol{\varepsilon}, T, \rho) = T(\boldsymbol{M} : \boldsymbol{\varepsilon}) - \frac{1}{2\rho}T^2.$$

Here ρ is the a penalty parameter, and T is the Lagrange multiplier.

The stress is obtained from

$$\begin{aligned}\boldsymbol{\sigma} &= \frac{\partial W}{\partial \boldsymbol{\varepsilon}} \\ &= \lambda\,\mathrm{tr}\,\boldsymbol{\varepsilon} + 2\mu_t\,\boldsymbol{\varepsilon} + T\boldsymbol{M}.\end{aligned} \tag{3.31}$$

In addition we have the condition

$$\frac{\partial W}{\partial T} = 0,$$

so that

$$\boldsymbol{M} : \boldsymbol{\varepsilon} - \frac{T}{\rho} = 0, \tag{3.32}$$

or

$$T = \rho(\boldsymbol{M} : \boldsymbol{\varepsilon}).$$

We assume that $\alpha = \gamma = 0$ in this section. For $T \in \mathcal{L}^2(\Omega)$, where β plays the role of a penalty parameter, the extensional term in the weak formulation (see (3.9b)) is

$$a^{\mathrm{ti}}(T, \boldsymbol{v}) = \int_\Omega T(\boldsymbol{M} : \boldsymbol{\varepsilon}(\boldsymbol{v}))\,dx. \tag{3.33}$$

With a test function $\vartheta \in \mathcal{L}^2(\Omega)$, we can write the weak form of (3.32) as

$$\int_\Omega \vartheta\Big(T - \beta(\boldsymbol{M} : \boldsymbol{\varepsilon}(\boldsymbol{u}))\Big)\,dx = 0.$$

The corresponding discrete form with $\boldsymbol{u}_h \in [\mathcal{Q}_1(\Omega_e)]^d$ and T_h, $\vartheta_h \in \mathcal{P}_0(\Omega_e)$ at element level is

$$\int_{\Omega_e} \vartheta_h \big(T_h - \beta(\boldsymbol{M} : \boldsymbol{\varepsilon}(\boldsymbol{u}_h))\big)\, dx = 0.$$

Since $\vartheta_h \in \mathcal{P}_0(\Omega_e)$, we have

$$\int_{\Omega_e} \big(T_h - \beta(\boldsymbol{M} : \boldsymbol{\varepsilon}(\boldsymbol{u}_h))\big)\, dx = 0.$$

Since T_h is piecewise constant, we have

$$T_h \int_{\Omega_e} dx = \beta \int_{\Omega_e} (\boldsymbol{M} : \boldsymbol{\varepsilon}(\boldsymbol{u}_h))\, dx,$$

or

$$T_h = \frac{\beta}{|\Omega_e|} \int_{\Omega_e} (\boldsymbol{M} : \boldsymbol{\varepsilon}(\boldsymbol{u}_h))\, dx.$$

We substitute in the discrete form of (3.33) to obtain

$$\begin{aligned}
\int_{\Omega} T_h(\boldsymbol{M} : \boldsymbol{\varepsilon}(\boldsymbol{v}_h))\, dx &= \sum_{\Omega_e \in \mathcal{T}_h} \frac{\beta}{|\Omega_e|} \left(\int_{\Omega_e} \boldsymbol{M} : \boldsymbol{\varepsilon}(\boldsymbol{u}_h)\, dx \right) \left(\int_{\Omega_e} \boldsymbol{M} : \boldsymbol{\varepsilon}(\boldsymbol{v}_h)\, dx \right) \\
&= \sum_{\Omega_e \in \mathcal{T}_h} \frac{\beta}{|\Omega_e|} \left(\int_{\Omega_e} \Pi_0(\boldsymbol{M} : \boldsymbol{\varepsilon}(\boldsymbol{u}_h))\, dx \right) \left(\int_{\Omega_e} \Pi_0(\boldsymbol{M} : \boldsymbol{\varepsilon}(\boldsymbol{v}_h))\, dx \right) \\
&= \sum_{\Omega_e \in \mathcal{T}_h} \frac{\beta}{|\Omega_e|} \left(\int_{\Omega_e} dx \right) \left(\int_{\Omega_e} \Pi_0(\boldsymbol{M} : \boldsymbol{\varepsilon}(\boldsymbol{u}_h)) \Pi_0(\boldsymbol{M} : \boldsymbol{\varepsilon}(\boldsymbol{v}_h))\, dx \right) \\
&= \sum_{\Omega_e \in \mathcal{T}_h} \beta \int_{\Omega_e} \Pi_0(\boldsymbol{M} : \boldsymbol{\varepsilon}(\boldsymbol{u}_h)) \Pi_0(\boldsymbol{M} : \boldsymbol{\varepsilon}(\boldsymbol{v}_h))\, dx, \qquad (3.34)
\end{aligned}$$

Using the fact that $\boldsymbol{M} : \boldsymbol{\varepsilon}(\boldsymbol{u}_h) \in \mathcal{P}_1(\Omega_e)$, and is integrated exactly using one-point quadrature, the expression (3.34) is therefore the same as (3.28), so that the perturbed Lagrangian approximation is equivalent to under-integration of the extensional term.

3.4 An equivalent mixed finite element method

Here we show that the under-integrated formulation in Section 3.3 is also equivalent to a mixed displacement-tension $(\boldsymbol{u}, t)$ finite element formulation. This is analogous to the well-known displacement-pressure or $\mathcal{Q}_1 - \mathcal{P}_0$ formulation for incompressibility. We focus here on near-inextensibility.

3.4.1 Governing equations and weak formulation

Returning to (2.9), we write the elasticity relation in the form

$$\boldsymbol{\sigma} = -t\boldsymbol{M} + \hat{\boldsymbol{\sigma}},$$

where

$$t = -\beta \nabla \cdot \boldsymbol{M}\boldsymbol{u},$$

and

$$\hat{\boldsymbol{\sigma}}(\boldsymbol{u}) = \lambda(\operatorname{tr}\boldsymbol{\varepsilon}(\boldsymbol{u}))\boldsymbol{I} + 2\mu_t\boldsymbol{\varepsilon}(\boldsymbol{u}) + \alpha\big((\nabla\cdot\boldsymbol{M}\boldsymbol{u})\boldsymbol{I} + (\operatorname{tr}\boldsymbol{\varepsilon}(\boldsymbol{u}))\boldsymbol{M}\big) + \gamma\big(\boldsymbol{\varepsilon}(\boldsymbol{u})\boldsymbol{M} + \boldsymbol{M}\boldsymbol{\varepsilon}(\boldsymbol{u})\big).$$

We note that

$$\boldsymbol{M} : \boldsymbol{\varepsilon}(\boldsymbol{u}) = \nabla\cdot\boldsymbol{M}\boldsymbol{u}.$$

The governing equations are now

$$-\operatorname{div}\hat{\boldsymbol{\sigma}}(\boldsymbol{u}) + \operatorname{div}(t\boldsymbol{M}) = \boldsymbol{f}, \tag{3.35a}$$

$$t = -\beta\nabla\cdot\boldsymbol{M}\boldsymbol{u}. \tag{3.35b}$$

For convenience, we assume an homogeneous Dirichlet boundary condition:

$$\boldsymbol{u} = 0 \quad \text{on} \quad \partial\Omega. \tag{3.36}$$

Taking the inner product of the equilibrium equation (3.35a) with a sufficiently smooth function $\boldsymbol{v}$, such that $\boldsymbol{v}|_{\partial\Omega} = 0$, and integrating by parts, we obtain

$$a'(\boldsymbol{u},\boldsymbol{v}) + b'(\boldsymbol{v},t) = l_f(\boldsymbol{v}),$$

where $a'(\cdot,\cdot)$ and $b'(\cdot,\cdot)$ are defined respectively by

$$\begin{aligned} a'(\boldsymbol{u},\boldsymbol{v}) &:= \lambda\int_\Omega(\nabla\cdot\boldsymbol{u})(\nabla\cdot\boldsymbol{v})\,dx + 2\mu_t\int_\Omega\boldsymbol{\varepsilon}(\boldsymbol{u}):\boldsymbol{\varepsilon}(\boldsymbol{v})\,dx + \alpha\int_\Omega\Big((\nabla\cdot\boldsymbol{M}\boldsymbol{u})(\nabla\cdot\boldsymbol{v}) + (\nabla\cdot\boldsymbol{u})(\nabla\cdot\boldsymbol{M}\boldsymbol{v})\Big)\,dx \\ &\quad + \gamma\int_\Omega\Big(\boldsymbol{\varepsilon}(\boldsymbol{u})\boldsymbol{M}:\boldsymbol{\varepsilon}(\boldsymbol{v}) + \boldsymbol{M}\boldsymbol{\varepsilon}(\boldsymbol{u}):\boldsymbol{\varepsilon}(\boldsymbol{v})\Big)\,dx, \qquad (3.37) \\ b'(\boldsymbol{v},t) &:= -\int_\Omega(\nabla\cdot\boldsymbol{M}\boldsymbol{v})t\,dx, \qquad (3.38) \end{aligned}$$

and $l_f(\cdot)$ is the linear functional defined by

$$l_f(\boldsymbol{v}) := \int_\Omega\boldsymbol{f}\cdot\boldsymbol{v}\,dx. \tag{3.39}$$

Similarly, multiplying equation (3.35b) with a sufficiently smooth function q and integrating over Ω, we obtain

$$-c'(t,q) + b'(\boldsymbol{u},q) = 0,$$

where the bilinear functional $c'(\cdot,\cdot)$ is defined by

$$c'(t,q) := \frac{1}{\beta}\int_\Omega tq\,dx. \tag{3.40}$$

We define the function spaces

$$\mathcal{X} := \left[\mathcal{H}_0^1(\Omega)\right]^2, \quad \text{with norm } \|\cdot\|_{\mathcal{X}} = |\cdot|_{1,\Omega},$$

and

$$\mathcal{M} := \mathcal{L}_0^2(\Omega) = \left\{q \in \mathcal{L}^2(\Omega) : \int_\Omega q\,dx = 0\right\}, \quad \text{with norm } \|\cdot\|_{\mathcal{M}} = \|\cdot\|_{0,\Omega}.$$

The weak formulation of the problem is then as follows: find a pair of functions $(\boldsymbol{u}, t) \in \mathcal{X} \times \mathcal{M}$ such that

$$a'(\boldsymbol{u},\boldsymbol{v}) + b'(\boldsymbol{v},t) = l_f(\boldsymbol{v}) \quad \forall \boldsymbol{v} \in \mathcal{X}, \tag{3.41a}$$

$$-c'(t,q) + b'(\boldsymbol{u},q) = 0 \qquad \forall q \in \mathcal{M}. \tag{3.41b}$$

The weak formulation (3.41) is clearly equivalent to (3.8), making allowances for the differences in boundary conditions.

To obtain the corresponding discrete problem of (3.41), we suppose that $\mathcal{X}_h \subset \mathcal{X}$ and $\mathcal{M}_h \subset \mathcal{M}$ are finite dimensional linear subspaces of the Hilbert spaces $\mathcal{X}$ and $\mathcal{M}$, respectively, and defined as follows:

$$\mathcal{X}_h := \left\{\boldsymbol{v}_h \in \mathcal{X} : \boldsymbol{v}_h|_{\Omega_e} \in [\mathcal{Q}_1(\Omega_e)]^2 \quad \forall \Omega_e \in \mathcal{T}_h,\ \boldsymbol{v}_h|_{\partial\Omega} = \boldsymbol{0}\right\},$$

$$\mathcal{M}_h := \{q_h \in \mathcal{M} : q_h|_{\Omega_e} \in \mathcal{P}_0(\Omega_e) \quad \forall \Omega_e \in \mathcal{T}_h\}.$$

Consider the following approximation of the problem (3.41): find $(\boldsymbol{u}_h, t_h) \in \mathcal{X}_h \times \mathcal{M}_h$ such that

$$a'(\boldsymbol{u}_h,\boldsymbol{v}_h) + b'(\boldsymbol{v}_h,t_h) = l_f(\boldsymbol{v}_h) \quad \forall \boldsymbol{v}_h \in \mathcal{X}_h, \tag{3.42a}$$

$$-c'(t_h,q_h) + b'(\boldsymbol{u}_h,q_h) = 0 \qquad \forall q_h \in \mathcal{M}_h. \tag{3.42b}$$

From (3.42b), we have at element level

$$\begin{aligned}
&-\frac{1}{\beta}\int_{\Omega_e} t_h q_h\,dx - \int_{\Omega_e} (\nabla\cdot \boldsymbol{M}\boldsymbol{u}_h) q_h\,dx = 0,\\
\Rightarrow &\int_{\Omega_e} \left(\frac{1}{\beta}t_h + \nabla\cdot \boldsymbol{M}\boldsymbol{u}_h\right) q_h = 0,\\
\Rightarrow &\int_{\Omega_e} \frac{1}{\beta}t_h + \nabla\cdot \boldsymbol{M}\boldsymbol{u}_h = 0,\\
\Rightarrow & t_h \frac{|\Omega_e|}{\beta} = -\int_{\Omega_e} \nabla\cdot \boldsymbol{M}\boldsymbol{u}_h\,dx.
\end{aligned}$$

Thus, the discrete tension is given by

$$t_h = -\frac{\beta}{|\Omega_e|} \int_{\Omega_e} \nabla \cdot \boldsymbol{M}\boldsymbol{u}_h \, dx. \tag{3.43}$$

We substitute into the discrete form $b'(\boldsymbol{v}_h, t_h)$ to obtain

$$\begin{aligned}
b'(\boldsymbol{v}_h, t_h) &= -\sum_{\Omega_e \in \mathcal{T}_h} \left(\int_{\Omega_e} \nabla \cdot \boldsymbol{M}\boldsymbol{v}_h \, dx \right) \left(-\frac{\beta}{|\Omega_e|} \int_{\Omega_e} \nabla \cdot \boldsymbol{M}\boldsymbol{u}_h \, dx \right) \\
&= \sum_{\Omega_e \in \mathcal{T}_h} \frac{\beta}{|\Omega_e|} \left(\int_{\Omega_e} \nabla \cdot \boldsymbol{M}\boldsymbol{v}_h \, dx \right) \left(\int_{\Omega_e} \nabla \cdot \boldsymbol{M}\boldsymbol{u}_h \, dx \right) \\
&= \sum_{\Omega_e \in \mathcal{T}_h} \frac{\beta}{|\Omega_e|} \left(\int_{\Omega_e} \Pi_0(\nabla \cdot \boldsymbol{M}\boldsymbol{v}_h) \, dx \right) \left(\int_{\Omega_e} \Pi_0(\nabla \cdot \boldsymbol{M}\boldsymbol{u}_h) \, dx \right) \\
&= \sum_{\Omega_e \in \mathcal{T}_h} \beta \int_{\Omega_e} \Pi_0(\nabla \cdot \boldsymbol{M}\boldsymbol{v}_h) \Pi_0(\nabla \cdot \boldsymbol{M}\boldsymbol{u}_h) \, dx \\
&= \sum_{\Omega_e \in \mathcal{T}_h} \beta |\Omega_e| \Pi_0(\nabla \cdot \boldsymbol{M}\boldsymbol{v}_h) \Pi_0(\nabla \cdot \boldsymbol{M}\boldsymbol{u}_h)
\end{aligned}$$

which is the same as (3.28). The third line is obtained by recognizing that $\nabla \cdot \boldsymbol{M}\boldsymbol{v}_h$ is linear on the element, so that the integral is integrated exactly using one-point integration.

Comparing with (3.30), we see that the mixed formulation (3.42) is equivalent to the selectively under-integrated formulation.

Chapter 4

Numerical tests

In this chapter, we present a series of results to illustrate the various features discussed in the previous chapters. For material parameters that satisfy the pointwise conditions (2.57), we first investigate the behaviour of compressible and nearly incompressible materials with reference to Table 2.1. Next, we explore the behaviour of nearly inextensible materials.

Two model problems are presented: Cook's membrane and bending of a beam.

4.1 Material parameters

All examples are under conditions of plane strain and based on four- and nine-noded quadrilateral elements with standard bilinear and biquadratic interpolation of the displacement field. We set $\nu_l = \nu_t = \nu$ and $\gamma = 0$, and choose values of ν and p that satisfy the conditions (2.57) for pointwise stability (see also Figure 2.2).

As summarized earlier in Table 2.1, for general states of stress in plane strain, incompressible behaviour occurs only for the case $p = 1$ and $\nu = 1/2$. To investigate the behaviour at near-incompressibility, we choose $\nu = 0.49995$. For conditions (2.57b) and (2.57c) to be satisfied, we will require $p \geq 1$ for this case.

We are also interested in the behaviour for values of $p < 1$ and which satisfy (2.57). For this purpose, we select two values of ν, viz. -0.5 and $+0.3$, and in accordance with (2.57), consider values of p in the following ranges:

$$\nu = 0.3 \;\Rightarrow\; p > (0.3)^2 = 0.09 \quad \text{and} \quad p > \frac{2(0.3)^2}{1-0.3} \simeq 0.257,$$

$$\nu = -0.5 \;\Rightarrow\; p > (-0.5)^2 = 0.25 \quad \text{and} \quad p > \frac{2(-0.5)^2}{1+0.5} \simeq 0.333.$$

Define $\hat{a} := (\widehat{Ox, \boldsymbol{a}})$, the angle between the x-axis and the fibre direction $\boldsymbol{a}$. For each problem, the following range of values for $\hat{a}$, also illustrated in Figure 4.1, will be considered:

$$\hat{a} = \left\{0, \frac{\pi}{8}, \frac{\pi}{6}, \frac{\pi}{4}, \frac{\pi}{3}, \frac{3\pi}{8}, \frac{\pi}{2}, \frac{5\pi}{8}, \frac{3\pi}{4}, \frac{7\pi}{8}, \pi\right\}.$$

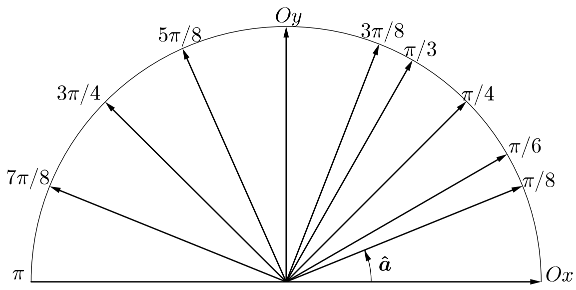

Figure 4.1: Fibre directions at different angles

The results in the examples that follow are for the following element choices:

Exact	The analytical solution
Q_1_CG	The standard displacement formulation of order 1
Q_2_CG	The standard displacement formulation of order 2
$Q_1\_CG\_UI_\lambda$	The standard displacement formulation with under-integration of the volumetric (λ-) term
$Q_1\_CG\_UI_\beta$	The standard displacement formulation with under-integration of the extensional (β-) term
$Q_1\_CG\_UI_{\beta\lambda}$	The standard displacement formulation with under-integration of the volumetric and the extensional terms

The diameter of an element Ω_e is defined by $h := \text{diam}\{\Omega_e\}$.

4.2 Cook's membrane

The Cook's membrane test consists of a tapered panel fixed along one edge and subject to a shearing load at the opposite edge as depicted in Figure 4.2. The applied load is $f = 100$ and $E_t = 250$. This test problem has no analytical solution. A mesh of 32 elements per side is used. The vertical tip displacement at corner C is measured. To investigate locking of the proposed formulations, we compare the results with those obtained using the standard Q_2-element.

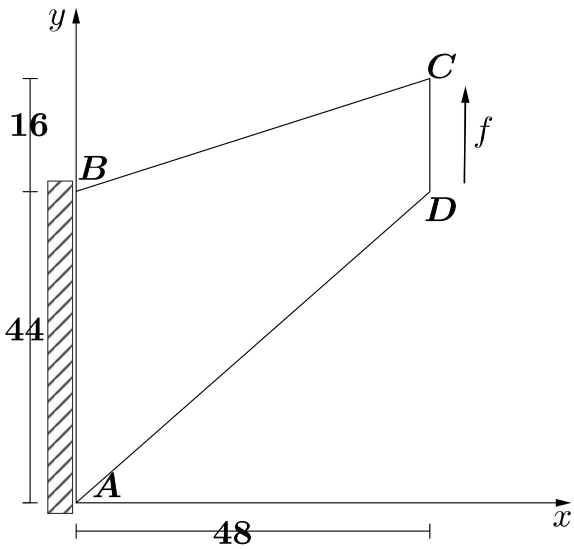

Figure 4.2: Cook's membrane geometry and boundary conditions

Figures 4.3 and 4.4 show semilog plots of the tip displacement vs p for various fibre directions for $\nu = 0.3$ and $\nu = -0.5$ respectively. For small values of p, $(0.35 \leq p \leq 3)$ as shown in the left figures, the conforming method Q_1_CG is uniformly convergent. For high values of p, $(4 \leq p \leq 10^7)$, as shown in the right figures, the conforming Q_1_CG shows locking behaviour, which is avoided when the extensional term is under-integrated $(Q_1\_CG\_UI_\beta)$. Also shown are curves for the standard Q_2-element, which appears to exhibit locking at higher values of p, for particular fibre angles.

Figure 4.5 shows semilog plots of the tip displacement vs p for various fibre directions, and for the various element choices. For moderate values of p $(1 \leq p \leq 5)$, the Q_1_CG formulation behaves well away from $p = 1$, with evidence of locking behaviour as $p \to 1$. This corresponds to the well-known volumetric locking, which is avoided when the volumetric term is under-integrated $(Q_1\_CG\_UI_\lambda)$. Notice that for $Q_1\_CG\_UI_\beta$ there is still locking, as the locking is purely volumetric. For higher values of p $(10 \leq p \leq 10^5)$, the Q_1_CG method shows locking behaviour as p gets bigger, and convergent behaviour is seen with $Q_1\_CG\_UI_\beta$. Notice that under-integrating only the volumetric term $(Q_1\_CG\_UI_\lambda)$ has no effect since the locking is purely extensional. $Q_1\_CG\_UI_{\beta\lambda}$ shows locking-free behaviour everywhere.

Figure 4.6 shows tip displacements for various fibre orientations, where the degree of anisotropy is fixed at $p = 10^5$ (top) and $p = 10^7$ (bottom). Note the poor performance of Q_2_CG. Similar behaviour is reported in [34]. Whether this indicates mild locking would depend on further parameter-explicit analysis, which is currently absent for the transversely isotropic problem at near-inextensibility.

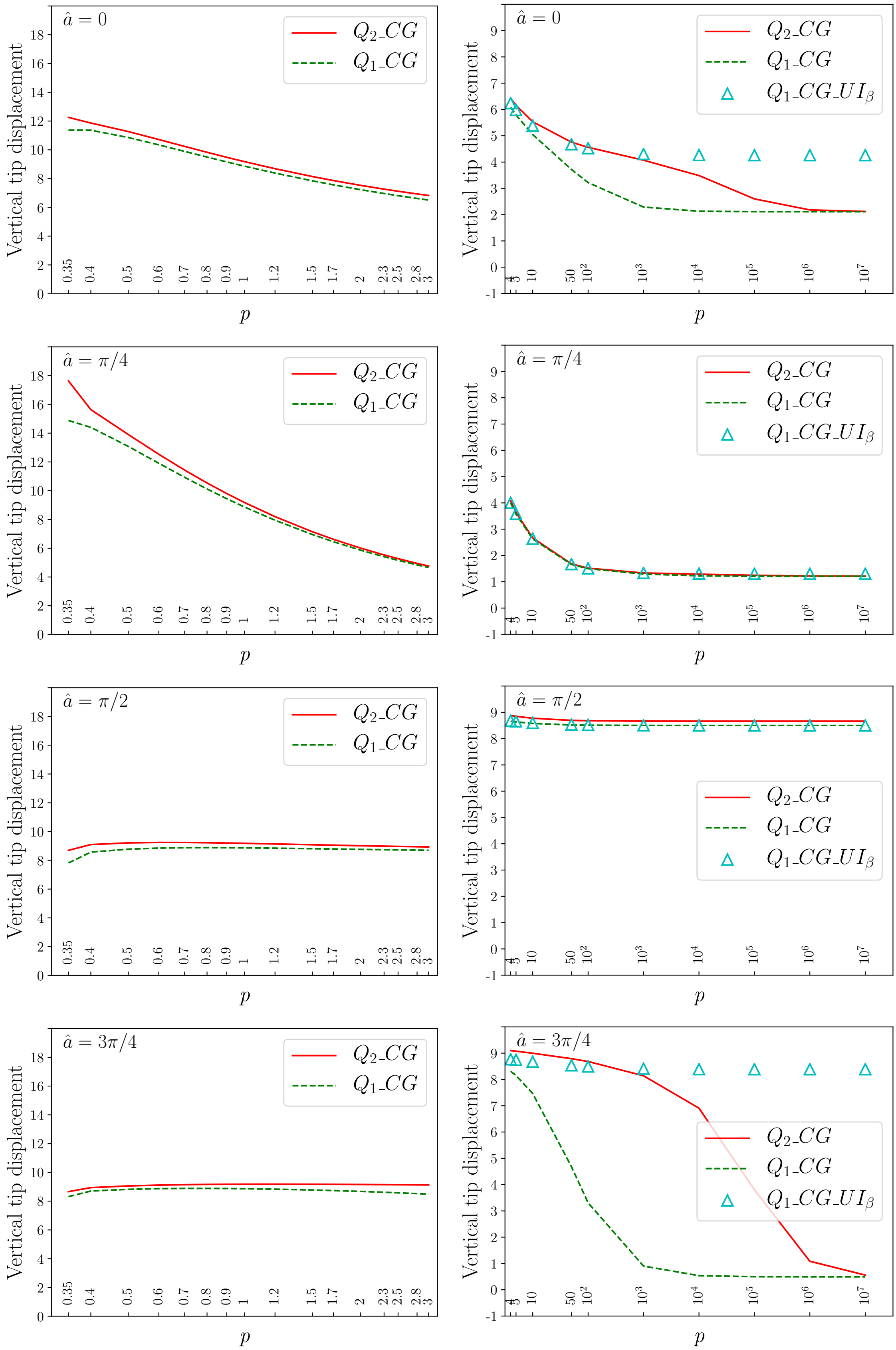

Figure 4.3: Tip displacement vs p for the Cook's membrane problem, with $\nu = 0.3$

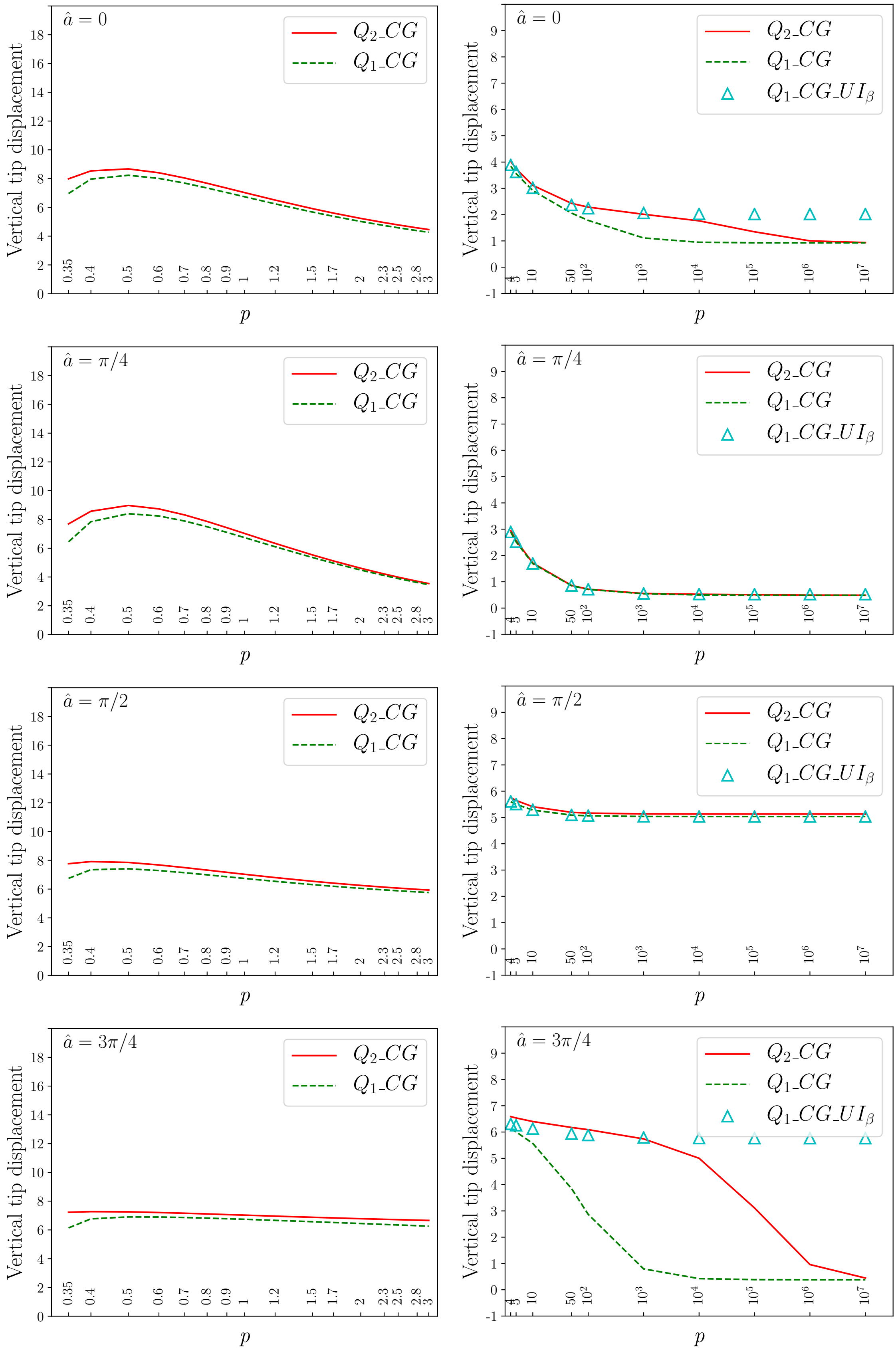

Figure 4.4: Tip displacement vs p for the Cook's membrane problem, with $\nu = -0.5$

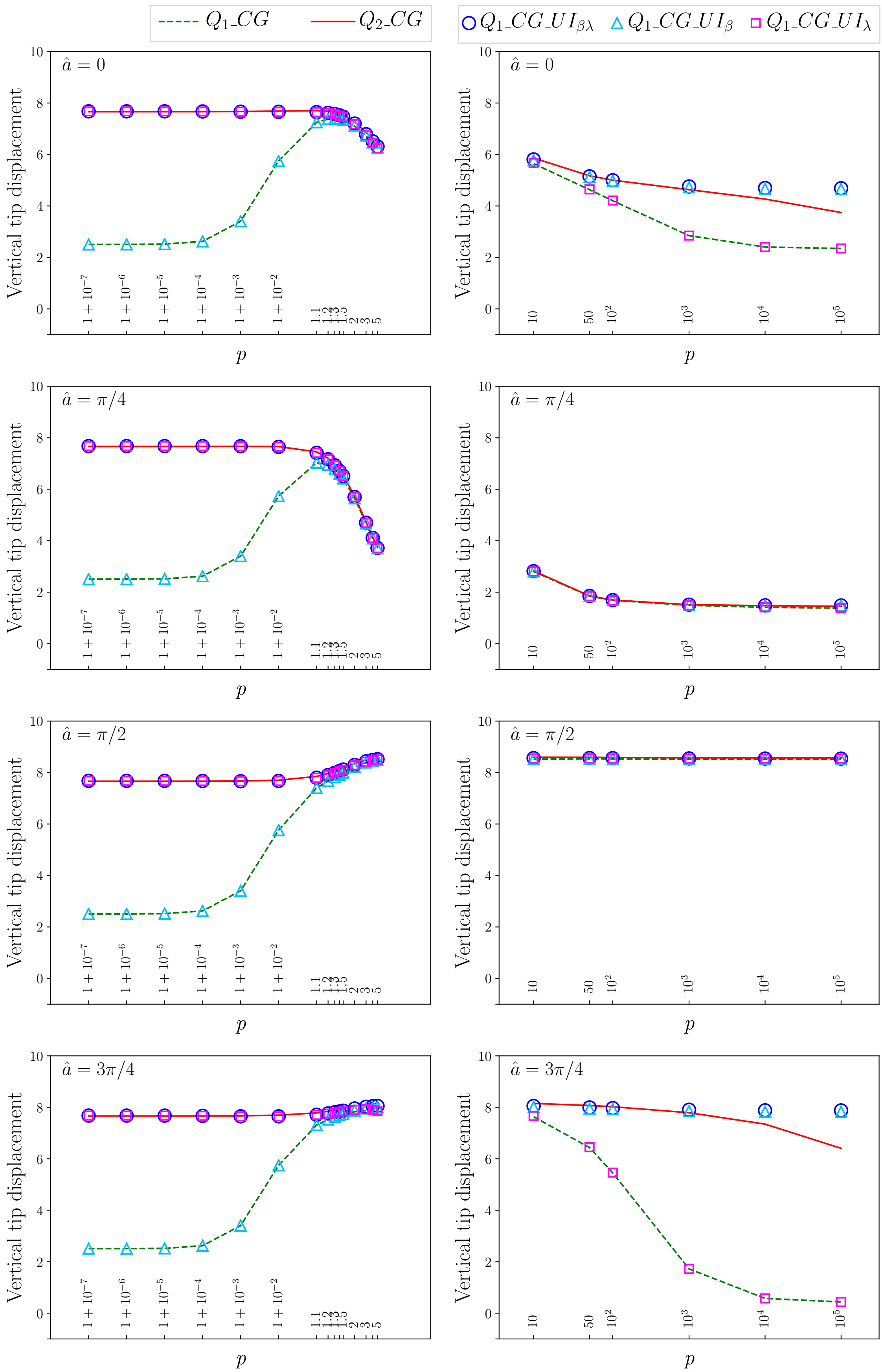

Figure 4.5: Tip displacement vs p for the Cook's membrane problem. Moderate (left) and high values of p (right), with $\nu = 0.49995$

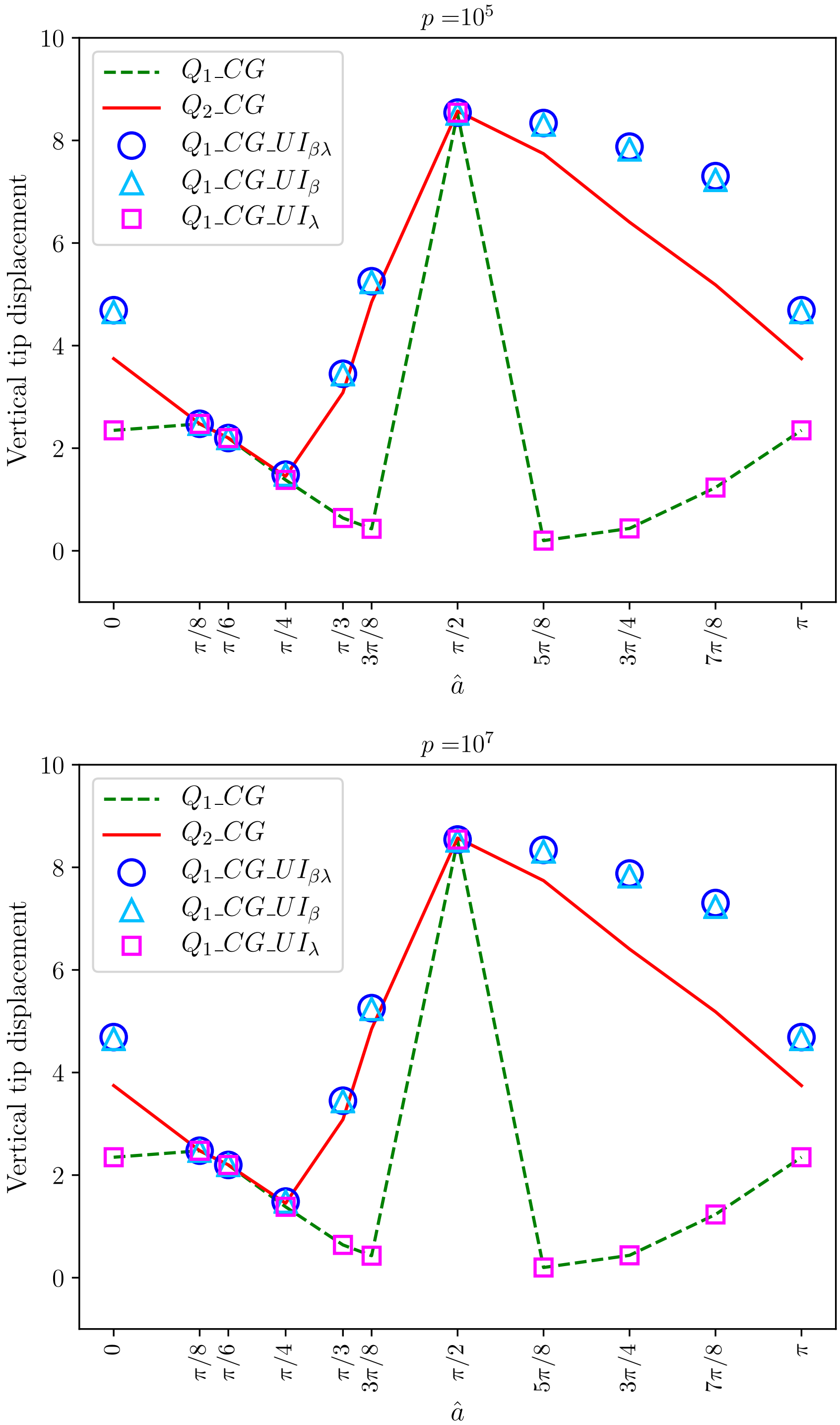

Figure 4.6: Tip displacement for Cook's membrane problem measured at different fibre orientations, for $p = 10^5$ (top) and for $p = 10^7$ (bottom), with $\nu = 0.49995$

4.3 Bending of a beam

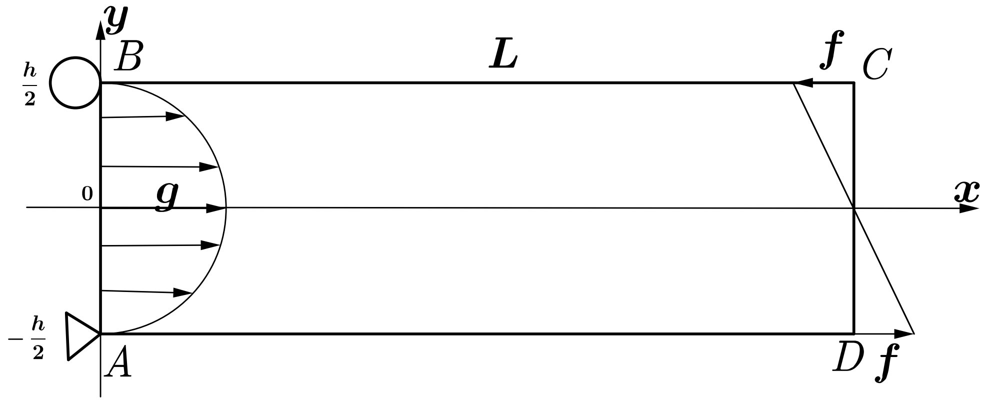

Figure 4.7: Beam geometry and boundary conditions

We consider the beam shown in Figure 4.7, subject to a linearly varying load along the edge CD. The horizontal displacement $\boldsymbol{u}$ is constrained at node B, while the node A is constrained in both directions. The beam has length $L = 10$ and height $h = 2$ and the applied load has a maximum value $f = 3000$. Here, $E_t = 1500$. The boundary conditions are

$$\begin{cases} u(0, y) = g(y), \\ v(0, -\frac{h}{2}) = 0, \end{cases}$$

where

$$g(y) = -\frac{f}{h}\mathbb{S}_{31}\left(y^2 - \frac{h^2}{4}\right).$$

The compliance coefficients $\mathbb{S}_{ij}$ are given in Appendix A. The analytical solution is

$$\begin{cases} u(x, y) = & -\frac{2f}{h}\left(\mathbb{S}_{11}xy + \frac{1}{2}\mathbb{S}_{31}\left(y^2 - \frac{h^2}{4}\right)\right), \\ v(x, y) = & -\frac{f}{h}\left(\mathbb{S}_{21}\left(y^2 - \frac{h^2}{4}\right) - \mathbb{S}_{11}x^2\right). \end{cases}$$

The linearly varying load $\hat{f}$ with maximum f is

$$\hat{f}(y) = -\frac{2f}{h}y.$$

A mesh of 80×16 elements is used, and the vertical displacement at corner C is measured. Locking behaviour is investigated by comparison with the analytical solution.

Figures 4.8 and 4.9 show semilog plots of the tip displacement vs p for various directions fibre for $\nu = 0.3$

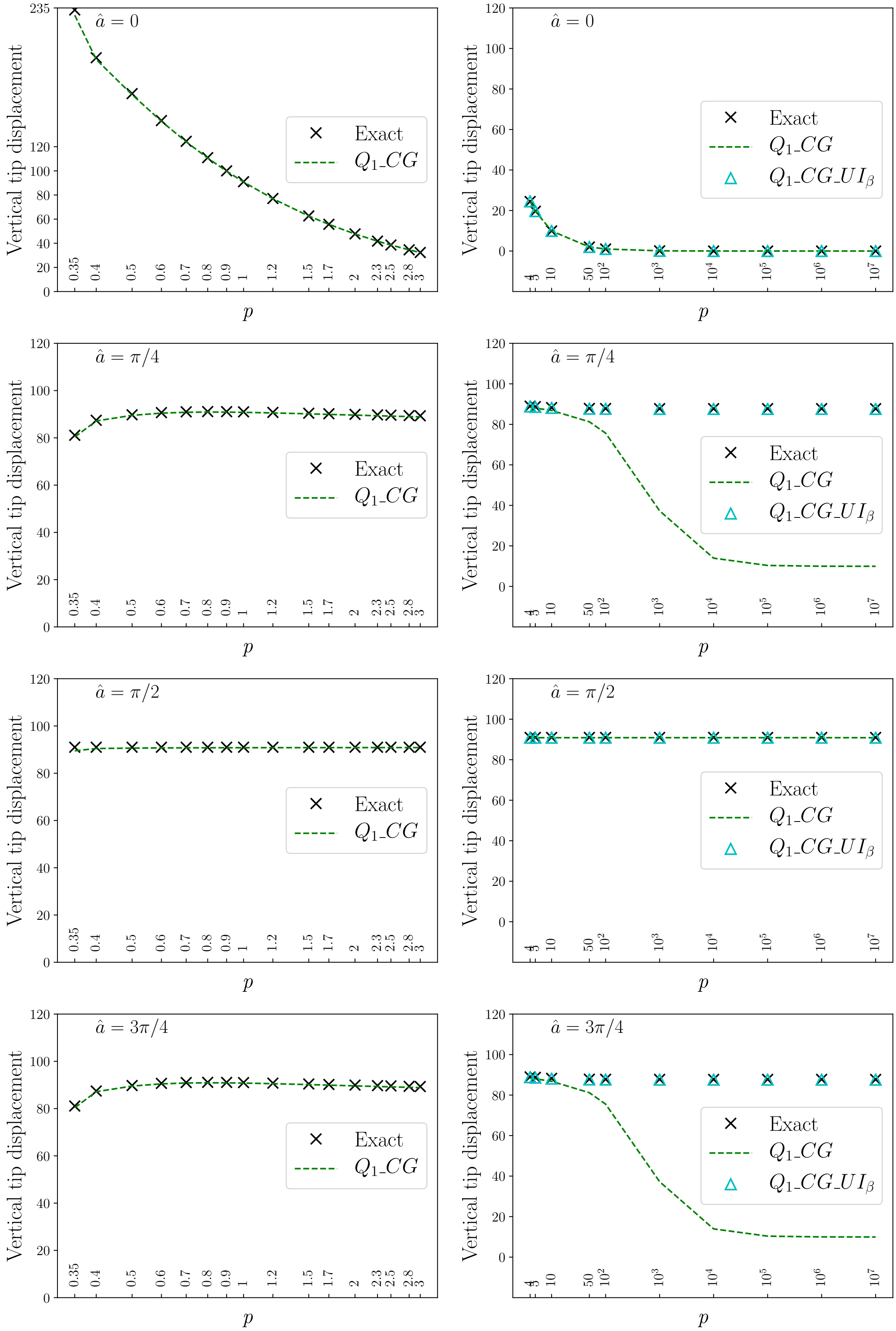

Figure 4.8: Tip displacement vs p for the beam problem, with $\nu = 0.3$

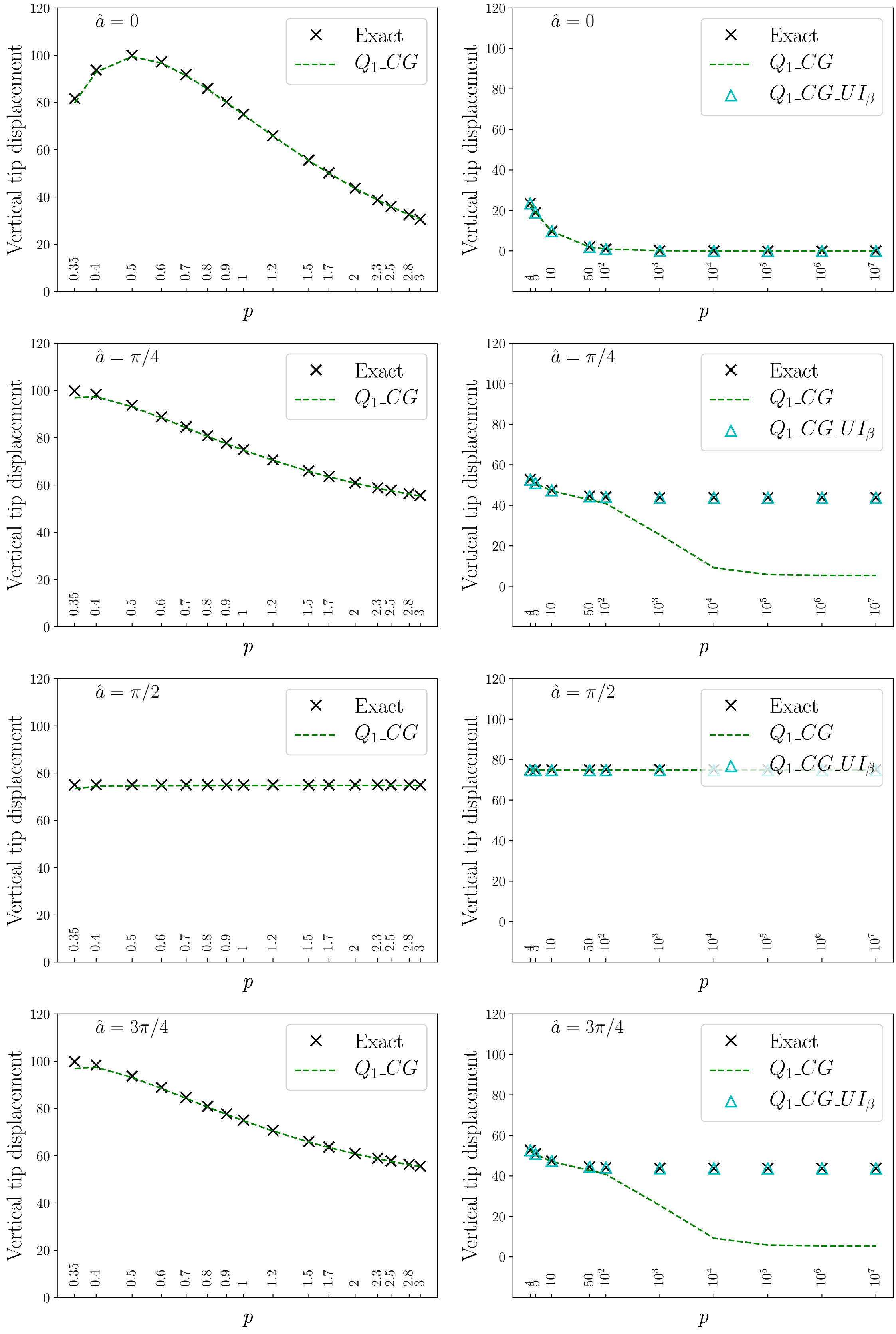

Figure 4.9: Tip displacement vs p for the beam problem, with $\nu = -0.5$

and $\nu = -0.5$ respectively. For small values of p, $(0.35 \leq p \leq 3)$ as shown in the left figures, the conforming method Q_1_CG is convergent. For high values of p, $(4 \leq p \leq 10^7)$, as shown in the right figures, the conforming Q_1_CG shows locking behaviour which is avoided when the extensional term is under-integrated $(Q_1\_CG\_UI_\beta)$.

In Figure 4.10, which shows semilog plots of tip displacement for different values of p, with various fibre direction. The same behaviour as appears for the Cook's example is seen, i.e. for moderate values of p away from $p = 1$ (approximately, $1 < p \leq 5$), there is locking-free behaviour with $Q_1\_CG\_UI_\lambda$ (left figures). For high values of p, purely extensional locking with Q_1_CG is overcome by using $Q_1\_CG\_UI_\beta$ (right figures). $Q_1\_CG\_UI_{\beta\lambda}$ shows locking-free behaviour for any value of p.

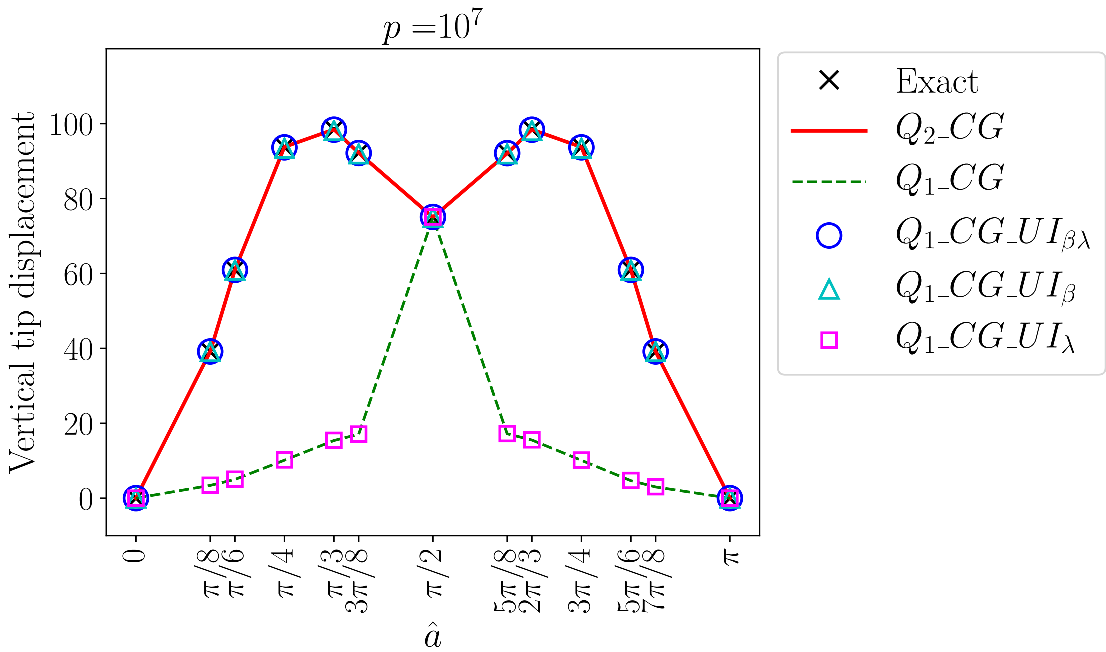

Figure 4.11: Tip displacement for the beam problem measured at different fibre orientations, for $p = 10^7$ and $\nu = 0.49995$

Figure 4.11 shows tip displacements for various fibre orientations where the degree of anisotropy is fixed at $p = 10^7$. Extensional locking of Q_1_CG is observed except for the angles 0 and $\pi/2$. For the angle $\pi/2$ no locking is observed. This can be accounted for by two factors: first, with this orientation the property of near-inextensibility in the vertical direction has a negligible effect on the bending-dominated deformation; and secondly, as previously discussed, the presence of anisotropy serves to circumvent volumetric locking.

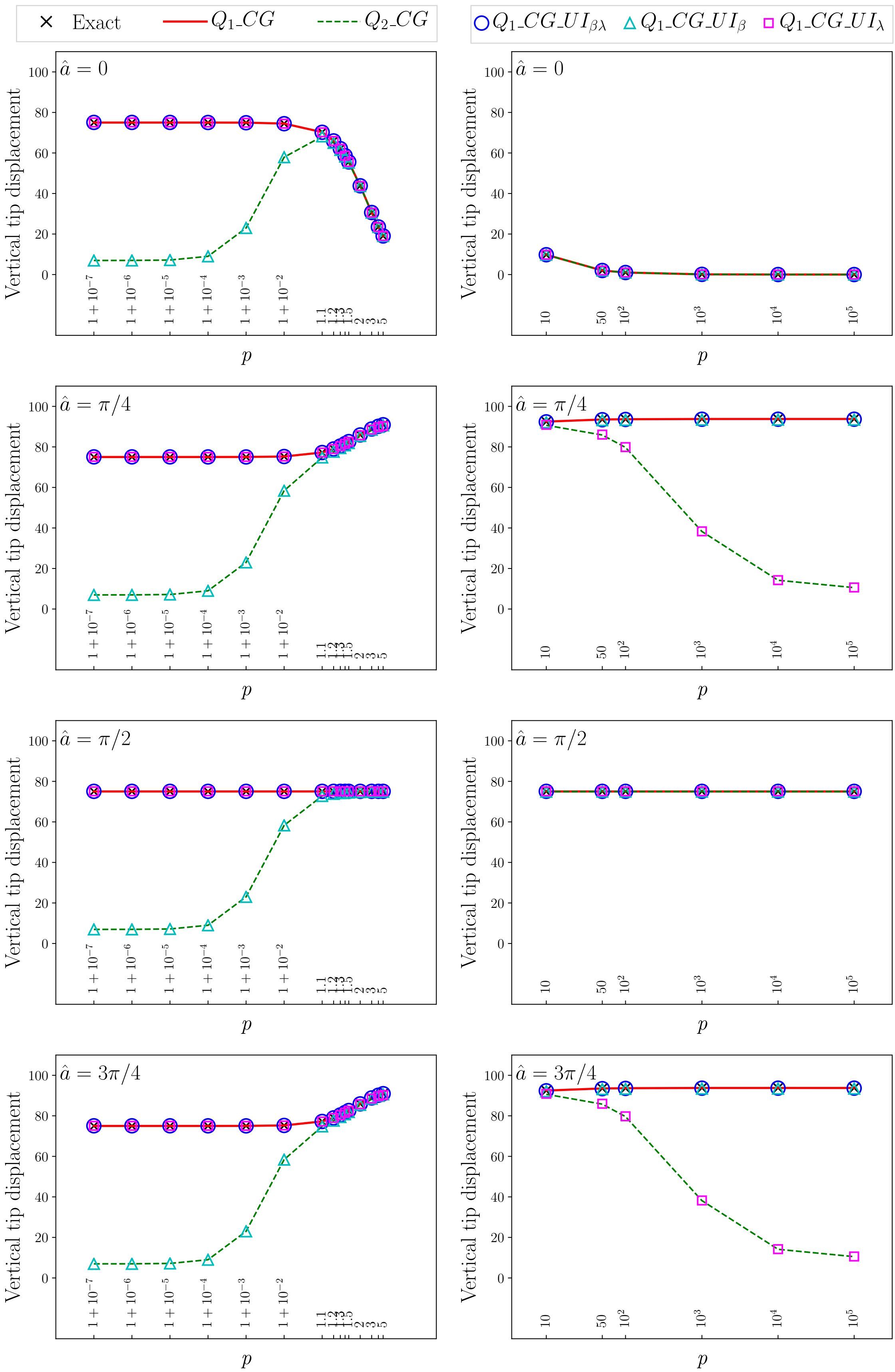

Figure 4.10: Tip displacement vs p for the beam problem. Moderate (left) and high (right), with $\nu = 0.49995$

The following set of results, Figures 4.12-4.13, show convergence plots of $\mathcal{H}^1$-relative error for the fibre orientations considered, and for values of $p = 1.0001$ (left figures), 3 (middle figures) and 10^4 (right figures). The $\mathcal{H}^1$-relative error is defined by

$$e_{\text{relative}} := \frac{\|\boldsymbol{u} - \boldsymbol{u}_h\|_{1,\Omega}}{\|\boldsymbol{u}\|_{1,\Omega}}. \tag{4.1}$$

For $p = 1.0001$, left figures, $Q_1\_CG\_UI_\lambda$ and $Q_1\_CG\_UI_{\beta\lambda}$ show optimal convergence for any fibre direction at the superlinear rate 1.83.

For $p = 3$, middle figures, all formulations at any fibre direction are superlinearly convergent at rate 1.7.

For $p = 10^4$, right figures, optimal convergence at the rate 1.86 for $Q_1\_CG\_UI_\beta$ and $Q_1\_CG\_UI_{\beta\lambda}$, and poor convergence for Q_1_CG and $Q_1\_CG\_UI_\lambda$ are shown. When the fibre direction is at an angle $\pi/2$, the error plots show convergence at the superlinear rate 1.64 for Q_1_CG.

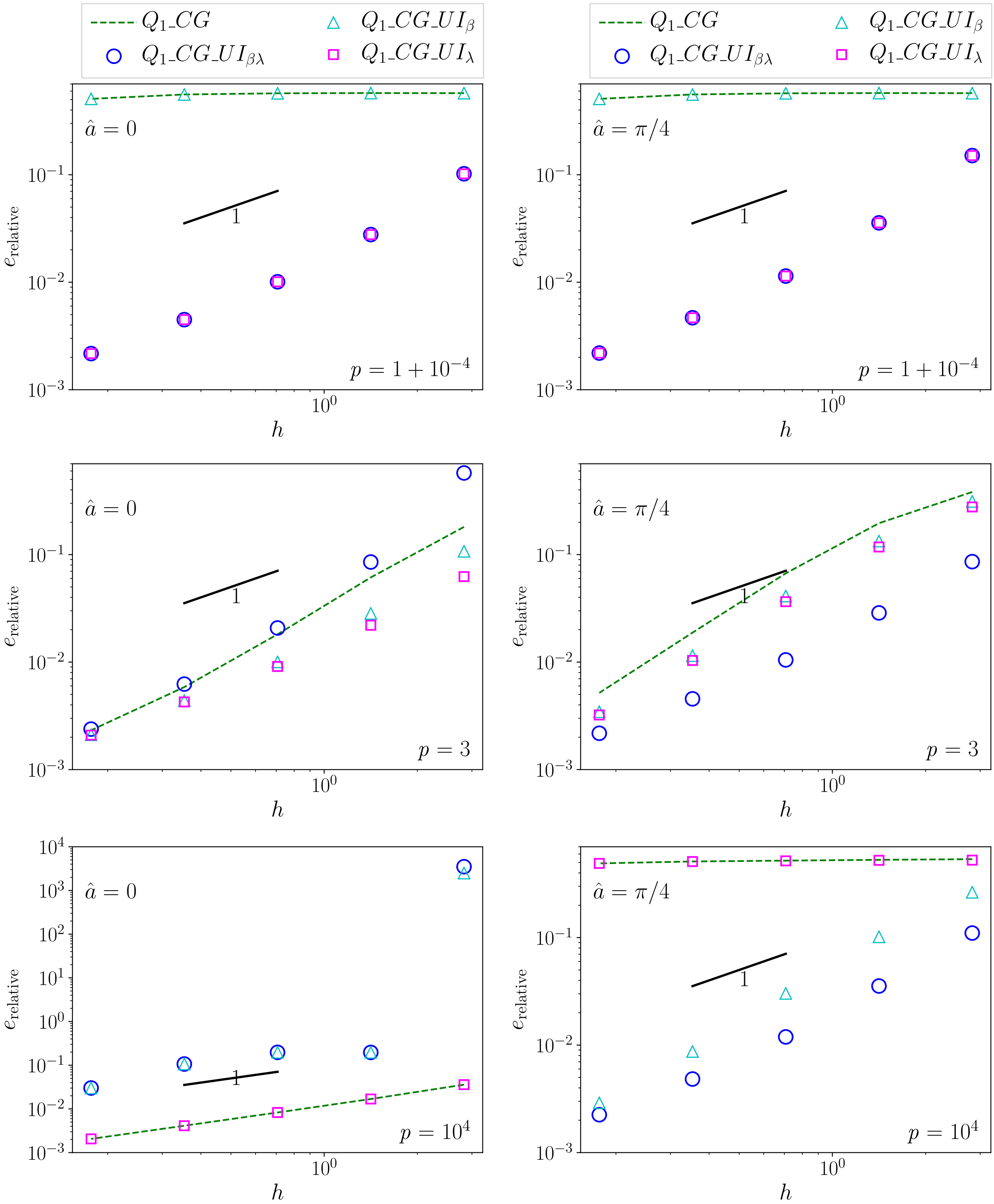

Figure 4.12: Comparison of relative $\mathcal{H}^1$-errors for conforming and under-integrated elements on quadrilaterals, for fibres at angle 0 (left) and $\pi/4$ (right), with $\nu = 0.49995$. For $p = 1.0001$ (top), $p = 3$ (middle) and $p = 10^4$(bottom)

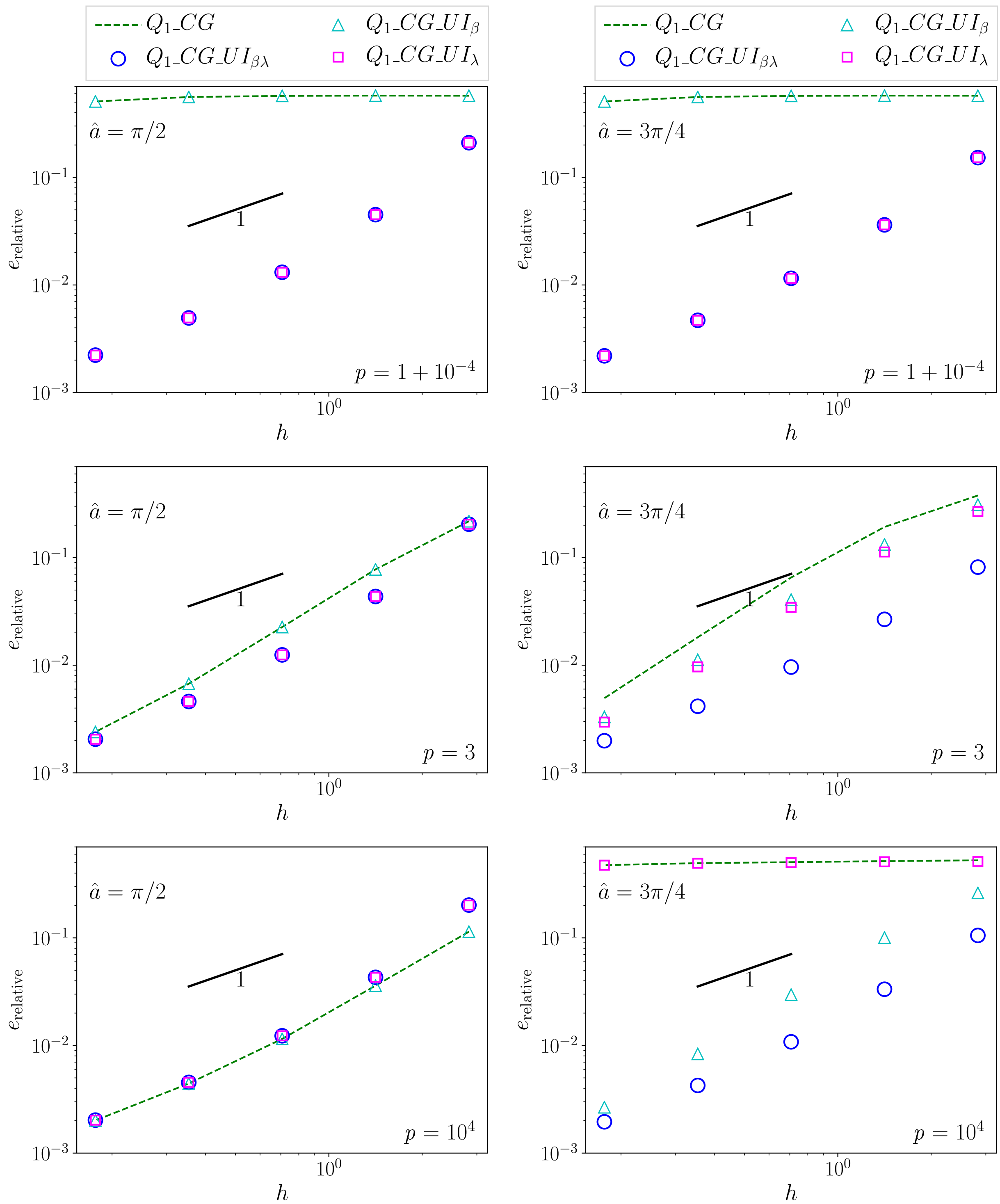

Figure 4.13: Comparison of relative $\mathcal{H}^1$-errors for conforming and under-integrated elements on quadrilaterals, for fibres at angle $\pi/2$ (left) and $3\pi/4$ (right), with $\nu = 0.49995$. For $p = 1.0001$ (top), $p = 3$ (middle) and $p = 10^4$(bottom)

Chapter 5

Discontinuous Galerkin methods

In this chapter, we investigate the use of interior penalty discontinuous Galerkin (IPDG) formulations for transversely isotropic linear elasticity. The objective is to construct discontinuous Galerkin (DG) formulations that are uniformly convergent in the incompressible and inextensible limits. The study focuses on the use of low order triangles, though much of the analysis is valid in two and three dimensions.

The outline of this chapter is as follows. In Section 5.1, various notations and the DG space are presented. The DG formulations are introduced in Section 5.2, their well-posedness established, and an a priori error bound derived. The likelihood of extensional locking is deduced from the error estimate, and an alternative formulation, based on selective under-integration, is introduced and analyzed in Section 5.3. The resulting error bound has a structure similar to that for the bound corresponding to isotropic elasticity, suggesting the locking-free behaviour of this formulation.

5.1 Notation

Discretization. The domain Ω is partitioned into a triangular/tetrahedral conforming mesh, comprising N_e disjoint subdomains Ω_e. The boundary $\partial\Omega_e$ of each element consists of edges/faces E, with outward unit normal $\boldsymbol{n}_e$. The set of all elements is denoted by $\mathcal{T}_h := \{\Omega_e\}_e$, $e \in \{1, \ldots, N_e\}$.

We define the following diameters:

$$h_E := \operatorname{diam}(E), \quad h_e := \operatorname{diam}(\Omega_e), \quad \text{and} \quad h := \max_{\Omega_e \in \mathcal{T}_h} \{h_e\},$$

and boundaries on edges or sets of edges:

Γ_D	the set of all Dirichlet boundary edges
Γ_N	the set of all Neumann boundary edges
Γ_i	the set of all interior boundary edges
Γ_{iD}	the union of all interior edges and all Dirichlet boundary edges
Γ	the union of all interior edges, all Dirichlet boundary edges, and all Neumann boundary edges
$\partial\Omega_e^i$	the set of all interior edges of a given element Ω_e
$\partial\Omega_e^D$	the set of all Dirichlet boundary edges of a given element Ω_e
$\partial\Omega_e^{iD}$	the union of all interior edges and all Dirichlet boundary edges of a given element Ω_e

Jumps and averages. Let $\Omega_i, \Omega_e \in \mathcal{T}_h$ be two neighbouring elements, sharing an interior edge $E = \partial\Omega_i \cap \partial\Omega_e$, and let $\boldsymbol{n}$ be the outward normal to Ω_i.

Define the following product space:

$$[T(\Gamma)]^d := \prod_{\Omega_e \in \mathcal{T}_h} [\mathcal{L}^2(\partial\Omega_e)]^d.$$

For any vector quantity $\boldsymbol{v} \in [T(\Gamma)]^d$ and any second order tensor $\boldsymbol{\tau} \in [T(\Gamma)]^{d\times d}$, we define the jumps

$$\lfloor \boldsymbol{v} \rfloor = (\boldsymbol{v}_i - \boldsymbol{v}_e) \otimes \boldsymbol{n}, \qquad [\boldsymbol{v}] = (\boldsymbol{v}_i - \boldsymbol{v}_e) \cdot \boldsymbol{n}, \qquad \lfloor \boldsymbol{\tau} \rfloor = (\boldsymbol{\tau}_i - \boldsymbol{\tau}_e)\boldsymbol{n},$$

and the averages

$$\{\boldsymbol{v}\} = \frac{1}{2}(\boldsymbol{v}_i + \boldsymbol{v}_e), \qquad \{\boldsymbol{\tau}\} = \frac{1}{2}(\boldsymbol{\tau}_i + \boldsymbol{\tau}_e),$$

where subscripts i and e denote values on the elements Ω_i and Ω_e, respectively.

For an element at edge Ω_e, the jumps are

$$\lfloor \boldsymbol{v} \rfloor = \boldsymbol{v} \otimes \boldsymbol{n}, \qquad [\boldsymbol{v}] = \boldsymbol{v} \cdot \boldsymbol{n}, \qquad \lfloor \boldsymbol{\tau} \rfloor = \boldsymbol{\tau}\boldsymbol{n},$$

and the averages

$$\{\boldsymbol{v}\} = \boldsymbol{v}, \qquad \{\boldsymbol{\tau}\} = \boldsymbol{\tau}.$$

Note that we have

$$[\{\cdot\}] = 0,\ [[\cdot]] = 0,\ \{\{\cdot\}\} = \{\cdot\} \text{ and } \{[\cdot]\} = [\cdot].$$

Discrete space and norm. We define the discrete space $\mathcal{V}_{DG}^h$ by

$$\mathcal{V}_{DG}^h := \left\{ \boldsymbol{v} \in [\mathcal{L}^2(\Omega)]^d : \boldsymbol{v}|_{\Omega_e} \in [\mathcal{P}_1(\Omega_e)]^d,\ \ \forall\, \Omega_e \in \mathcal{T}_h \right\}, \tag{5.1}$$

where $\mathcal{P}_1(\Omega)$ is the space of polynomials on Ω of maximum total degree 1.

The space $\mathcal{V}_{DG}^h$ is endowed with the norm (see for example [19, 45])

$$||\boldsymbol{u}||_{DG}^2 := \sum_{\Omega_e \in \mathcal{T}_h} \|\boldsymbol{\varepsilon}(\boldsymbol{u})\|_{0,\Omega_e}^2 + \frac{1}{2} \sum_{E \in \Gamma_{iD}} \frac{1}{h_E} \|\lfloor \boldsymbol{u} \rfloor\|_{0,E}^2. \tag{5.2}$$

5.2 Discontinuous Galerkin finite element approximations

5.2.1 Discontinuous Galerkin formulation

The derivation of the DG formulation follows the idea proposed in [2]. We start by multiplying the equilibrium equation (3.2) with a test function $\boldsymbol{v}$, and by integrating over an elemental domain Ω_e to obtain

$$-\int_{\Omega_e} \operatorname{div} \boldsymbol{\sigma}(\boldsymbol{u}) \cdot \boldsymbol{v} \, dx = \int_{\Omega_e} \boldsymbol{f} \cdot \boldsymbol{v} \, dx.$$

By applying integration by parts, we get

$$\int_{\Omega_e} \boldsymbol{\sigma}(\boldsymbol{u}) : \boldsymbol{\varepsilon}(\boldsymbol{v}) \, dx = \int_{\partial\Omega_e} \boldsymbol{\sigma}(\boldsymbol{u}) : \boldsymbol{v} \otimes \boldsymbol{n} \, ds + \int_{\Omega_e} \boldsymbol{f} \cdot \boldsymbol{v} \, dx.$$

Summing over all elements,

$$\sum_{\Omega_e \in \mathcal{T}_h} \int_{\Omega_e} \boldsymbol{\sigma}(\boldsymbol{u}) : \boldsymbol{\varepsilon}(\boldsymbol{v}) \, dx = \sum_{\Omega_e \in \mathcal{T}_h} \int_{\partial\Omega_e} \boldsymbol{\sigma}(\boldsymbol{u}) : \boldsymbol{v} \otimes \boldsymbol{n} \, ds + \sum_{\Omega_e \in \mathcal{T}_h} \int_{\Omega_e} \boldsymbol{f} \cdot \boldsymbol{v} \, dx.$$

Next, we use the "magic formula" (see [19]) to write

$$\sum_{\Omega_e \in \mathcal{T}_h} \int_{\Omega_e} \boldsymbol{\sigma}(\boldsymbol{u}) : \boldsymbol{\varepsilon}(\boldsymbol{v}) \, dx = \sum_{E \in \Gamma} \int_E \{\boldsymbol{\sigma}(\boldsymbol{u})\} : \lfloor \boldsymbol{v} \rfloor \, ds + \sum_{E \in \Gamma_i} \int_E \lfloor \boldsymbol{\sigma}(\boldsymbol{u}) \rfloor \cdot \{\boldsymbol{v}\} \, ds + \sum_{\Omega_e \in \mathcal{T}_h} \int_{\Omega_e} \boldsymbol{f} \cdot \boldsymbol{v} \, dx.$$

We assume that the exact solution is smooth ($\boldsymbol{u} \in [\mathcal{H}^2(\Omega)]^d$) and the stress is continuous, giving

$$\lfloor \boldsymbol{\sigma}(\boldsymbol{u}) \rfloor = \boldsymbol{0},$$

which leaves us with

$$\sum_{\Omega_e \in \mathcal{T}_h} \int_{\Omega_e} \boldsymbol{\sigma}(\boldsymbol{u}) : \boldsymbol{\varepsilon}(\boldsymbol{v}) \, dx = \sum_{E \in \Gamma} \int_E \{\boldsymbol{\sigma}(\boldsymbol{u})\} : \lfloor \boldsymbol{v} \rfloor \, ds + \sum_{\Omega_e \in \mathcal{T}_h} \int_{\Omega_e} \boldsymbol{f} \cdot \boldsymbol{v} \, dx.$$

We add a term to symmetrize the problem and get

$$\sum_{\Omega_e\in\mathcal{T}_h}\int_{\Omega_e}\boldsymbol{\sigma}(\boldsymbol{u}):\boldsymbol{\varepsilon}(\boldsymbol{v})\,dx=\sum_{E\in\Gamma}\int_E\{\boldsymbol{\sigma}(\boldsymbol{u})\}:\lfloor\boldsymbol{v}\rfloor\,ds+\sum_{E\in\Gamma}\int_E\{\boldsymbol{\sigma}(\boldsymbol{v})\}:\lfloor\boldsymbol{u}\rfloor\,ds+\sum_{\Omega_e\in\mathcal{T}_h}\int_{\Omega_e}\boldsymbol{f}\cdot\boldsymbol{v}\,dx,$$

noting that $\lfloor\boldsymbol{u}\rfloor=\boldsymbol{0}$ from the smoothness of the exact solution.

We add a stabilization term to obtain the symmetric interior penalty formulation

$$\sum_{\Omega_e\in\mathcal{T}_h}\int_{\Omega_e}\boldsymbol{\sigma}(\boldsymbol{u}):\boldsymbol{\varepsilon}(\boldsymbol{v})\,dx+\sum_{E\in\Gamma}\int_E\frac{k}{h_E}\mathbb{C}\lfloor\boldsymbol{u}\rfloor:\lfloor\boldsymbol{v}\rfloor\,ds=\sum_{E\in\Gamma}\int_E\{\boldsymbol{\sigma}(\boldsymbol{u})\}:\lfloor\boldsymbol{v}\rfloor\,ds+\sum_{E\in\Gamma}\int_E\{\boldsymbol{\sigma}(\boldsymbol{v})\}:\lfloor\boldsymbol{u}\rfloor\,ds$$
$$+\sum_{\Omega_e\in\mathcal{T}_h}\int_{\Omega_e}\boldsymbol{f}\cdot\boldsymbol{v}\,dx,$$

where k is a non-negative stabilization parameter.

Finally, to obtain the full IPDG formulations, we apply the boundary conditions given by (3.5), and introduce a parameter θ such that

$$\sum_{\Omega_e\in\mathcal{T}_h}\int_{\Omega_e}\boldsymbol{\sigma}(\boldsymbol{u}):\boldsymbol{\varepsilon}(\boldsymbol{v})\,dx-\sum_{E\in\Gamma_{iD}}\int_E\{\boldsymbol{\sigma}(\boldsymbol{u})\}:\lfloor\boldsymbol{v}\rfloor\,ds+\theta\sum_{E\in\Gamma_{iD}}\int_E\lfloor\boldsymbol{u}\rfloor:\{\boldsymbol{\sigma}(\boldsymbol{v})\}\,ds+\sum_{E\in\Gamma_{iD}}\int_E\frac{k}{h_E}\mathbb{C}\lfloor\boldsymbol{u}\rfloor:\lfloor\boldsymbol{v}\rfloor\,ds$$
$$=\sum_{\Omega_e\in\mathcal{T}_h}\int_{\Omega_e}\boldsymbol{f}\cdot\boldsymbol{v}\,dx+\sum_{E\in\Gamma_N}\boldsymbol{h}\cdot\boldsymbol{v}\,ds+\theta\sum_{E\in\Gamma_D}\int_E(\boldsymbol{g}\otimes\boldsymbol{n}):\boldsymbol{\sigma}(\boldsymbol{v})\,ds+\sum_{E\in\Gamma_D}\int_E\frac{k}{h_E}\mathbb{C}(\boldsymbol{g}\otimes\boldsymbol{n}):(\boldsymbol{v}\otimes\boldsymbol{n})\,ds.$$

Here θ is a switch that distinguishes the three methods, ($\theta=1$ for the Nonsymmetric Interior Penalty Galerkin (NIPG) method, $\theta=-1$ for Symmetric Interior Penalty Galerkin (SIPG), and $\theta=0$ for Incomplete Interior Penalty Galerkin (IIPG)).

The general IPDG weak formulation is as follows [19, 45]:

for all $\boldsymbol{v}\in\mathcal{V}^h_{DG}$, find $\boldsymbol{u}_h\in\mathcal{V}^h_{DG}$ such that

$$a_h(\boldsymbol{u}_h,\boldsymbol{v})=l_h(\boldsymbol{v}),\tag{5.3}$$

where

$$a_h(\boldsymbol{u},\boldsymbol{v})=\sum_{\Omega_e\in\mathcal{T}_h}\int_{\Omega_e}\boldsymbol{\sigma}(\boldsymbol{u}):\boldsymbol{\varepsilon}(\boldsymbol{v})\,dx-\sum_{E\in\Gamma_{iD}}\int_E\{\boldsymbol{\sigma}(\boldsymbol{u})\}:\lfloor\boldsymbol{v}\rfloor\,ds+\theta\sum_{E\in\Gamma_{iD}}\int_E\lfloor\boldsymbol{u}\rfloor:\{\boldsymbol{\sigma}(\boldsymbol{v})\}\,ds$$
$$+\sum_{E\in\Gamma_{iD}}\int_E\frac{k}{h_E}\mathbb{C}\lfloor\boldsymbol{u}\rfloor:\lfloor\boldsymbol{v}\rfloor\,ds,\tag{5.4}$$

and

$$l_h(\boldsymbol{v}) = \sum_{\Omega_e \in \mathcal{T}_h} \int_{\Omega_e} \boldsymbol{f} \cdot \boldsymbol{v}\, dx + \sum_{E \in \Gamma_N} \int_E \boldsymbol{h} \cdot \boldsymbol{v}\, ds + \theta \sum_{E \in \Gamma_D} \int_E (\boldsymbol{g} \otimes \boldsymbol{n}) : \boldsymbol{\sigma}(\boldsymbol{v})\, ds + \sum_{E \in \Gamma_D} \int_E \frac{k}{h_E} \mathbb{C}(\boldsymbol{g} \otimes \boldsymbol{n}) : (\boldsymbol{v} \otimes \boldsymbol{n})\, ds. \tag{5.5}$$

Here the elasticity tensor $\mathbb{C}$ is as defined in (2.8), and the stress tensor $\boldsymbol{\sigma}$ is as defined in (2.9).

We note that it is possible to assign different stabilization parameters to the different terms in the stabilisation. Thus alternatively, we can define the bilinear form and the linear functional

$$\begin{aligned}
\hat{a}_h(\boldsymbol{u}, \boldsymbol{v}) &= \sum_{\Omega_e \in \mathcal{T}_h} \int_{\Omega_e} \boldsymbol{\sigma}(\boldsymbol{u}) : \boldsymbol{\varepsilon}(\boldsymbol{v})\, dx - \sum_{E \in \Gamma_{iD}} \int_E \{\boldsymbol{\sigma}(\boldsymbol{u})\} : \lfloor \boldsymbol{v} \rfloor\, ds + \theta \sum_{E \in \Gamma_{iD}} \int_E \lfloor \boldsymbol{u} \rfloor : \{\boldsymbol{\sigma}(\boldsymbol{v})\}\, ds \\
&+ k_\lambda \lambda \sum_{E \in \Gamma_{iD}} \frac{1}{h_E} \int_E [\boldsymbol{u}][\boldsymbol{v}]\, ds + k_\mu \mu_t \sum_{E \in \Gamma_{iD}} \frac{1}{h_E} \int_E \lfloor \boldsymbol{u} \rfloor : \lfloor \boldsymbol{v} \rfloor\, ds \\
&+ k_\alpha \alpha \sum_{E \in \Gamma_{iD}} \frac{1}{h_E} \int_E \Big((\boldsymbol{M} : \lfloor \boldsymbol{u} \rfloor)[\boldsymbol{v}] + [\boldsymbol{u}](\boldsymbol{M} : \lfloor \boldsymbol{v} \rfloor) \Big)\, ds \\
&+ k_\beta \beta \sum_{E \in \Gamma_{iD}} \frac{1}{h_E} \int_E (\boldsymbol{M} : \lfloor \boldsymbol{u} \rfloor)(\boldsymbol{M} : \lfloor \boldsymbol{v} \rfloor)\, ds \\
&+ k_\gamma \gamma \sum_{E \in \Gamma_{iD}} \frac{1}{h_E} \int_E (\lfloor \boldsymbol{u} \rfloor \boldsymbol{M} + \boldsymbol{M} \lfloor \boldsymbol{u} \rfloor) : \lfloor \boldsymbol{v} \rfloor\, ds,
\end{aligned} \tag{5.6}$$

and

$$\begin{aligned}
\hat{l}_h(\boldsymbol{v}) &= \sum_{\Omega_e \in \mathcal{T}_h} \int_{\Omega_e} \boldsymbol{f} \cdot \boldsymbol{v}\, dx + \sum_{E \in \Gamma_N} \int_E \boldsymbol{h} \cdot \boldsymbol{v}\, ds + \theta \sum_{E \in \Gamma_D} \int_E (\boldsymbol{g} \otimes \boldsymbol{n}) : \boldsymbol{\sigma}(\boldsymbol{v})\, ds \\
&+ k_\lambda \lambda \sum_{E \in \Gamma_D} \frac{1}{h_E} \int_E (\boldsymbol{g} \cdot \boldsymbol{n})(\boldsymbol{v} \cdot \boldsymbol{n})\, ds + k_\mu \mu_t \sum_{E \in \Gamma_D} \frac{1}{h_E} \int_E \boldsymbol{g} \cdot \boldsymbol{v}\, ds \\
&+ k_\alpha \alpha \sum_{E \in \Gamma_D} \frac{1}{h_E} \int_E \Big((\boldsymbol{M} : \boldsymbol{g} \otimes \boldsymbol{n})(\boldsymbol{v} \cdot \boldsymbol{n}) + (\boldsymbol{g} \cdot \boldsymbol{n})(\boldsymbol{M} : \boldsymbol{v} \otimes \boldsymbol{n}) \Big)\, ds \\
&+ k_\beta \beta \sum_{E \in \Gamma_D} \frac{1}{h_E} \int_E (\boldsymbol{M} : \boldsymbol{g} \otimes \boldsymbol{n})(\boldsymbol{M} : \boldsymbol{v} \otimes \boldsymbol{n})\, ds \\
&+ k_\gamma \gamma \sum_{E \in \Gamma_D} \frac{1}{h_E} \int_E \Big((\boldsymbol{g} \otimes \boldsymbol{n}) \boldsymbol{M} + \boldsymbol{M} (\boldsymbol{g} \otimes \boldsymbol{n}) \Big) : \boldsymbol{v} \otimes \boldsymbol{n}\, ds,
\end{aligned} \tag{5.7}$$

where $k_\lambda, k_\mu, k_\alpha, k_\beta$ and k_γ are non-negative stabilization parameters.

In what follows, we confine attention to homogeneous bodies, so that the fibre direction $\boldsymbol{a}$ is constant.

5.2.2 Continuity

The bilinear form $a_h(\cdot,\cdot)$ is continuous with respect to the DG-norm $||\cdot||_{DG}$ if there exists a positive constant C such that

$$|a_h(\boldsymbol{u},\boldsymbol{v})| \leq C||\boldsymbol{u}||_{DG}||\boldsymbol{v}||_{DG}, \qquad \forall \boldsymbol{u},\boldsymbol{v} \in \mathcal{V}_{DG}^h.$$

We have

$$\begin{aligned}|a_h(\boldsymbol{u},\boldsymbol{v})| \leq & \left|\sum_{\Omega_e\in\mathcal{T}_h}\int_{\Omega_e}\boldsymbol{\sigma}(\boldsymbol{u}):\boldsymbol{\varepsilon}(\boldsymbol{v})\,dx\right| + \left|\sum_{E\in\Gamma_{iD}}\int_E\{\boldsymbol{\sigma}(\boldsymbol{u})\}:\lfloor\boldsymbol{v}\rfloor\,ds\right| + \left|\sum_{E\in\Gamma_{iD}}\int_E\lfloor\boldsymbol{u}\rfloor:\{\boldsymbol{\sigma}(\boldsymbol{v})\}\,ds\right| \\ & + \left|\sum_{E\in\Gamma_{iD}}\int_E\frac{k}{h_E}\mathbb{C}\lfloor\boldsymbol{u}\rfloor:\lfloor\boldsymbol{v}\rfloor\,ds\right|. \end{aligned} \tag{5.8}$$

We bound each term at the right hand side:

$$\begin{aligned}\left|\sum_{\Omega_e\in\mathcal{T}_h}\int_{\Omega_e}\boldsymbol{\sigma}(\boldsymbol{u}):\boldsymbol{\varepsilon}(\boldsymbol{v})\,dx\right| &\leq \left(\sum_{\Omega_e\in\mathcal{T}_h}||\boldsymbol{\sigma}(\boldsymbol{u})||^2_{0,\Omega_e}\right)^{1/2}\left(\sum_{\Omega_e\in\mathcal{T}_h}||\boldsymbol{\varepsilon}(\boldsymbol{v})||^2_{0,\Omega_e}\right)^{1/2} \\ &\leq C\left(\sum_{\Omega_e\in\mathcal{T}_h}||\boldsymbol{\varepsilon}(\boldsymbol{u})||^2_{0,\Omega_e}\right)^{1/2}\left(\sum_{\Omega_e\in\mathcal{T}_h}||\boldsymbol{\varepsilon}(\boldsymbol{v})||^2_{0,\Omega_e}\right)^{1/2} \\ &\leq C||\boldsymbol{u}||_{DG}||\boldsymbol{v}||_{DG}\end{aligned}$$

$$\begin{aligned}\left|\sum_{E\in\Gamma_{iD}}\int_E\{\boldsymbol{\sigma}(\boldsymbol{u})\}:\lfloor\boldsymbol{v}\rfloor\,ds\right| &\leq \left(\sum_{E\in\Gamma_{iD}}h_E||\{\boldsymbol{\sigma}(\boldsymbol{u})\}||^2_{0,E}\right)^{1/2}\left(\sum_{E\in\Gamma_{iD}}\frac{1}{h_E}||\lfloor\boldsymbol{v}\rfloor||^2_{0,E}\right)^{1/2} \\ &\leq C\left(\sum_{\Omega_e\in\mathcal{T}_h}h_e||\boldsymbol{\sigma}(\boldsymbol{u})||^2_{0,\partial\Omega_e^{iD}}\right)^{1/2}\left(\sum_{E\in\Gamma_{iD}}\frac{1}{h_E}||\lfloor\boldsymbol{v}\rfloor||^2_{0,E}\right)^{1/2} \\ &\leq C\left(\sum_{\Omega_e\in\mathcal{T}_h}||\boldsymbol{\varepsilon}(\boldsymbol{u})||^2_{0,\Omega_e}\right)^{1/2}\left(\sum_{E\in\Gamma_{iD}}\frac{1}{h_E}||\lfloor\boldsymbol{v}\rfloor||^2_{0,E}\right)^{1/2} \\ &\leq C||\boldsymbol{u}||_{DG}||\boldsymbol{v}||_{DG}\end{aligned}$$

Similarly,

$$\left|\sum_{E\in\Gamma_{iD}}\int_E\lfloor\boldsymbol{u}\rfloor:\{\boldsymbol{\sigma}(\boldsymbol{v})\}\,ds\right| \leq C||\boldsymbol{u}||_{DG}||\boldsymbol{v}||_{DG}$$

$$\begin{aligned}\left|\sum_{E\in\Gamma_{iD}}\int_E \frac{k}{h_E}\mathbb{C}\lfloor \boldsymbol{u}\rfloor : \lfloor \boldsymbol{v}\rfloor\, ds\right| &\leq k\left(\sum_{E\in\Gamma_{iD}}\frac{1}{h_E}||\mathbb{C}\lfloor \boldsymbol{u}\rfloor||^2_{0,E}\right)^{1/2}\left(\sum_{E\in\Gamma_{iD}}\frac{1}{h_E}||\lfloor \boldsymbol{v}\rfloor||^2_{0,E}\right)^{1/2}\\ &\leq C\left(\sum_{E\in\Gamma_{iD}}\frac{1}{h_E}||\lfloor \boldsymbol{u}\rfloor||^2_{0,E}\right)^{1/2}\left(\sum_{E\in\Gamma_{iD}}\frac{1}{h_E}||\lfloor \boldsymbol{v}\rfloor||^2_{0,E}\right)^{1/2}\\ &\leq C||\boldsymbol{u}||_{DG}||\boldsymbol{v}||_{DG}\end{aligned}$$

Thus,

$$|a_h(\boldsymbol{u},\boldsymbol{v})| \leq C||\boldsymbol{u}||_{DG}||\boldsymbol{v}||_{DG},$$

in which C is a constant dependent on material parameters $\lambda, \mu_t, \alpha, \beta$ and γ.

5.2.3 Consistency

Given the exact solution $\boldsymbol{u} \in [\mathcal{H}^2(\Omega)]^d$, the problem (5.3) is consistent if for any $\boldsymbol{v} \in \mathcal{V}^h_{DG}$

$$a_h(\boldsymbol{u},\boldsymbol{v}) - l_h(\boldsymbol{v}) = 0.$$

The proof of consistency is straightforward and may be carried out in a single argument for all three cases.

Let $\boldsymbol{u} \in [\mathcal{H}^2(\Omega)]^d$ be the exact solution of the problem; then we have

$$[\boldsymbol{u}] = 0, \quad \text{and} \quad \lfloor \boldsymbol{u}\rfloor = \lfloor \boldsymbol{\sigma}(\boldsymbol{u})\rfloor_{|E} = \boldsymbol{0} \qquad \forall\, E \in \Gamma_i,$$

and

$$\lfloor \boldsymbol{u}\rfloor = \boldsymbol{g}\otimes\boldsymbol{n} \quad \text{and} \quad [\boldsymbol{u}] = \boldsymbol{g}\cdot\boldsymbol{n} \qquad \text{on } \Gamma_D.$$

Therefore, we can write

$$a_h(\boldsymbol{u},\boldsymbol{v}) - l_h(\boldsymbol{v}) = \sum_{\Omega_e\in\mathcal{T}_h}\int_{\Omega_e}\boldsymbol{\sigma}(\boldsymbol{u}) : \boldsymbol{\varepsilon}(\boldsymbol{v})\, dx - \sum_{E\in\Gamma_{iD}}\int_E \{\boldsymbol{\sigma}(\boldsymbol{u})\} : \lfloor \boldsymbol{v}\rfloor\, ds - \sum_{\Omega_e\in\mathcal{T}_h}\int_{\Omega_e}\boldsymbol{f}\cdot\boldsymbol{v}\, dx - \sum_{E\in\Gamma_N}\int_E \boldsymbol{h}\cdot\boldsymbol{v}\, ds.$$

The exact solution $\boldsymbol{u}$ satisfies the weak form, so that

$$\begin{aligned}\sum_{\Omega_e\in\mathcal{T}_h}\int_{\Omega_e}\boldsymbol{\sigma}(\boldsymbol{u}) : \boldsymbol{\varepsilon}(\boldsymbol{v})\, dx &= \sum_{\Omega_e\in\mathcal{T}_h}\int_{\Omega_e}\boldsymbol{f}\cdot\boldsymbol{v}\, dx + \sum_{\Omega_e\in\mathcal{T}_h}\int_{\partial\Omega_e}\boldsymbol{\sigma}(\boldsymbol{u}) : \boldsymbol{v}\otimes\boldsymbol{n}\, dx\\ &= \sum_{\Omega_e\in\mathcal{T}_h}\int_{\Omega_e}\boldsymbol{f}\cdot\boldsymbol{v}\, dx + \sum_{E\in\Gamma}\int_E \{\boldsymbol{\sigma}(\boldsymbol{u})\} : \lfloor \boldsymbol{v}\rfloor\, ds + \sum_{E\in\Gamma_i}\int_E \lfloor \boldsymbol{\sigma}(\boldsymbol{u})\rfloor \cdot \{\boldsymbol{v}\}\, ds\\ &= \sum_{\Omega_e\in\mathcal{T}_h}\int_{\Omega_e}\boldsymbol{f}\cdot\boldsymbol{v}\, dx + \sum_{E\in\Gamma_{iD}}\int_E \{\boldsymbol{\sigma}(\boldsymbol{u})\} : \lfloor \boldsymbol{v}\rfloor\, ds + \sum_{E\in\Gamma_N}\int_E \boldsymbol{h}\cdot\boldsymbol{v}\, ds.\end{aligned}$$

Hence, we can conclude that the problem is consistent.

5.2.4 Coercivity

The bilinear form a_h is coercive if, for any $\boldsymbol{v} \in \mathcal{V}_{DG}^h$, there exists a positive constant K such that

$$a_h(\boldsymbol{v}, \boldsymbol{v}) \geq K \|\boldsymbol{v}\|_{DG}^2.$$

To prove coercivity, each IP method will be investigated separately, as different approaches are used for each of them.

The bilinear form $a_h(\cdot, \cdot)$ define by (5.8) which uses a fixed stabilization parameter k for all stabilization terms is used here.

NIPG ($\theta = 1$) For the non-symmetric IPDG case, for any $\boldsymbol{v} \in \mathcal{V}_{DG}^h$, we have

$$a_h(\boldsymbol{v}, \boldsymbol{v}) = \sum_{\Omega_e \in \mathcal{T}_h} \int_{\Omega_e} \boldsymbol{\sigma}(\boldsymbol{v}) : \boldsymbol{\varepsilon}(\boldsymbol{v})\, dx + \sum_{E \in \Gamma_{iD}} \int_E \frac{k}{h_E} \mathbb{C} \lfloor \boldsymbol{v} \rfloor : \lfloor \boldsymbol{v} \rfloor\, ds. \tag{5.9}$$

The proof of coercivity in Section 3.1.2 also holds for $\boldsymbol{v} \in \mathcal{V}_{DG}^h$ so that

$$\int_{\Omega_e} \boldsymbol{\sigma}(\boldsymbol{v}) : \boldsymbol{\varepsilon}(\boldsymbol{v})\, dx \geq \Lambda_{min} \|\boldsymbol{\varepsilon}(\boldsymbol{v})\|_{0,\Omega_e}^2. \tag{5.10}$$

By choosing $\boldsymbol{\varepsilon} = \lfloor \boldsymbol{v} \rfloor$ in (3.18), we have for $\boldsymbol{v} \in \mathcal{V}_{DG}^h$

$$\sum_{E \in \Gamma_{iD}} \int_E \frac{k}{h_E} \mathbb{C} \lfloor \boldsymbol{v} \rfloor : \lfloor \boldsymbol{v} \rfloor\, ds \geq k \Lambda_{min} \sum_{E \in \Gamma_{iD}} \frac{1}{h_E} \| \lfloor \boldsymbol{v} \rfloor \|_{0,E}^2.$$

Therefore,

$$\begin{aligned} a_h(\boldsymbol{v}, \boldsymbol{v}) &\geq \Lambda_{min} \sum_{\Omega_e \in \mathcal{T}_h} \|\boldsymbol{\varepsilon}(\boldsymbol{v})\|_{0,\Omega_e}^2 + k \Lambda_{min} \sum_{E \in \Gamma_{iD}} \frac{1}{h_E} || \lfloor \boldsymbol{v} \rfloor ||_{0,E}^2 \\ &= K ||\boldsymbol{v}||_{DG}^2 \end{aligned} \tag{5.11}$$

with

$$K = \Lambda_{min} \min\{1, 2k\} > 0. \tag{5.12}$$

We conclude that the bilinear form is coercive for the NIPG case.

SIPG ($\theta = -1$) For the SIPG case, the bilinear form can be written as follows, for any $\boldsymbol{v} \in \mathcal{V}^h_{DG}$:

$$a_h(\boldsymbol{v},\boldsymbol{v}) = \sum_{\Omega_e\in\mathcal{T}_h}\int_{\Omega_e}\mathbb{C}\boldsymbol{\varepsilon}(\boldsymbol{v}) : \boldsymbol{\varepsilon}(\boldsymbol{v})\,dx - 2\sum_{E\in\Gamma_{iD}}\int_E\{\mathbb{C}\boldsymbol{\varepsilon}(\boldsymbol{v})\} : \lfloor\boldsymbol{v}\rfloor\,ds + \sum_{E\in\Gamma_{iD}}\int_E\frac{k}{h_E}\mathbb{C}\lfloor\boldsymbol{v}\rfloor : \lfloor\boldsymbol{v}\rfloor\,ds. \tag{5.13}$$

Note that since the elasticity tensor $\mathbb{C}$ possess major symmetries and is positive definite, then there exists a unique square root $\mathbb{C}^{1/2}$ such that, for any second-order tensors $\boldsymbol{A}$ and $\boldsymbol{B}$, we have:

$$\mathbb{C}\boldsymbol{A} : \boldsymbol{B} = \mathbb{C}^{1/2}\boldsymbol{A} : \mathbb{C}^{1/2}\boldsymbol{B}. \tag{5.14}$$

We have

$$\begin{aligned}\mathscr{A} :=& -2\sum_{E\in\Gamma_{iD}}\int_E\{\mathbb{C}\boldsymbol{\varepsilon}(\boldsymbol{v})\} : \lfloor\boldsymbol{v}\rfloor\,ds\\ =& -2\sum_{E\in\Gamma_{iD}}\int_E\mathbb{C}^{1/2}\{\boldsymbol{\varepsilon}(\boldsymbol{v})\} : \mathbb{C}^{1/2}\lfloor\boldsymbol{v}\rfloor\,ds.\end{aligned}$$

Thus,

$$\begin{aligned}\mathscr{A} \geq& -2\left(\sum_{E\in\Gamma_{iD}}\|h_E^{1/2}\mathbb{C}^{1/2}\{\boldsymbol{\varepsilon}(\boldsymbol{v})\}\|^2_{0,E}\right)^{1/2}\left(\sum_{E\in\Gamma_{iD}}\|h_E^{-1/2}\mathbb{C}^{1/2}\lfloor\boldsymbol{v}\rfloor\|^2_{0,E}\right)^{1/2}\\ \geq& -2\left(\sum_{\Omega_e\in\mathcal{T}_h}h_e\|\mathbb{C}^{1/2}\boldsymbol{\varepsilon}(\boldsymbol{v})\|^2_{0,\partial\Omega_e^{iD}}\right)^{1/2}\left(\sum_{E\in\Gamma_{iD}}\|h_E^{-1/2}\mathbb{C}^{1/2}\lfloor\boldsymbol{v}\rfloor\|^2_{0,E}\right)^{1/2} \quad \text{(using (C.3d))}\\ \geq& -2C\left(\sum_{\Omega_e\in\mathcal{T}_h}\|\mathbb{C}^{1/2}\boldsymbol{\varepsilon}(\boldsymbol{v})\|^2_{0,\Omega_e}\right)^{1/2}\left(\sum_{E\in\Gamma_{iD}}\|h_E^{-1/2}\mathbb{C}^{1/2}\lfloor\boldsymbol{v}\rfloor\|^2_{0,E}\right)^{1/2} \quad \text{(using (C.3a))}\\ \geq& -C\epsilon\left(\sum_{\Omega_e\in\mathcal{T}_h}\|\mathbb{C}^{1/2}\boldsymbol{\varepsilon}(\boldsymbol{v})\|^2_{0,\Omega_e}\right) - \frac{1}{\epsilon}\left(\sum_{E\in\Gamma_{iD}}\|h_E^{-1/2}\mathbb{C}^{1/2}\lfloor\boldsymbol{v}\rfloor\|^2_{0,E}\right)\\ =& -\epsilon C\sum_{\Omega_e\in\mathcal{T}_h}\int_{\Omega_e}\mathbb{C}^{1/2}\boldsymbol{\varepsilon}(\boldsymbol{v}) : \mathbb{C}^{1/2}\boldsymbol{\varepsilon}(\boldsymbol{v})\,dx - \frac{1}{\epsilon}\sum_{E\in\Gamma_{iD}}\frac{1}{h_E}\int_E\mathbb{C}^{1/2}\lfloor\boldsymbol{v}\rfloor : \mathbb{C}^{1/2}\lfloor\boldsymbol{v}\rfloor\,ds\\ =& -\epsilon C\sum_{\Omega_e\in\mathcal{T}_h}\int_{\Omega_e}\mathbb{C}\boldsymbol{\varepsilon}(\boldsymbol{v}) : \boldsymbol{\varepsilon}(\boldsymbol{v})\,dx - \frac{1}{\epsilon}\sum_{E\in\Gamma_{iD}}\frac{1}{h_E}\int_E\mathbb{C}\lfloor\boldsymbol{v}\rfloor : \lfloor\boldsymbol{v}\rfloor\,ds.\end{aligned}$$

Therefore, we have

$$a_h(\boldsymbol{v},\boldsymbol{v}) \geq (1-\epsilon C)\sum_{\Omega_e\in\mathcal{T}_h}\int_{\Omega_e}\mathbb{C}\boldsymbol{\varepsilon}(\boldsymbol{v}) : \boldsymbol{\varepsilon}(\boldsymbol{v})\,dx + \left(k - \frac{1}{\epsilon}\right)\sum_{E\in\Gamma_{iD}}\frac{1}{h_E}\int_E\mathbb{C}\lfloor\boldsymbol{v}\rfloor : \lfloor\boldsymbol{v}\rfloor\,ds.$$

We set the coefficient in the first term to a constant $m > 0$, let $\epsilon = \dfrac{1-m}{C}$, and restrict m to $0 < m < 1$ to ensure $\epsilon > 0$.

Then

$$2\left(k-\frac{1}{\epsilon}\right)\geq m \Leftrightarrow k-\frac{C}{1-m}\geq\frac{m}{2}$$
$$\Leftrightarrow k\geq\frac{m}{2}+\frac{C}{1-m}.$$

With this choice of k, we have

$$\begin{aligned} a_h(\boldsymbol{v},\boldsymbol{v}) &\geq m\left(\sum_{\Omega_e\in\mathcal{T}_h}\int_{\Omega_e}\mathbb{C}\boldsymbol{\varepsilon}(\boldsymbol{v}):\boldsymbol{\varepsilon}(\boldsymbol{v})\,dx+\frac{1}{2}\sum_{E\in\Gamma_{iD}}\frac{1}{h_E}\int_E\mathbb{C}\lfloor\boldsymbol{v}\rfloor:\lfloor\boldsymbol{v}\rfloor\,ds\right)\\ &\geq m\Lambda_{min}\left(\sum_{\Omega_e\in\mathcal{T}_h}\|\boldsymbol{\varepsilon}(\boldsymbol{v})\|^2_{0,\Omega_e}+\frac{1}{2}\sum_{E\in\Gamma_{iD}}\frac{1}{h_E}\|\lfloor\boldsymbol{v}\rfloor\|^2_{0,E}\right)\\ &=K\|\boldsymbol{v}\|^2_{DG}, \end{aligned}\tag{5.15}$$

with

$$K=m\Lambda_{min}.\tag{5.16}$$

Therefore, we can conclude that the bilinear form a_h is coercive for SIPG.

IIPG ($\theta=0$) The corresponding bilinear form is written as follows, for any $\boldsymbol{v}\in\mathcal{V}^h_{DG}$:

$$a_h(\boldsymbol{v},\boldsymbol{v})=\sum_{\Omega_e\in\mathcal{T}_h}\int_{\Omega_e}\mathbb{C}\boldsymbol{\varepsilon}(\boldsymbol{v}):\boldsymbol{\varepsilon}(\boldsymbol{v})\,dx-\sum_{E\in\Gamma_{iD}}\int_E\{\mathbb{C}\boldsymbol{\varepsilon}(\boldsymbol{v})\}:\lfloor\boldsymbol{v}\rfloor\,ds+\sum_{E\in\Gamma_{iD}}\int_E\frac{k}{h_E}\mathbb{C}\lfloor\boldsymbol{v}\rfloor:\lfloor\boldsymbol{v}\rfloor\,ds.$$

The only difference between this form and the SIPG bilinear form is the coefficient in the second term; thus the proof of coercivity for IIPG case is identical to that for the SIPG case up to a constant.

We summarize these results.

5.2.5 Theorem. *The bilinear functional $a_h(\cdot,\cdot)$ defined in (5.3) is coercive if:*

(a) when $\theta=1$, $k>0$;

(b) when $\theta\in\{0,-1\}$,

$$k\geq\frac{m}{2}+\frac{C}{1-m},$$

where C is a positive constant to be calculated, and $0<m<1$.

5.2.6 Error bound

As shown in [45], one has uniform (λ-independent) convergence for the isotropic problem when linear triangles are used. We present here a corresponding bound for transversely isotropic materials, assuming a constant fibre direction $\boldsymbol{a}$.

To establish the bound, we adopt the same approach as in [45]; that is, splitting the error using the linear Crouzeix-Raviart interpolant ([13, 21]) $\Pi_e \boldsymbol{u} \in \left[\mathcal{P}_1(\Omega_e)\right]^d$, for $\boldsymbol{u} \in \left[\mathcal{H}^2(\Omega_e)\right]^d$, which is defined by

$$\Pi_e \boldsymbol{u}(\bar{\boldsymbol{x}}_E) := \frac{1}{h_E} \int_E \boldsymbol{u} \, ds \quad \forall\, E \in \partial\Omega_e, \tag{5.17}$$

where $\bar{\boldsymbol{x}}_E$ is the midpoint of edge E.

The corresponding global interpolant $\Pi : \left[\mathcal{H}^2(\Omega_e)\right]^d \to \mathcal{V}_{DG}^h$ is defined by

$$\Pi \boldsymbol{u}_{|\Omega_e} = \Pi_e \boldsymbol{u} \quad \forall\, \Omega_e \in \mathcal{T}_h.$$

5.2.1 Proposition. *The interpolant has the following properties:*

$$\int_E (\boldsymbol{u} - \Pi_e \boldsymbol{u}) \, ds = \boldsymbol{0}, \tag{5.18a}$$

$$\int_E (\boldsymbol{u} - \Pi_e \boldsymbol{u}) \cdot \boldsymbol{n}_e \, ds = 0, \tag{5.18b}$$

$$\int_{\Omega_e} \nabla \cdot (\boldsymbol{u} - \Pi_e \boldsymbol{u}) \, dx = 0, \tag{5.18c}$$

$$\int_{\Omega_e} \boldsymbol{M} : \boldsymbol{\varepsilon}(\boldsymbol{u} - \Pi_e \boldsymbol{u}) \, dx = 0. \tag{5.18d}$$

Proof. The proofs of (5.18a), (5.18b) and (5.18c) are given in [45], and repeated here.

To prove (5.18a), by definition, for $\boldsymbol{u} \in \left[\mathcal{H}^2(\Omega_e)\right]^d$, we have

$$\int_E \boldsymbol{u} \, ds = h_E \Pi_e \boldsymbol{u}(\bar{\boldsymbol{x}}_E),$$

thus it follows directly.

To prove (5.18b), we have

$$\int_E (\boldsymbol{u} - \Pi_e \boldsymbol{u}) \cdot \boldsymbol{n}_e \, ds = \boldsymbol{n}_e \cdot \int_E (\boldsymbol{u} - \Pi_e \boldsymbol{u}) \, ds = \boldsymbol{0} \cdot \boldsymbol{n}_e = 0.$$

For (5.18c), using Green's formula, we have

$$\int_{\Omega_e} \nabla \cdot (\boldsymbol{u} - \Pi_e \boldsymbol{u}) \, dx = \int_{\partial\Omega_e} (\boldsymbol{u} - \Pi_e \boldsymbol{u}) \cdot \boldsymbol{n}_e \, ds = \sum_{E \in \partial\Omega_e} \int_E (\boldsymbol{u} - \Pi_e \boldsymbol{u}) \cdot \boldsymbol{n}_e \, ds = 0.$$

For (5.18d), using integration by parts, we have

$$\int_{\Omega_e} \boldsymbol{M} : \boldsymbol{\varepsilon}(\boldsymbol{u} - \Pi_e \boldsymbol{u}) \, dx = \int_{\partial\Omega_e} (\boldsymbol{u} - \Pi_e \boldsymbol{u}) \otimes \boldsymbol{n}_e : \boldsymbol{M} \, ds - \int_{\Omega_e} (\nabla \cdot \boldsymbol{M}) \cdot (\boldsymbol{u} - \Pi_e \boldsymbol{u}) \, ds = 0.$$

□

5.2.2 Proposition. *The following interpolation error estimates hold:*

$$\|\boldsymbol{u} - \Pi_e \boldsymbol{u}\|_{0,\Omega_e} + h_e |\boldsymbol{u} - \Pi_e \boldsymbol{u}|_{1,\Omega_e} \leq C h_e^2 |\boldsymbol{u}|_{2,\Omega_e}, \tag{5.19a}$$

$$|\boldsymbol{u} - \Pi_e \boldsymbol{u}|_{2,\Omega_e} = |\boldsymbol{u}|_{2,\Omega_e}, \tag{5.19b}$$

$$\|\nabla \cdot (\boldsymbol{u} - \Pi_e \boldsymbol{u})\|_{0,\Omega_e} \leq C h_e |\nabla \cdot \boldsymbol{u}|_{1,\Omega_e}, \tag{5.19c}$$

$$|\nabla \cdot (\boldsymbol{u} - \Pi_e \boldsymbol{u})|_{1,\Omega_e} = |\nabla \cdot \boldsymbol{u}|_{1,\Omega_e}, \tag{5.19d}$$

$$\|\boldsymbol{M} : \boldsymbol{\varepsilon}(\boldsymbol{u} - \Pi_e \boldsymbol{u})\|_{0,\Omega_e} \leq C h_e |\boldsymbol{M} : \boldsymbol{\varepsilon}(\boldsymbol{u})|_{1,\Omega_e}, \tag{5.19e}$$

$$|\boldsymbol{M} : \boldsymbol{\varepsilon}(\boldsymbol{u} - \Pi_e \boldsymbol{u})|_{1,\Omega_e} = |\boldsymbol{M} : \boldsymbol{\varepsilon}(\boldsymbol{u})|_{1,\Omega_e} \tag{5.19f}$$

where $C > 0$ is in each case a constant independent of h_e and $\boldsymbol{u}$.

Proof. The proofs for (5.19a)-(5.19d) are given in [45] and repeated here.

Proof of (5.19a). From the standard interpolation estimate,

$$\|\boldsymbol{u} - \Pi_e \boldsymbol{u}\|_{0,\Omega_e} \leq C h_e^2 |\boldsymbol{u}|_{2,\Omega_e},$$

and

$$|\boldsymbol{u} - \Pi_e \boldsymbol{u}|_{1,\Omega_e} \leq \|\boldsymbol{u} - \Pi_e \boldsymbol{u}\|_{1,\Omega_e} \leq C h_e |\boldsymbol{u}|_{2,\Omega_e},$$

which gives (5.19a).

Proof of (5.19f). Setting $\boldsymbol{U} = \boldsymbol{u} - \Pi_e \boldsymbol{u}$, then since $\Pi_e \boldsymbol{u} \in \left[\mathcal{P}_1(\Omega_e)\right]^d$, it follows that

$$|\boldsymbol{U}|_{2,\Omega_e} = |\boldsymbol{u}|_{2,\Omega_e}, \tag{5.20a}$$

$$|\nabla \cdot \boldsymbol{U}|_{1,\Omega_e} = |\nabla \cdot \boldsymbol{u}|_{1,\Omega_e}, \tag{5.20b}$$

$$\text{and} \quad |\boldsymbol{\varepsilon}(\boldsymbol{U})|_{1,\Omega_e} = |\boldsymbol{\varepsilon}(\boldsymbol{u})|_{1,\Omega_e}. \tag{5.20c}$$

With a constant fibre direction $\boldsymbol{a}$, it follows from (5.20c) that

$$|\boldsymbol{M} : \boldsymbol{\varepsilon}(\boldsymbol{U})|_{1,\Omega_e} = |\boldsymbol{M} : \boldsymbol{\varepsilon}(\boldsymbol{u})|_{1,\Omega_e}. \tag{5.21}$$

Applying Proposition A.2.12 in [45] to $\boldsymbol{U}$ gives

$$\|\boldsymbol{U}\|_{2,\Omega_e}^2 \leq C\left(|\boldsymbol{U}|_{2,\Omega_e}^2 + \sum_{E\in\partial\Omega_e}\left|\int_E \boldsymbol{U}\, ds\right|^2\right)$$
$$= C|\boldsymbol{u}|_{2,\Omega_e}^2.$$

Applying Proposition A.2.11 in [45] to $\nabla\cdot\boldsymbol{U}$ gives

$$\left\|\nabla\cdot\boldsymbol{U} - \frac{1}{|\Omega_e|}\int_{\Omega_e}\nabla\cdot\boldsymbol{U}\, dx\right\|_{0,\Omega_e} \leq Ch_e|\nabla\cdot\boldsymbol{U}|_{1,\Omega_e},$$

and with (5.18c) and $(5.20)_2$ we obtain (5.19c).

Proof of (5.19e). Lemma A.3 in [45] applied to $\boldsymbol{M} : \boldsymbol{\varepsilon}(\boldsymbol{U})$ gives

$$\left\|\boldsymbol{M} : \boldsymbol{\varepsilon}(\boldsymbol{U}) - \frac{1}{|\Omega_e|}\int_{\Omega_e}\boldsymbol{M} : \boldsymbol{\varepsilon}(\boldsymbol{U})\, dx\right\|_{0,\Omega_e} \leq Ch_e|\boldsymbol{M} : \boldsymbol{\varepsilon}(\boldsymbol{U})|_{1,\Omega_e}.$$

With (5.18d) and (5.21), we obtain (5.19e). □

Let $\boldsymbol{u} \in \left[\mathcal{H}^2(\Omega_e)\right]^d$ be the exact solution to the problem (5.3), and $\boldsymbol{u}_h \in \mathcal{V}_{DG}^h$ its corresponding finite element approximation. The approximation error is denoted by

$$\boldsymbol{e} := \boldsymbol{u} - \boldsymbol{u}_h.$$

Let us define

$$\boldsymbol{\eta} := \boldsymbol{u} - \Pi\boldsymbol{u}, \quad \text{and} \quad \boldsymbol{\xi} := \Pi\boldsymbol{u} - \boldsymbol{u}_h,$$

so that in particular $\boldsymbol{\xi}_{|\Omega_e} \in [\mathcal{P}_1(\Omega_e)]^d$.

Thus,

$$\boldsymbol{e} = \boldsymbol{\eta} + \boldsymbol{\xi},$$

and the DG-norm of the error is

$$||\boldsymbol{e}||_{DG}^2 \leq ||\boldsymbol{\eta}||_{DG}^2 + ||\boldsymbol{\xi}||_{DG}^2.$$

To obtain the error bound, each term is bounded separately.

Starting with $||\boldsymbol{\eta}||_{DG}^2$, since $\boldsymbol{\eta} \in \mathcal{V}_{DG}^h$, we have, from (5.2),

$$||\boldsymbol{\eta}||_{DG}^2 = \sum_{\Omega_e\in\mathcal{T}_h}\|\boldsymbol{\varepsilon}(\boldsymbol{\eta})\|_{0,\Omega_e}^2 + \frac{1}{2}\sum_{E\in\Gamma_{iD}}\frac{1}{h_E}\|\lfloor\boldsymbol{\eta}\rfloor\|_{0,E}^2.$$

Using (C.3b) and (C.3d),

$$
\begin{aligned}
||\boldsymbol{\eta}||^2_{DG} &\leq C\Big(\sum_{\Omega_e\in\mathcal{T}_h} \|\nabla\boldsymbol{\eta}\|^2_{0,\Omega_e} + \sum_{\Omega_e\in\mathcal{T}_h}\sum_{E\in\partial\Omega_e^{iD}} \frac{1}{h_E}\|\boldsymbol{\eta}\|^2_{0,E}\Big) \\
&\leq C\Big(\sum_{\Omega_e\in\mathcal{T}_h} |\boldsymbol{\eta}|^2_{1,\Omega_e} + \sum_{\Omega_e\in\mathcal{T}_h} \big(h_e^{-2}\|\boldsymbol{\eta}\|^2_{0,\Omega_e} + |\boldsymbol{\eta}|^2_{1,\Omega_e}\big)\Big) \\
&\leq C \sum_{\Omega_e\in\mathcal{T}_h} h_e^2 |\boldsymbol{u}|^2_{2,\Omega_e} \,.
\end{aligned} \tag{5.22}
$$

Next, we bound $||\boldsymbol{\xi}||^2_{DG}$. From consistency of the bilinear form a_h, we have

$$a_h(\boldsymbol{e},\boldsymbol{\xi}) = 0.$$

Thus,

$$a_h(\boldsymbol{\xi},\boldsymbol{\xi}) = a_h(\boldsymbol{e}-\boldsymbol{\eta},\boldsymbol{\xi}) = -a_h(\boldsymbol{\eta},\boldsymbol{\xi}).$$

From coercivity of the bilinear form a_h, we have

$$|a_h(\boldsymbol{\xi},\boldsymbol{\xi})| \geq K||\boldsymbol{\xi}||^2_{DG}.$$

Thus,

$$|a_h(\boldsymbol{\eta},\boldsymbol{\xi})| \geq K||\boldsymbol{\xi}||^2_{DG}. \tag{5.23}$$

It then suffices to find an upper bound to $|a_h(\boldsymbol{\eta},\boldsymbol{\xi})|$. For that, the technique is to extract a factor of $||\boldsymbol{\xi}||_{DG}$, leaving some function in terms of $\boldsymbol{\eta}$ which will be bounded by norms of the exact solution $\boldsymbol{u}$ from each term using the interpolant estimates given by (5.19).

It is also useful to note that $\boldsymbol{\xi}\in[\mathcal{P}_1(\Omega)]^d$ so that $\boldsymbol{\varepsilon}(\boldsymbol{\xi}), \nabla\cdot\boldsymbol{\xi}$, and $\nabla\boldsymbol{\xi}$ are constants.

We have

$$|a_h(\boldsymbol{\eta},\boldsymbol{\xi})| \leq |a_h^{iso}(\boldsymbol{\eta},\boldsymbol{\xi})| + |a_h^{ti}(\boldsymbol{\eta},\boldsymbol{\xi})|,$$

where the isotropic part is bounded as follows (see [19]):

$$|a_h^{iso}(\boldsymbol{\eta},\boldsymbol{\xi})| \leq C||\boldsymbol{\xi}||_{DG}\left(\sum_{\Omega_e\in\mathcal{T}_h} h_e^2\left(\mu_t^2|\boldsymbol{u}|^2_{2,\Omega_e} + \lambda^2|\nabla\cdot\boldsymbol{u}|^2_{1,\Omega_e}\right)\right)^{1/2}. \tag{5.24}$$

For the transversely isotropic part, we have

$$
\begin{aligned}
&|a_h^{ti}(\boldsymbol{\eta},\boldsymbol{\xi})| \leq \\
&\quad |\alpha|\Big|\sum_{\Omega_e\in\mathcal{T}_h}\int_{\Omega_e}(\boldsymbol{M}:\boldsymbol{\varepsilon}(\boldsymbol{\eta}))(\nabla\cdot\boldsymbol{\xi})+(\nabla\cdot\boldsymbol{\eta})(\boldsymbol{M}:\boldsymbol{\varepsilon}(\boldsymbol{\xi}))\;dx\Big| + |\beta|\Big|\sum_{\Omega_e\in\mathcal{T}_h}\int_{\Omega_e}(\boldsymbol{M}:\boldsymbol{\varepsilon}(\boldsymbol{\eta}))(\boldsymbol{M}:\boldsymbol{\varepsilon}(\boldsymbol{\xi}))\;dx\Big| \\
&+2|\gamma|\Big|\sum_{\Omega_e\in\mathcal{T}_h}\int_{\Omega_e}\boldsymbol{\varepsilon}(\boldsymbol{\eta})\boldsymbol{M}:\boldsymbol{\varepsilon}(\boldsymbol{\xi})\;dx\Big| + \theta\Big|\sum_{E\in\Gamma_{iD}}\int_E\{\boldsymbol{\sigma}^{ti}(\boldsymbol{\xi})\}:\lfloor\boldsymbol{\eta}\rfloor\;ds\Big| \\
&+|\alpha|\Big|\sum_{E\in\Gamma_{iD}}\int_E\{(\boldsymbol{M}:\boldsymbol{\varepsilon}(\boldsymbol{\eta}))\mathbf{I}+(\nabla\cdot\boldsymbol{\eta})\boldsymbol{M}\}:\lfloor\boldsymbol{\xi}\rfloor\;ds\Big| + |\beta|\Big|\sum_{E\in\Gamma_{iD}}\int_E\{(\boldsymbol{M}:\boldsymbol{\varepsilon}(\boldsymbol{\eta}))\boldsymbol{M}\}:\lfloor\boldsymbol{\xi}\rfloor\;ds\Big| \\
&+|\gamma|\Big|\sum_{E\in\Gamma_{iD}}\int_E\{\boldsymbol{\varepsilon}(\boldsymbol{\eta})\boldsymbol{M}+\boldsymbol{M}\boldsymbol{\varepsilon}(\boldsymbol{\eta})\}:\lfloor\boldsymbol{\xi}\rfloor\;ds\Big| + k|\alpha|\Big|\sum_{E\in\Gamma_{iD}}\frac{1}{h_E}\int_E\Big([\boldsymbol{\eta}](\boldsymbol{M}:\lfloor\boldsymbol{\xi}\rfloor)+(\boldsymbol{M}:\lfloor\boldsymbol{\eta}\rfloor)[\boldsymbol{\xi}]\Big)\;ds\Big| \\
&+k|\beta|\Big|\sum_{E\in\Gamma_{iD}}\frac{1}{h_E}\int_E(\boldsymbol{M}:\lfloor\boldsymbol{\eta}\rfloor)(\boldsymbol{M}:\lfloor\boldsymbol{\xi}\rfloor)\;ds\Big| + k|\gamma|\Big|\sum_{E\in\Gamma_{iD}}\frac{1}{h_E}\int_E(\lfloor\boldsymbol{\eta}\rfloor\boldsymbol{M}+\boldsymbol{M}\lfloor\boldsymbol{\eta}\rfloor):\lfloor\boldsymbol{\xi}\rfloor\;ds\Big|.
\end{aligned}
$$

From the properties of the interpolants, we have

$$
\begin{aligned}
&\int_{\Omega_e}(\boldsymbol{M}:\boldsymbol{\varepsilon}(\boldsymbol{\eta}))(\nabla\cdot\boldsymbol{\xi})\;dx=(\nabla\cdot\boldsymbol{\xi})\int_{\Omega_e}(\boldsymbol{M}:\boldsymbol{\varepsilon}(\boldsymbol{\eta}))\;dx=0 \quad \text{(using (5.18d))}\\
&\int_{\Omega_e}(\nabla\cdot\boldsymbol{\eta})(\boldsymbol{M}:\boldsymbol{\varepsilon}(\boldsymbol{\xi}))\;dx=(\boldsymbol{M}:\boldsymbol{\varepsilon}(\boldsymbol{\xi}))\int_{\Omega_e}(\nabla\cdot\boldsymbol{\eta})\;dx=0 \quad \text{(using (5.18c))}\\
&\int_{\Omega_e}(\boldsymbol{M}:\boldsymbol{\varepsilon}(\boldsymbol{\eta}))(\boldsymbol{M}:\boldsymbol{\varepsilon}(\boldsymbol{\xi}))\;dx=(\boldsymbol{M}:\boldsymbol{\varepsilon}(\boldsymbol{\xi}))\int_{\Omega_e}(\boldsymbol{M}:\boldsymbol{\varepsilon}(\boldsymbol{\eta}))\;dx=0 \quad \text{(using (5.18d))}.
\end{aligned}
$$

Since

$$
\boldsymbol{\sigma}^{ti}(\boldsymbol{\xi})=\alpha\big((\boldsymbol{M}:\boldsymbol{\varepsilon}(\boldsymbol{\xi}))\boldsymbol{I}+(\nabla\cdot\boldsymbol{\xi})\boldsymbol{M}\big)+\beta(\boldsymbol{M}:\boldsymbol{\varepsilon}(\boldsymbol{\xi}))\boldsymbol{M}+\gamma\big(\boldsymbol{\varepsilon}(\boldsymbol{\xi})\boldsymbol{M}+\boldsymbol{M}\boldsymbol{\varepsilon}(\boldsymbol{\xi})\big)\in[\mathcal{P}_0(\Omega_e)]^{d\times d},
$$

it follows that

$$
\int_E\{\boldsymbol{\sigma}^{ti}(\boldsymbol{\xi})\}:\lfloor\boldsymbol{\eta}\rfloor\;ds=\{\boldsymbol{\sigma}^{ti}(\boldsymbol{\xi})\}:\int_E\lfloor\boldsymbol{\eta}\rfloor\;ds=0 \quad \text{(using (5.18a))}.
$$

Therefore, we have

$$
\begin{aligned}
&|a_h^{ti}(\boldsymbol{\eta},\boldsymbol{\xi})| \leq \\
&\quad \underbrace{2|\gamma|\Big|\sum_{\Omega_e\in\mathcal{T}_h}\int_{\Omega_e}\boldsymbol{\varepsilon}(\boldsymbol{\eta})\boldsymbol{M}:\boldsymbol{\varepsilon}(\boldsymbol{\xi})\;dx\Big|}_{I} + \underbrace{|\alpha|\Big|\sum_{E\in\Gamma_{iD}}\int_E\{(\boldsymbol{M}:\boldsymbol{\varepsilon}(\boldsymbol{\eta}))\mathbf{I}+(\nabla\cdot\boldsymbol{\eta})\boldsymbol{M}\}:\lfloor\boldsymbol{\xi}\rfloor\;ds\Big|}_{II} \\
&\quad + \underbrace{|\beta|\Big|\sum_{E\in\Gamma_{iD}}\int_E\{(\boldsymbol{M}:\boldsymbol{\varepsilon}(\boldsymbol{\eta}))\boldsymbol{M}\}:\lfloor\boldsymbol{\xi}\rfloor\;ds\Big|}_{III} + \underbrace{|\gamma|\Big|\sum_{E\in\Gamma_{iD}}\int_E\{\boldsymbol{\varepsilon}(\boldsymbol{\eta})\boldsymbol{M}+\boldsymbol{M}\boldsymbol{\varepsilon}(\boldsymbol{\eta})\}:\lfloor\boldsymbol{\xi}\rfloor\;ds\Big|}_{IV} \\
&\quad + \underbrace{k|\alpha|\Big|\sum_{E\in\Gamma_{iD}}\frac{1}{h_E}\int_E\Big([\boldsymbol{\eta}](\boldsymbol{M}:\lfloor\boldsymbol{\xi}\rfloor)+(\boldsymbol{M}:\lfloor\boldsymbol{\eta}\rfloor)[\boldsymbol{\xi}]\Big)\;ds\Big|}_{V} + \underbrace{k|\beta|\Big|\sum_{E\in\Gamma_{iD}}\frac{1}{h_E}\int_E(\boldsymbol{M}:\lfloor\boldsymbol{\eta}\rfloor)(\boldsymbol{M}:\lfloor\boldsymbol{\xi}\rfloor)\;ds\Big|}_{VI} \\
&\quad + \underbrace{k|\gamma|\Big|\sum_{E\in\Gamma_{iD}}\frac{1}{h_E}\int_E(\lfloor\boldsymbol{\eta}\rfloor\boldsymbol{M}+\boldsymbol{M}\lfloor\boldsymbol{\eta}\rfloor):\lfloor\boldsymbol{\xi}\rfloor\;ds\Big|}_{VII}. \qquad (5.25)
\end{aligned}
$$

We now bound each term in (5.25).

First, a bound for I:

$$
\begin{aligned}
I &= 2|\gamma|\Big|\sum_{\Omega_e\in\mathcal{T}_h}\int_{\Omega_e}\boldsymbol{\varepsilon}(\boldsymbol{\eta})\boldsymbol{M}:\boldsymbol{\varepsilon}(\boldsymbol{\xi})\;dx\Big| \\
&\leq 2|\gamma|\left(\sum_{\Omega_e\in\mathcal{T}_h}\|\boldsymbol{\varepsilon}(\boldsymbol{\eta})\boldsymbol{M}\|_{0,\Omega_e}^2\right)^{1/2}\left(\sum_{\Omega_e\in\mathcal{T}_h}\|\boldsymbol{\varepsilon}(\boldsymbol{\xi})\|_{0,\Omega_e}^2\right)^{1/2} \\
&\leq C|\gamma|\left(\sum_{\Omega_e\in\mathcal{T}_h}\|\boldsymbol{\varepsilon}(\boldsymbol{\eta})\|_{0,\Omega_e}^2\right)^{1/2}\left(\sum_{\Omega_e\in\mathcal{T}_h}\|\boldsymbol{\varepsilon}(\boldsymbol{\xi})\|_{0,\Omega_e}^2\right)^{1/2} \qquad (\text{since } |\varepsilon\boldsymbol{M}|^2\leq C|\varepsilon|^2) \\
&\leq C|\gamma|\|\boldsymbol{\xi}\|_{DG}\left(\sum_{\Omega_e\in\mathcal{T}_h}\|\nabla\boldsymbol{\eta}\|_{0,\Omega_e}^2\right)^{1/2} \\
&\leq C|\gamma|\|\boldsymbol{\xi}\|_{DG}\left(\sum_{\Omega_e\in\mathcal{T}_h}|\boldsymbol{\eta}|_{1,\Omega_e}^2\right)^{1/2} \\
&\leq C|\gamma|\|\boldsymbol{\xi}\|_{DG}\left(\sum_{\Omega_e\in\mathcal{T}_h}h_e^2|\boldsymbol{u}|_{2,\Omega_e}^2\right)^{1/2} \qquad (\text{using } (5.19\text{a})).
\end{aligned}
$$

Next, a bound for II, which we split into two terms II_a and II_b. Using triangular inequality, we have:

$$
\begin{aligned}
II_a &:= |\alpha| \Big| \sum_{E\in\Gamma_{iD}} \int_E \{(\boldsymbol{M} : \boldsymbol{\varepsilon}(\boldsymbol{\eta}))\mathbf{I}\} : \lfloor \boldsymbol{\xi} \rfloor \; ds \Big| \\
&\leq |\alpha| \left(\sum_{E\in\Gamma_{iD}} h_E \|\{(\boldsymbol{M} : \boldsymbol{\varepsilon}(\boldsymbol{\eta}))\boldsymbol{I}\}\|_{0,E}^2 \right)^{1/2} \left(\sum_{E\in\Gamma_{iD}} \frac{1}{h_E} \|\lfloor \boldsymbol{\xi} \rfloor\|_{0,E}^2 \right)^{1/2} \\
&\leq C|\alpha| \|\boldsymbol{\xi}\|_{DG} \left(\sum_{E\in\Gamma_{iD}} h_E \|\{\boldsymbol{M} : \boldsymbol{\varepsilon}(\boldsymbol{\eta})\}\|_{0,E}^2 \right)^{1/2} \\
&\leq C|\alpha| \|\boldsymbol{\xi}\|_{DG} \left(\sum_{\Omega_e\in\mathcal{T}_h} h_e \|\boldsymbol{M} : \boldsymbol{\varepsilon}(\boldsymbol{\eta})\|_{0,\partial\Omega_e^{iD}}^2 \right)^{1/2} \qquad \text{(using (C.3d))} \\
&\leq C\alpha \|\boldsymbol{\xi}\|_{DG} \left(\sum_{\Omega_e\in\mathcal{T}_h} \|\boldsymbol{M} : \boldsymbol{\varepsilon}(\boldsymbol{\eta})\|_{0,\Omega_e}^2 + h_e^2 |\boldsymbol{M} : \boldsymbol{\varepsilon}(\boldsymbol{\eta})|_{1,\Omega_e}^2 \right)^{1/2} \qquad \text{(using (C.3b))} \\
&\leq C|\alpha| \|\boldsymbol{\xi}\|_{DG} \left(\sum_{\Omega_e\in\mathcal{T}_h} h_e^2 |\boldsymbol{M} : \boldsymbol{\varepsilon}(\boldsymbol{u})|_{1,\Omega_e}^2 \right)^{1/2} \qquad \text{(using (5.19e) and (5.19f))}.
\end{aligned}
$$

and

$$
\begin{aligned}
II_b &:= |\alpha| \Big| \sum_{E\in\Gamma_{iD}} \int_E \{(\nabla\cdot\boldsymbol{\eta})\boldsymbol{M}\} : \lfloor \boldsymbol{\xi} \rfloor \; ds \Big| \\
&\leq |\alpha| \left(\sum_{E\in\Gamma_{iD}} h_E \|\{(\nabla\cdot\boldsymbol{\eta})\boldsymbol{M}\}\|_{0,E}^2 \right)^{1/2} \left(\sum_{E\in\Gamma_{iD}} \frac{1}{h_E} \|\lfloor \boldsymbol{\xi} \rfloor\|_{0,E}^2 \right)^{1/2} \\
&\leq C|\alpha| \|\boldsymbol{\xi}\|_{DG} \left(\sum_{\Omega_e\in\mathcal{T}_h} h_e \|\nabla\cdot\boldsymbol{\eta}\|_{0,\partial\Omega_e^{iD}}^2 \right)^{1/2} \qquad \text{(using (C.3d) and } |(\nabla\cdot\boldsymbol{v})\boldsymbol{M}|^2 \leq |\nabla\cdot\boldsymbol{v}|^2) \\
&\leq C|\alpha| \|\boldsymbol{\xi}\|_{DG} \left(\sum_{\Omega_e\in\mathcal{T}_h} \|\nabla\cdot\boldsymbol{\eta}\|_{0,\Omega_e}^2 + h_e^2 |\nabla\cdot\boldsymbol{\eta}|_{1,\Omega_e}^2 \right)^{1/2} \qquad \text{(using (C.3b))} \\
&\leq C|\alpha| \|\boldsymbol{\xi}\|_{DG} \left(\sum_{\Omega_e\in\mathcal{T}_h} h_e^2 |\nabla\cdot\boldsymbol{u}|_{1,\Omega_e}^2 \right)^{1/2} \qquad \text{(using (5.19c) and (5.19d))}.
\end{aligned}
$$

Term III is bounded as follows:

$$
\begin{aligned}
III &= |\beta| \Big| \sum_{E\in\Gamma_{iD}} \int_E \{(\boldsymbol{M}:\boldsymbol{\varepsilon}(\boldsymbol{\eta}))\boldsymbol{M}\} : \lfloor \boldsymbol{\xi} \rfloor \, ds \Big| \\
&\le |\beta| \left(\sum_{E\in\Gamma_{iD}} h_E \|\{(\boldsymbol{M}:\boldsymbol{\varepsilon}(\boldsymbol{\eta}))\boldsymbol{M}\}\|_{0,E}^2 \right)^{1/2} \left(\sum_{E\in\Gamma_{iD}} \frac{1}{h_E} \|\lfloor \boldsymbol{\xi} \rfloor\|_{0,E}^2 \right)^{1/2} \qquad (\text{since } |(\boldsymbol{M}:\varepsilon)\boldsymbol{M}|^2 \le |\boldsymbol{M}:\varepsilon|^2) \\
&\le |\beta| \|\boldsymbol{\xi}\|_{DG} \left(\sum_{E\in\Gamma_{iD}} h_E \|\{\boldsymbol{M}:\boldsymbol{\varepsilon}(\boldsymbol{\eta})\}\|_{0,E}^2 \right)^{1/2} \\
&\le C|\beta| \|\boldsymbol{\xi}\|_{DG} \left(\sum_{\Omega_e\in\mathcal{T}_h} h_e \|\boldsymbol{M}:\boldsymbol{\varepsilon}(\boldsymbol{\eta})\|_{0,\partial\Omega_e^{iD}}^2 \right)^{1/2} \qquad (\text{using (C.3d)}) \\
&\le C|\beta| \|\boldsymbol{\xi}\|_{DG} \left(\sum_{\Omega_e\in\mathcal{T}_h} \|\boldsymbol{M}:\boldsymbol{\varepsilon}(\boldsymbol{\eta})\|_{0,\Omega_e}^2 + h_e^2 |\boldsymbol{M}:\boldsymbol{\varepsilon}(\boldsymbol{\eta})|_{1,\Omega_e} \right)^{1/2} \qquad (\text{using (C.3b)} \\
&\le C|\beta| \|\boldsymbol{\xi}\|_{DG} \left(\sum_{\Omega_e\in\mathcal{T}_h} h_e^2 |\boldsymbol{M}:\boldsymbol{\varepsilon}(\boldsymbol{u})|_{1,\Omega_e}^2 \right)^{1/2} \qquad (\text{using (5.19e) and (5.19f)}).
\end{aligned}
$$

The term IV is split into two terms, IV_a and IV_b:

$$
\begin{aligned}
IV_a &:= |\gamma| \Big| \sum_{E\in\Gamma_{iD}} \int_E \{\boldsymbol{\varepsilon}(\boldsymbol{\eta})\boldsymbol{M}\} : \lfloor \boldsymbol{\xi} \rfloor \, ds \Big| \\
&\le |\gamma| \left(\sum_{E\in\Gamma_{iD}} h_E \|\{\boldsymbol{\varepsilon}(\boldsymbol{\eta})\boldsymbol{M}\}\|_{0,E}^2 \right)^{1/2} \left(\sum_{E\in\Gamma_{iD}} \frac{1}{h_E} \|\lfloor \boldsymbol{\xi} \rfloor\|_{0,E}^2 \right)^{1/2} \\
&\le |\gamma| \|\boldsymbol{\xi}\|_{DG} \left(\sum_{E\in\Gamma_{iD}} h_E \|\{\boldsymbol{\varepsilon}(\boldsymbol{\eta})\}\|_{0,E}^2 \right)^{1/2} \qquad (\text{since } |\varepsilon\boldsymbol{M}|^2 \le C|\varepsilon|^2) \\
&\le C|\gamma| \|\boldsymbol{\xi}\|_{DG} \left(\sum_{\Omega_e\in\mathcal{T}_h} h_e \|\boldsymbol{\varepsilon}(\boldsymbol{\eta})\|_{0,\partial\Omega_e^{iD}}^2 \right)^{1/2} \qquad (\text{using (C.3d)}) \\
&\le C|\gamma| \|\boldsymbol{\xi}\|_{DG} \left(\sum_{\Omega_e\in\mathcal{T}_h} h_e \|\nabla\boldsymbol{\eta}\|_{0,\partial\Omega_e^{iD}}^2 \right)^{1/2} \\
&\le C|\gamma| \|\boldsymbol{\xi}\|_{DG} \left(\sum_{\Omega_e\in\mathcal{T}_h} \|\nabla\boldsymbol{\eta}\|_{0,\Omega_e}^2 + h_e^2 |\nabla\boldsymbol{\eta}|_{1,\Omega_e}^2 \right)^{1/2} \qquad (\text{using (C.3b)}) \\
&\le C|\gamma| \|\boldsymbol{\xi}\|_{DG} \left(\sum_{\Omega_e\in\mathcal{T}_h} |\boldsymbol{\eta}|_{1,\Omega_e}^2 + h_e^2 |\boldsymbol{\eta}|_{2,\Omega_e}^2 \right)^{1/2} \\
&\le C|\gamma| \|\boldsymbol{\xi}\|_{DG} \left(\sum_{\Omega_e\in\mathcal{T}_h} h_e^2 |\boldsymbol{u}|_{2,\Omega_e}^2 \right)^{1/2} .
\end{aligned}
$$

Following similar steps, we have

$$
\begin{aligned}
IV_b &:= |\gamma| \Big| \sum_{E \in \Gamma_{iD}} \int_E \{\boldsymbol{M}\boldsymbol{\varepsilon}(\boldsymbol{\eta})\} : \lfloor \boldsymbol{\xi} \rfloor \; ds \Big| \\
&\leq C |\gamma| \|\boldsymbol{\xi}\|_{DG} \left(\sum_{\Omega_e \in \mathcal{T}_h} h_e^2 |\boldsymbol{u}|_{2,\Omega_e}^2 \right)^{1/2} .
\end{aligned}
$$

Term V is split into two terms, V_a and V_b.

$$
\begin{aligned}
V_a &:= k|\alpha| \Big| \sum_{E \in \Gamma_{iD}} \frac{1}{h_E} \int_E [\boldsymbol{\eta}] (\boldsymbol{M} : \lfloor \boldsymbol{\xi} \rfloor) \; ds \Big| \\
&\leq k|\alpha| \left(\sum_{E \in \Gamma_{iD}} \frac{1}{h_E} \|[\boldsymbol{\eta}]\|_{0,E}^2 \right)^{1/2} \left(\sum_{E \in \Gamma_{iD}} \frac{1}{h_E} \|\boldsymbol{M} : \lfloor \boldsymbol{\xi} \rfloor\|_{0,E}^2 \right)^{1/2} \\
&\leq C|\alpha| \|\boldsymbol{\xi}\|_{DG} \left(\sum_{E \in \Gamma_{iD}} \frac{1}{h_E} \|[\boldsymbol{\eta}]\|_{0,E}^2 \right)^{1/2} \qquad \text{(since } |\boldsymbol{M} : \lfloor \boldsymbol{\xi} \rfloor|^2 < C |\lfloor \boldsymbol{\xi} \rfloor|^2\text{)} \\
&\leq C|\alpha| \|\boldsymbol{\xi}\|_{DG} \left(\sum_{\Omega_e \in \mathcal{T}_h} \sum_{E \in \partial\Omega_e^{iD}} \frac{2}{h_E} \|\boldsymbol{\eta}\|_{0,E} \right)^{1/2} \qquad \text{(using (C.3c))} \\
&\leq C|\alpha| \|\boldsymbol{\xi}\|_{DG} \left(\sum_{\Omega_e \in \mathcal{T}_h} \sum_{E \in \partial\Omega_e^{iD}} \frac{2}{h_E} \|\boldsymbol{\eta}\|_{0,E} \right)^{1/2} \qquad \text{(using (C.3c))} \\
&\leq C|\alpha| \|\boldsymbol{\xi}\|_{DG} \left(\sum_{\Omega_e \in \mathcal{T}_h} h_e^{-2} \|\boldsymbol{\eta}\|_{0,\Omega_e} + |\boldsymbol{\eta}|_{1,\Omega_e} \right)^{1/2} \qquad \text{(using (C.3b))} \\
&\leq C|\alpha| \|\boldsymbol{\xi}\|_{DG} \left(\sum_{\Omega_e \in \mathcal{T}_h} h_e^2 |\boldsymbol{u}|_{2,\Omega_e}^2 \right)^{1/2} \qquad \text{(using (5.19a))}.
\end{aligned}
$$

Following similar steps, we have

$$
V_b := k|\alpha| \Big| \sum_{E \in \Gamma_{iD}} \frac{1}{h_E} \int_E [\boldsymbol{\xi}] (\boldsymbol{M} : \lfloor \boldsymbol{\eta} \rfloor) \; ds \Big| \leq C\alpha \|\boldsymbol{\xi}\|_{DG} \left(\sum_{\Omega_e \in \mathcal{T}_h} h_e^2 |\boldsymbol{u}|_{2,\Omega_e}^2 \right)^{1/2} .
$$

To bound the term VI, we have

$$
\begin{aligned}
VI &= k|\beta|\Big|\sum_{E\in\Gamma_{iD}}\frac{1}{h_E}\int_E (\boldsymbol{M}:\lfloor\boldsymbol{\eta}\rfloor)(\boldsymbol{M}:\lfloor\boldsymbol{\xi}\rfloor)\;ds\Big|\\
&\le k|\beta|\left(\sum_{E\in\Gamma_{iD}}\frac{1}{h_E}\|\boldsymbol{M}:\lfloor\boldsymbol{\xi}\rfloor\|_{0,E}^2\right)^{1/2}\left(\sum_{E\in\Gamma_{iD}}\frac{1}{h_E}\|\boldsymbol{M}:\lfloor\boldsymbol{\eta}\rfloor\|_{0,E}^2\right)^{1/2}\\
&\le C|\beta|\|\boldsymbol{\xi}\|_{DG}\left(\sum_{E\in\Gamma_{iD}}\frac{1}{h_E}\|\lfloor\boldsymbol{\eta}\rfloor\|_{0,E}^2\right)^{1/2} \qquad (\text{since } |\boldsymbol{M}:\lfloor\boldsymbol{\eta}\rfloor|^2<C|\lfloor\boldsymbol{\eta}\rfloor|^2)\\
&\le C|\beta|\|\boldsymbol{\xi}\|_{DG}\left(\sum_{\Omega_e\in\mathcal{T}_h}\sum_{E\in\partial\Omega_e^{iD}}\frac{2}{h_E}\|\boldsymbol{\eta}\|_{0,E}\right)^{1/2} \qquad (\text{using (C.3c)})\\
&\le C|\beta|\|\boldsymbol{\xi}\|_{DG}\left(\sum_{\Omega_e\in\mathcal{T}_h}h_e^{-2}\|\boldsymbol{\eta}\|_{0,\Omega_e}+|\boldsymbol{\eta}|_{1,\Omega_e}\right)^{1/2} \qquad (\text{using (C.3b)})\\
&\le C|\beta|\|\boldsymbol{\xi}\|_{DG}\left(\sum_{\Omega_e\in\mathcal{T}_h}h_e^2|\boldsymbol{u}|_{2,\Omega_e}^2\right)^{1/2} \qquad (\text{using (5.19a)}).
\end{aligned}
$$

Finally, the term VII is bounded as follows:

$$
\begin{aligned}
VII_a &:= k|\gamma|\Big|\sum_{E\in\Gamma_{iD}}\frac{1}{h_E}\int_E \lfloor\boldsymbol{\eta}\rfloor\boldsymbol{M}:\lfloor\boldsymbol{\xi}\rfloor\;ds\Big|\\
&\le k|\gamma|\left(\sum_{E\in\Gamma_{iD}}\frac{1}{h_E}\|\lfloor\boldsymbol{\eta}\rfloor\boldsymbol{M}\|_{0,E}^2\right)^{1/2}\left(\sum_{E\in\Gamma_{iD}}\frac{1}{h_E}\|\lfloor\boldsymbol{\xi}\rfloor\|_{0,E}^2\right)^{1/2}\\
&\le C|\gamma|\|\boldsymbol{\xi}\|_{DG}\left(\sum_{E\in\Gamma_{iD}}\frac{1}{h_E}\|\lfloor\boldsymbol{\eta}\rfloor\|_{0,E}^2\right)^{1/2} \qquad (\text{since}|\lfloor\boldsymbol{\eta}\rfloor\boldsymbol{M}|^2\le|\lfloor\boldsymbol{\eta}\rfloor|^2)\\
&\le C|\gamma|\|\boldsymbol{\xi}\|_{DG}\left(\sum_{\Omega_e\in\mathcal{T}_h}h_e^2|\boldsymbol{u}|_{2,\Omega_e}^2\right)^{1/2} \qquad (\text{similar to } VI).
\end{aligned}
$$

Following similar steps, we have

$$
VII_b := k|\gamma|\Big|\sum_{E\in\Gamma_{iD}}\frac{1}{h_E}\int_E \boldsymbol{M}\lfloor\boldsymbol{\eta}\rfloor:\lfloor\boldsymbol{\xi}\rfloor\;ds\Big| \le C|\gamma|\|\boldsymbol{\xi}\|_{DG}\left(\sum_{\Omega_e\in\mathcal{T}_h}h_e^2|\boldsymbol{u}|_{2,\Omega_e}^2\right)^{1/2}.
$$

We use these results to bound $|a_h^{ti}(\boldsymbol{\eta},\boldsymbol{\xi})|$, which leads to

$$
|a_h^{ti}(\boldsymbol{\eta},\boldsymbol{\xi})| \le C||\boldsymbol{\xi}||_{DG}\left(\sum_{\Omega_e\in\mathcal{T}_h}h_e^2\Big((\alpha^2+\beta^2+\gamma^2)|\boldsymbol{u}|_{2,\Omega_e}^2+\alpha^2|\nabla\cdot\boldsymbol{u}|_{1,\Omega_e}^2+(\alpha^2+\beta^2)|\boldsymbol{M}:\boldsymbol{\varepsilon}(\boldsymbol{u})|_{1,\Omega_e}^2\Big)\right)^{1/2}. \tag{5.26}
$$

Thus, with (5.24) and (5.26), we have

$$|a_h^{ti}(\boldsymbol{\eta},\boldsymbol{\xi})| \leq C||\boldsymbol{\xi}||_{DG}\left(\sum_{\Omega_e\in\mathcal{T}_h} h_e^2\Big((\mu_t^2+\alpha^2+\beta^2+\gamma^2)|\boldsymbol{u}|^2_{2,\Omega_e}+(\lambda^2+\alpha^2)|\nabla\cdot\boldsymbol{u}|^2_{1,\Omega_e}+(\alpha^2+\beta^2)|\boldsymbol{M}:\boldsymbol{\varepsilon}(\boldsymbol{u})|^2_{1,\Omega_e}\Big)\right)^{1/2}. \tag{5.27}$$

Therefore, using (5.23), we obtain

$$||\boldsymbol{\xi}||^2_{DG} \leq \frac{C}{K^2}\sum_{\Omega_e\in\mathcal{T}_h} h_e^2\Big((\mu_t^2+\alpha^2+\beta^2+\gamma^2)|\boldsymbol{u}|^2_{2,\Omega_e}+(\lambda^2+\alpha^2)|\nabla\cdot\boldsymbol{u}|^2_{1,\Omega_e}+(\alpha^2+\beta^2)|\boldsymbol{M}:\boldsymbol{\varepsilon}(\boldsymbol{u})|^2_{1,\Omega_e}\Big), \tag{5.28}$$

where K is the coercivity constant defined by (5.12) for NIPG case, and by (5.16) for SIPG and IIPG cases. With (5.22) and (5.28), the full DG error bound is

$$||\boldsymbol{e}||^2_{DG} \leq \frac{C}{K^2}h^2\Big((\mu_t^2+\alpha^2+\beta^2+\gamma^2)|\boldsymbol{u}|^2_{2,\Omega}+(\lambda^2+\alpha^2)|\nabla\cdot\boldsymbol{u}|^2_{1,\Omega}+(\alpha^2+\beta^2)|\boldsymbol{M}:\boldsymbol{\varepsilon}(\boldsymbol{u})|^2_{1,\Omega}\Big). \tag{5.29}$$

Remark. For the case of isotropy, the error estimate is (see [19])

$$||\boldsymbol{e}||^2_{DG} \leq \frac{C}{K^2}h^2\left(\mu_t^2|\boldsymbol{u}|^2_{2,\Omega}+\lambda^2|\nabla\cdot\boldsymbol{u}|^2_{1,\Omega}\right). \tag{5.30}$$

Brenner & Sung in [8] have derived the following uniform estimate for the case of problems on polygonal domain $\Omega\subset\mathbb{R}^2$:

$$\|\boldsymbol{u}\|_{2,\Omega}+\lambda\|\nabla\cdot\boldsymbol{u}\|_{1,\Omega} \leq C\left(\|\boldsymbol{f}\|_{0,\Omega}+\|\boldsymbol{g}\|_{0,\Gamma_D}\right). \tag{5.31}$$

This allows the right-hand side of (5.30) to be bounded independent of λ, thus confirming the locking-free behaviour of the DG formulation in the incompressible limit.

A similar estimate for the transversely isotropic problem is not available; however, one would expect that an analogous estimate would allow the terms of the form

$$(\mu_t^2+\alpha^2+\gamma^2)|\boldsymbol{u}|^2_{2,\Omega}+(\lambda^2+\alpha^2)|\nabla\cdot\boldsymbol{u}|^2_{1,\Omega}+(\alpha^2+\beta^2)|\boldsymbol{M}:\boldsymbol{\varepsilon}(\boldsymbol{u})|^2_{1,\Omega} \tag{5.32}$$

to be bounded independent of λ and β.

The presence of β in the first term of (5.29) suggests that locking may occur in the inextensible limit. Numerical experiments discussed in Chapter 6 will explore these features.

The term that leads to the undesirable β-dependence in the error bound is term VI in (5.25). To circumvent the β-dependence, one would need to find a way to modify the formulation in such a way that this term is eliminated. We do so in the following section by making use of selective under-integration.

5.3 Under-integration

It has been shown in [19] that, for the case of isotropy and using bilinear elements, the undesirable λ-dependency of the error bound in the incompressible limit may be circumvented by under-integrating the problematic terms. The same approach is used here in order to overcome locking in the extensible limit: the β-stabilization term VI will be under-integrated.

We will adopt a form of the formulation in which the bilinear form is given by (5.6) with k_μ replaced by $2k + k_\mu$ and all other stabilization parameters are equal to k, assuming $k, k_\mu > 0$.

The resulting bilinear form is then,

$$\bar{a}_h(\boldsymbol{u}, \boldsymbol{v}) := a_h(\boldsymbol{u}, \boldsymbol{v}) + \mu_t \sum_{E \in \Gamma_{iD}} \frac{k_\mu}{h_E} \int_E \lfloor \boldsymbol{u} \rfloor : \lfloor \boldsymbol{v} \rfloor \, ds. \tag{5.33}$$

Note that this bilinear form is coercive, as is easily established using Theorem 5.2.5.

If we define by Π_0 the $\mathcal{L}^2$-orthogonal projection onto the space of constants, the new DG formulation with under-integration is:

$$\bar{a}_h^{UI}(\boldsymbol{u}, \boldsymbol{v}) = l_h^{UI}(\boldsymbol{v})$$

where

$$\bar{a}_h^{UI}(\boldsymbol{u}, \boldsymbol{v}) = \bar{a}_h(\boldsymbol{u}, \boldsymbol{v}) + k\beta \sum_{E \in \Gamma_{iD}} \frac{1}{h_E} \int_E (\boldsymbol{M} : \lfloor \boldsymbol{u} \rfloor)(\Pi_0 - \boldsymbol{I})(\boldsymbol{M} : \lfloor \boldsymbol{v} \rfloor) \, ds, \tag{5.34}$$

and

$$l_h^{UI}(\boldsymbol{v}) = l_h(\boldsymbol{v}) + k\beta \sum_{E \in \Gamma_D} \frac{1}{h_E} \int_E (\boldsymbol{M} : \boldsymbol{g} \otimes \boldsymbol{n})(\Pi_0 - \boldsymbol{I})(\boldsymbol{M} : \boldsymbol{v} \otimes \boldsymbol{n}) \, ds. \tag{5.35}$$

Note that under-integration of the edge term $\int_E \lfloor \cdot \rfloor : \{\boldsymbol{\sigma}(\cdot)\} \, ds$ is not necessary since for any $\boldsymbol{u} \in [\mathcal{P}_1(\Omega_e)]^d$, the integrand is linear, so that one-point integration is exact.

The effect of the formulation (5.34) is to replace the term VI in (5.25) with

$$\begin{aligned} VI^{UI} &:= k|\beta| \left| \sum_{E \in \Gamma_{iD}} \frac{1}{h_E} \int_E \Pi_0(\boldsymbol{M} : \lfloor \boldsymbol{\eta} \rfloor) \Pi_0(\boldsymbol{M} : \lfloor \boldsymbol{\xi} \rfloor) \, ds \right| \\ &= k|\beta| \left| \sum_{E \in \Gamma_{iD}} \frac{1}{h_E} \Pi_0(\boldsymbol{M} : \lfloor \boldsymbol{\xi} \rfloor) \boldsymbol{M} : \int_E \lfloor \boldsymbol{\eta} \rfloor \, ds \right| \\ &= 0. \end{aligned}$$

Thus these terms will also have no contribution to the error bound, as desired.

However, this has involved modification of the DG formulation itself, so that it is necessary to show coercivity and consistency of the modified bilinear form.

5.3.1 Consistency

With the continuous exact solution $\boldsymbol{u} \in [\mathcal{H}^2(\Omega)]^d$ satisfying properties given in Section 5.2.3, we have

$$\overline{a}_h^{UI}(\boldsymbol{u},\boldsymbol{v}) - l_h^{UI}(\boldsymbol{v}) = \sum_{\Omega_e\in\mathcal{T}_h}\int_{\Omega_e}\boldsymbol{\sigma}(\boldsymbol{u}):\boldsymbol{\varepsilon}(\boldsymbol{v})\,dx - \sum_{E\in\Gamma_{iD}}\int_E\{\boldsymbol{\sigma}(\boldsymbol{u})\}:\lfloor\boldsymbol{v}\rfloor\,ds - \sum_{\Omega_e\in\mathcal{T}_h}\int_{\Omega_e}\boldsymbol{f}\cdot\boldsymbol{v}\,dx - \sum_{E\in\Gamma_N}\int_E\boldsymbol{h}\cdot\boldsymbol{v}\,ds.$$

Since $\boldsymbol{u}$ satisfies the weak form,

$$\begin{aligned}\sum_{\Omega_e\in\mathcal{T}_h}\int_{\Omega_e}\boldsymbol{\sigma}(\boldsymbol{u}):\boldsymbol{\varepsilon}(\boldsymbol{v})\,dx &= \sum_{\Omega_e\in\mathcal{T}_h}\int_{\Omega_e}\boldsymbol{f}\cdot\boldsymbol{v}\,dx + \sum_{\Omega_e\in\mathcal{T}_h}\int_{\partial\Omega_e}\boldsymbol{\sigma}(\boldsymbol{u}):\boldsymbol{v}\otimes\boldsymbol{n}\,ds\\ &= \sum_{\Omega_e\in\mathcal{T}_h}\int_{\Omega_e}\boldsymbol{f}\cdot\boldsymbol{v}\,dx + \sum_{E\in\Gamma}\int_E\{\boldsymbol{\sigma}(\boldsymbol{u})\}:\lfloor\boldsymbol{v}\rfloor\,ds + \sum_{E\in\Gamma_i}\int_E\lfloor\boldsymbol{\sigma}(\boldsymbol{u})\rfloor\cdot\{\boldsymbol{v}\}\,ds\\ &= \sum_{\Omega_e\in\mathcal{T}_h}\int_{\Omega_e}\boldsymbol{f}\cdot\boldsymbol{v}\,dx + \sum_{E\in\Gamma_{iD}}\int_E\{\boldsymbol{\sigma}(\boldsymbol{u})\}:\lfloor\boldsymbol{v}\rfloor\,ds + \sum_{E\in\Gamma_N}\int_E\boldsymbol{h}\cdot\boldsymbol{v}\,ds.\end{aligned}$$

Therefore,

$$\overline{a}_h^{UI}(\boldsymbol{u},\boldsymbol{v}) - l_h^{UI}(\boldsymbol{v}) = 0$$

as desired.

5.3.2 Coercivity

Each IP method will be investigated separately.

NIPG $(\theta = 1)$ We have

$$\begin{aligned}\overline{a}_h^{UI}(\boldsymbol{v},\boldsymbol{v}) = &\sum_{\Omega_e\in\mathcal{T}_h}\int_{\Omega_e}\mathbb{C}\boldsymbol{\varepsilon}(\boldsymbol{v}):\boldsymbol{\varepsilon}(\boldsymbol{v})\,dx + \sum_{E\in\Gamma_{iD}}\frac{k}{h_E}\int_E\mathbb{C}\lfloor\boldsymbol{v}\rfloor:\lfloor\boldsymbol{v}\rfloor\,ds + \mu_t\sum_{E\in\Gamma_{iD}}\frac{k_\mu}{h_E}\int_E||\lfloor\boldsymbol{v}\rfloor||^2\,ds\\ &+\beta\sum_{E\in\Gamma_{iD}}\frac{k}{h_E}\int_E(\Pi_0-\boldsymbol{I})\big(\boldsymbol{M}:\lfloor\boldsymbol{v}\rfloor\big)\big(\boldsymbol{M}:\lfloor\boldsymbol{v}\rfloor\big)\,ds\\ =&a_h(\boldsymbol{v},\boldsymbol{v}) + \mu_t\sum_{E\in\Gamma_{iD}}\frac{k_\mu}{h_E}\int_E||\lfloor\boldsymbol{v}\rfloor||^2\,ds + \beta\sum_{E\in\Gamma_{iD}}\frac{k}{h_E}\int_E(\Pi_0-\boldsymbol{I})\big(\boldsymbol{M}:\lfloor\boldsymbol{v}\rfloor\big)\big(\boldsymbol{M}:\lfloor\boldsymbol{v}\rfloor\big)\,ds,\end{aligned} \tag{5.36}$$

note that $a_h(\boldsymbol{v},\boldsymbol{v})$ is defined as in (5.9).

We define

$$\mathscr{B} := \mu_t \sum_{E\in\Gamma_{iD}} \frac{k_\mu}{h_E} \int_E |\lfloor \boldsymbol{v} \rfloor|^2 \, ds + \beta \sum_{E\in\Gamma_{iD}} \frac{k}{h_E} \int_E (\Pi_0 - \boldsymbol{I})\big(\boldsymbol{M} : \lfloor \boldsymbol{v} \rfloor\big)\big(\boldsymbol{M} : \lfloor \boldsymbol{v} \rfloor\big) \, ds. \tag{5.37}$$

For ease, we set $\boldsymbol{m} = \boldsymbol{v}_i - \boldsymbol{v}_e$ and denote by $\boldsymbol{n}$ the outward unit normal vector, giving

$$\begin{aligned} |\lfloor \boldsymbol{v} \rfloor|^2 &= |\boldsymbol{m} \otimes \boldsymbol{n}|^2 = \boldsymbol{m}\cdot\boldsymbol{m}, \\ \boldsymbol{M} : \lfloor \boldsymbol{v} \rfloor &= (\boldsymbol{a}\otimes\boldsymbol{a}) : (\boldsymbol{m}\otimes\boldsymbol{n}) = (\boldsymbol{a}\cdot\boldsymbol{m})(\boldsymbol{a}\cdot\boldsymbol{n}). \end{aligned}$$

Then

$$\mathscr{B} = \mu_t \sum_{E\in\Gamma_{iD}} \frac{k_\mu}{h_E} \int_E \boldsymbol{m}\cdot\boldsymbol{m} \, ds + \beta \sum_{E\in\Gamma_{iD}} \frac{k}{h_E} \int_E \Big((\Pi_0 - \boldsymbol{I})(\boldsymbol{a}\cdot\boldsymbol{m})\Big)^2 (\boldsymbol{a}\cdot\boldsymbol{n})^2 \, ds. \tag{5.38}$$

We have

$$\begin{aligned} \boldsymbol{m}\cdot\boldsymbol{m} &\geq (\boldsymbol{a}\cdot\boldsymbol{m})^2 \\ &\geq (\boldsymbol{a}\cdot\boldsymbol{m})^2(\boldsymbol{a}\cdot\boldsymbol{n})^2 \qquad \text{(since } (\boldsymbol{a}\cdot\boldsymbol{n})^2 \leq 1\text{)} \\ &= (\boldsymbol{a}\cdot\boldsymbol{n})^2 \left(\frac{1}{2}(\boldsymbol{a}\cdot\boldsymbol{m})^2 + \frac{1}{2}(\boldsymbol{a}\cdot\boldsymbol{m})^2\right). \end{aligned}$$

Noting that

$$\int_E \Big(\Pi_0(\bullet)\Big)^2 ds \leq \int_E \bullet^2 \, ds,$$

then we have

$$\int_E \boldsymbol{m}\cdot\boldsymbol{m} \, ds \geq \int_E (\boldsymbol{a}\cdot\boldsymbol{n})^2 \left(\frac{1}{2}(\boldsymbol{a}\cdot\boldsymbol{m})^2 + \frac{1}{2}\Big(\Pi_0(\boldsymbol{a}\cdot\boldsymbol{m})\Big)^2\right) ds. \tag{5.39}$$

Going back to (5.38), using (5.39), we obtain

$$\mathscr{B} \geq \sum_{E\in\Gamma_{iD}} \frac{1}{h_E} \int_E (\boldsymbol{a}\cdot\boldsymbol{n})^2 \left[\left(\frac{k_\mu \mu_t}{2} - k\beta\right)(\boldsymbol{a}\cdot\boldsymbol{m})^2 + \left(\frac{k_\mu\mu_t}{2} + k\beta\right)\Big(\Pi_0(\boldsymbol{a}\cdot\boldsymbol{m})\Big)^2\right] ds.$$

The term on the right-hand-side is non-negative if

$$\begin{cases} \dfrac{k_\mu \mu}{2} - k\beta \geq 0, \\ \dfrac{k_\mu \mu}{2} + k\beta \geq 0, \end{cases} \quad \Leftrightarrow \quad \frac{2k|\beta|}{\mu_t} \leq k_\mu. \tag{5.40}$$

Going back to (5.36), by choosing k and k_μ as in (5.40), we have

$$\overline{a}_h^{UI}(\boldsymbol{v},\boldsymbol{v}) \geq a_h(\boldsymbol{v},\boldsymbol{v}).$$

From (5.11), we have

$$\overline{a}_h^{UI}(\boldsymbol{v},\boldsymbol{v}) \geq K||\boldsymbol{v}||_{DG}^2,$$

with

$$K = \Lambda_{min} \min\{1, 2k\}. \tag{5.41}$$

Thus, the under-integrated NIPG formulation is coercive.

SIPG $(\theta = -1)$ We have

$$\begin{aligned}\overline{a}_h^{UI}(\boldsymbol{v},\boldsymbol{v}) = &\sum_{\Omega_e \in \mathcal{T}_h} \int_{\Omega_e} \mathbb{C}\boldsymbol{\varepsilon}(\boldsymbol{v}) : \boldsymbol{\varepsilon}(\boldsymbol{v})\, dx - 2 \sum_{E\in\Gamma_{iD}} \int_E \lfloor \boldsymbol{v} \rfloor : \{\mathbb{C}\boldsymbol{\varepsilon}(\boldsymbol{v})\}\, ds + \sum_{E\in\Gamma_{iD}} \frac{k}{h_E} \int_E \mathbb{C}\lfloor \boldsymbol{v} \rfloor : \lfloor \boldsymbol{v} \rfloor\, ds \\ &+ \mu_t \sum_{E\in\Gamma_{iD}} \frac{k_\mu}{h_E} \int_E |\lfloor \boldsymbol{v} \rfloor|^2\, ds + \beta \sum_{E\in\Gamma_{iD}} \frac{k}{h_E} \int_E (\Pi_0 - \boldsymbol{I})\big(\boldsymbol{M} : \lfloor \boldsymbol{v} \rfloor\big)\big(\boldsymbol{M} : \lfloor \boldsymbol{v} \rfloor\big)\, ds \\ =&a_h(\boldsymbol{v},\boldsymbol{v}) + \mathscr{B},\end{aligned}$$

note that $a_h(\boldsymbol{v},\boldsymbol{v})$ is defined as in (5.13), and $\mathscr{B}$ as in (5.37).

From the NIPG coercivity proof above, for k and k_μ that satisfy (5.40), we have

$$\overline{a}_h^{UI}(\boldsymbol{v},\boldsymbol{v}) \geq a_h(\boldsymbol{v},\boldsymbol{v}).$$

From (5.15), we have:

$$\overline{a}_h^{UI}(\boldsymbol{v},\boldsymbol{v}) \geq K||\boldsymbol{v}||_{DG}^2,$$

with

$$K = m\Lambda_{min}, \tag{5.42}$$

such that $0 < m < 1$ and $k \geq \frac{m}{2} + \frac{C}{1-m}$, for a positive constant C to be determined.

IIPG $(\theta = 0)$ The proof of coercivity for IIPG with under-integration case is identical to that for the SIPG with under-integration case up to a constant.

5.3.3 Theorem. *The bilinear functional* $\overline{a}_h^{UI}(\cdot,\cdot)$ *defined in* (5.34) *is coercive if, for* $k, k_\mu > 0$

(a) when $\theta = 1$,

$$\frac{2k|\beta|}{\mu_t} \leq k_\mu;$$

(b) when $\theta \in \{-1, 0\}$,

$$\frac{2k|\beta|}{\mu_t} \leq k_\mu, \quad \text{and} \quad k \geq \frac{m}{2} + \frac{C}{1-m},$$

where C is a positive constant to be calculated, and $0 < m < 1$.

Error bound The approximation error is now bounded as follows:

$$||\boldsymbol{e}||_{DG}^2 \leq \frac{C}{K^2} h^2 \Big((\mu_t^2 + \gamma^2) |\boldsymbol{u}|_{2,\Omega}^2 + (\lambda^2 + \alpha^2) |\nabla \cdot \boldsymbol{u}|_{1,\Omega}^2 + (\alpha^2 + \beta^2) |\boldsymbol{M} : \boldsymbol{\varepsilon}(\boldsymbol{u})|_{1,\Omega}^2 \Big), \tag{5.43}$$

where K is the coercivity constant defined by (5.41) for NIPG case, and by (5.42) for SIPG and IIPG cases.

The first term on the right-hand side is independent of β. The bound (5.43) is now in a form that would be expected to lead to a uniform estimate, by analogy with the bound (5.31). The behaviour of the under-integrated DG formulation will be explored further in the next chapter.

Chapter 6

Numerical tests for discontinuous Galerkin approximations

In this chapter, we present a series of results to illustrate the various features discussed in Chapter 5. For material parameters that satisfy the pointwise conditions (2.57), we first investigate the behaviour of compressible and nearly incompressible materials with reference to Table 2.1. Next, we explore the behaviour of nearly inextensible materials.

We reconsider here the examples described in Chapter 4, that is, the Cook's membrane problem and the beam problem.

All examples are under conditions of plane strain and based on three- and six-noded triangular elements with standard linear and quadratic interpolation of the displacement field.

6.1 Material parameters

The choice for the values of the parameters are the same as those used in Chapter 4: that is, we set $\nu_l = \nu_t = \nu$ and $\gamma = 0$. Furthermore, we investigate behaviour for $\nu = -0.5$ and 0.3, and for the range of values of p that comply with the pointwise stability conditions (2.57). We also study the response for $\nu = 0.49995$ and $p \geq 1$, noting that standard approaches lead to volumetric locking behaviour in the limiting case of isotropy, with $p = 1$.

The conditions for coercivity in Chapter 5 assume equal values of the stabilization parameter for all terms except that involving μ_t. These are sufficient conditions that do not account, for example, for situations in which some or all of the other material parameters are positive. In such situations there is greater flexibility in the choice of the stabilization parameters. We have adopted the following choices, which are found to lead to stable approximations:

For $\nu = 0.49995$ and $\nu = 0.3$, we choose $k_\mu = k_\alpha = k_\gamma = 10$, and $k_\lambda = k_\beta = 100$.

For $\nu = -0.5$, we choose $k_\mu = k_\lambda = k_\beta = k_\gamma = 10$, and $k_\alpha = 100$.

The results in the examples that follow are for the following element choices:

$Exact$	The analytical solution
P_1_CG	The standard displacement formulation of order 1
P_2_CG	The standard displacement formulation of order 2
P_1_NIPG	The non-symmetric interior penalty method of order 1
P_1_SIPG	The symmetric interior penalty method of order 1
P_1_IIPG	The incomplete interior penalty method of order 1
$P_1\_NIPG\_UI_\beta$	The non-symmetric interior penalty method of order 1 with under-integration of the β- stabilization term
$P_1\_SIPG\_UI_\beta$	The symmetric interior penalty method of order 1 with under-integration of the β- stabilization term
$P_1\_IIPG\_UI_\beta$	The incomplete interior penalty method of order 1 with under-integration of the β- stabilization term

6.2 Cook's membrane

The problem is defined as in Section 4.2. A mesh of 32×32 elements is used.

To investigate locking of the proposed formulations, we compare the results with those obtained using the standard P_2-element.

Figures 6.1 and 6.2 show semilog plots of the tip displacement vs p for various fibre directions for $\nu = 0.3$ and $\nu = -0.5$. For small values of p, $(0.35 \le p \le 3)$ as shown in the left figures, the conforming method P_1_CG is locking-free. For high values of p, $(4 \le p \le 10^7)$, as shown in the right figures, the conforming P_1_CG and all three IPDG methods show locking behaviour which is avoided when the extensional stabilization terms are under-integrated. We note the extensional locking behaviour of the P_2-element.

Figure 6.3 shows semilog plots of the tip displacement vs p for a range of fibre angles, for the various element choices, and for moderate and high values of p. For moderate values of p $(1 \le p \le 5)$, all three IPDG methods show no locking. For higher values of p $(10 \le p \le 10^5)$, all three IPDG methods show locking behaviour with an increase in p. On the other hand, locking is avoided for the under-integrated formulations, for larger values of p. Figure 6.4 shows tip displacements for various fibre orientations, where the degree of anisotropy is fixed at $p = 10^5$ (left) and at $p = 10^7$ (right). Some deterioration in accuracy is observed for the conforming P_2-element as in the case of the Q_2-element in Section 4.2.

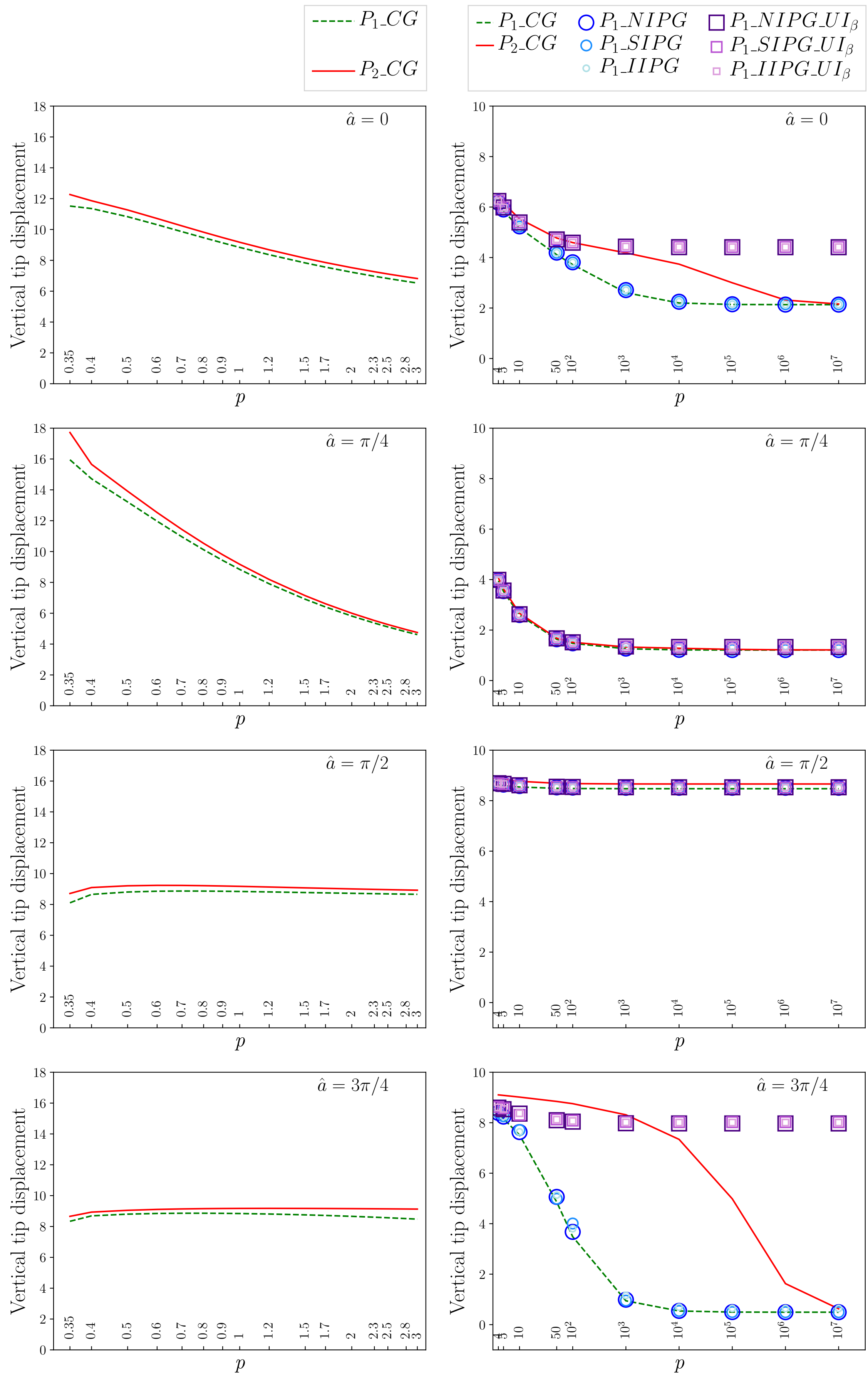

Figure 6.1: Tip displacement vs p for the Cook's membrane problem, with $\nu = 0.3$, for moderate (left) and high (right) values of p

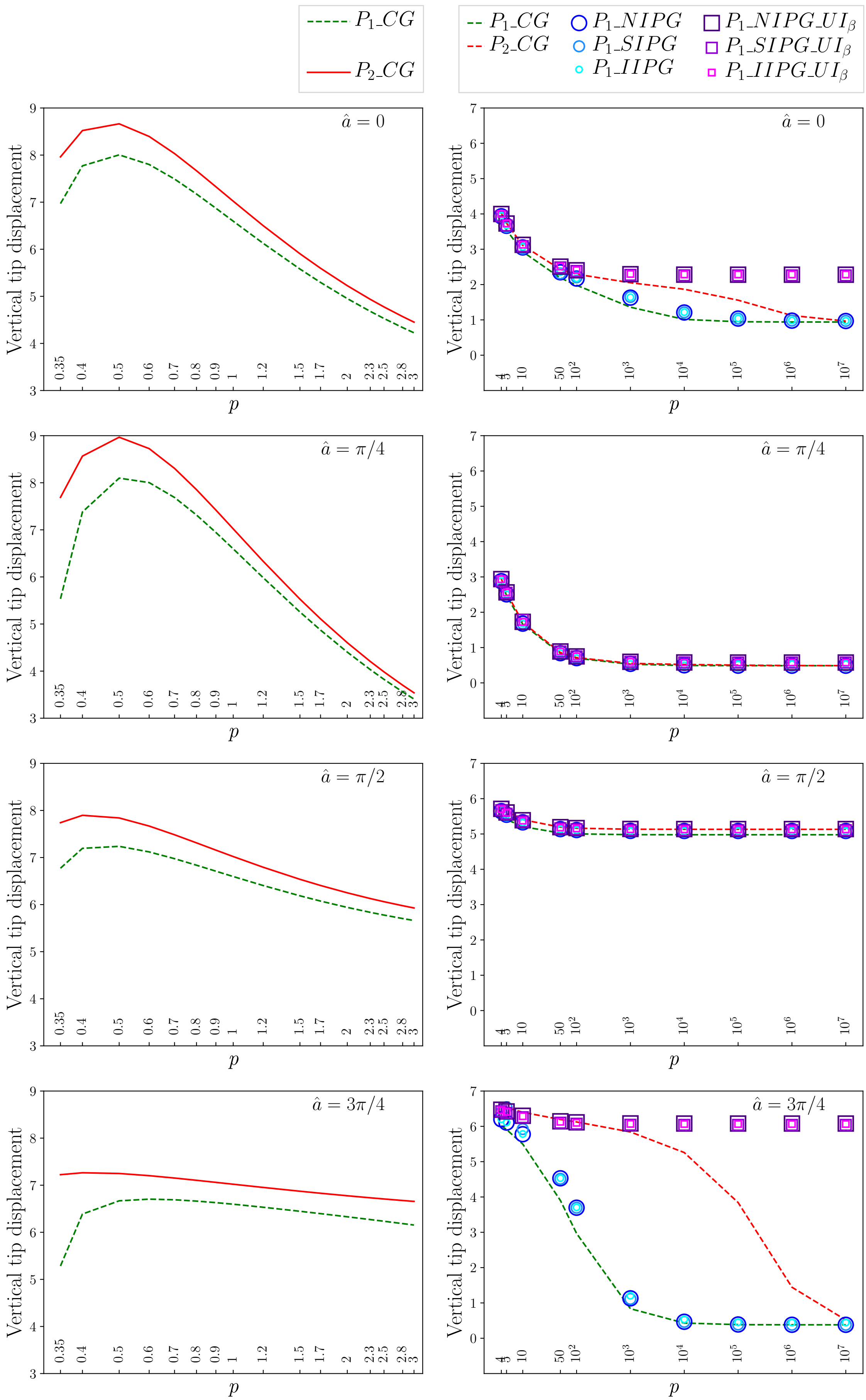

Figure 6.2: Tip displacement vs p for the Cook's membrane problem, with $\nu = -0.5$, for moderate (left) and high (right) values of p

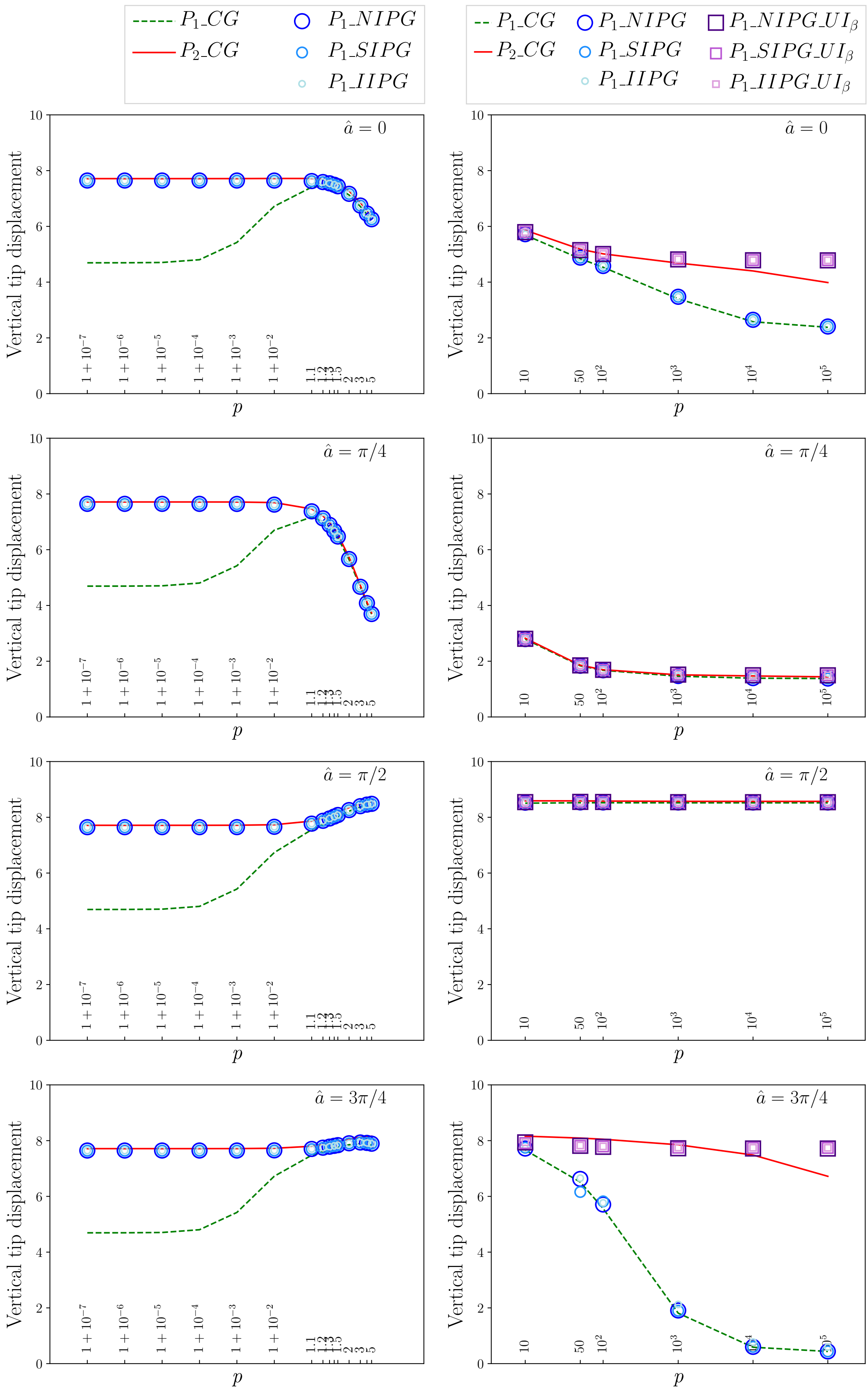

Figure 6.3: Tip displacement vs p for the Cook's membrane problem, with $\nu = 0.49995$. For moderate (left), and high (right) values of p

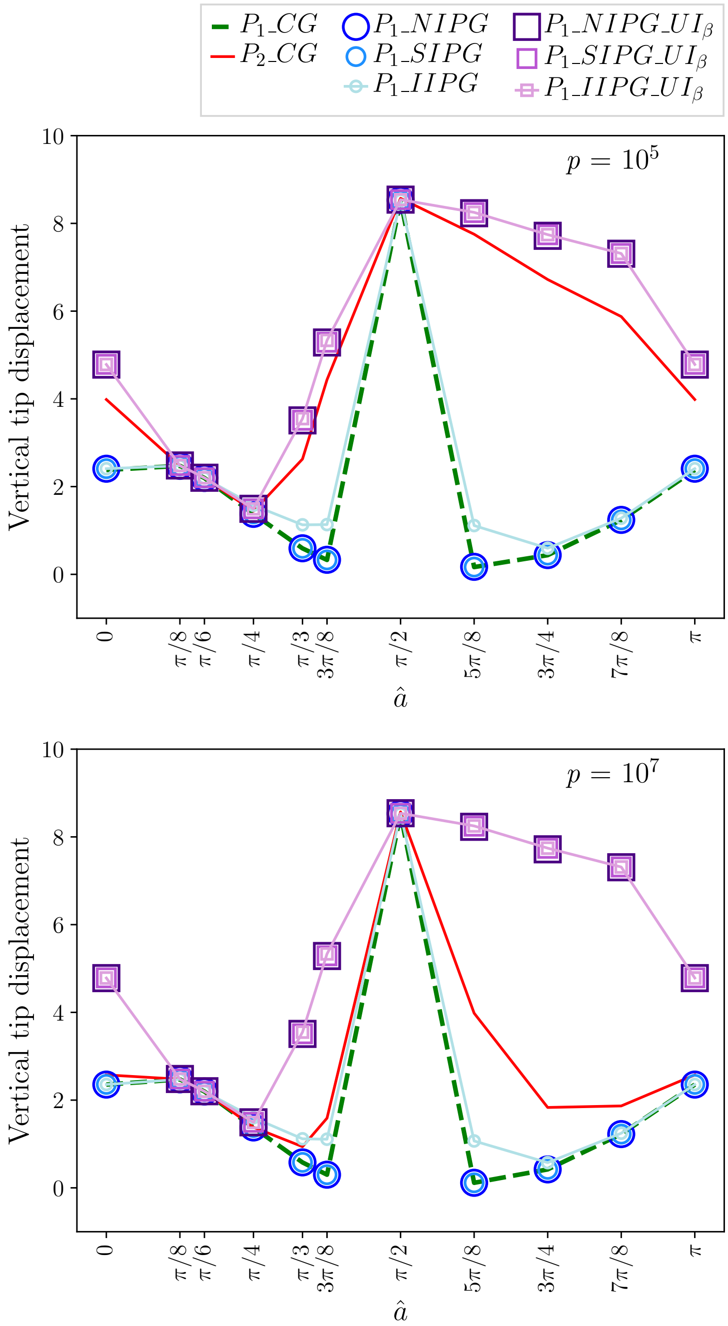

Figure 6.4: Tip displacement for Cook's membrane problem measured at different fibre orientations, for $p = 10^5$ (left) and for $p = 10^7$ (right), with $\nu = 0.49995$

6.3 Bending of a beam

The problem is defined as in Section 4.3. A mesh of 80×16 is used. Locking behaviour is investigated by comparison with the analytical solution.

Figures 6.1 and 6.2 show semilog plots of the tip displacement vs p for various directions fibre for $\nu = 0.3$ and $\nu = -0.5$ respectively. Similar behaviour as in the case of Cook's membrane is depicted; that is, uniform convergence of the conforming method for small values of p, $(0.35 \leq p \leq 3)$ as shown in the left figures, and locking of P_1_CG and all three IPDG methods for high values of p, $(4 \leq p \leq 10^7)$, which is overcome by under-integrating the extensional stabilization terms. For small values of p, $(0.35 \leq p \leq 3)$ as shown in the left figures, the conforming method P_1_CG is locking-free.

In Figure 6.7, which shows semilog plots of tip displacement for different values of p, with various fibre directions. The same behaviour as appears for the Cook's example is seen, i.e. the expected locking of P_1_CG as p approaches 1 is overcome by using IPDG methods (left figures). For high values of p there is a purely extensional locking with all IPDG methods, which is overcome by using under-integration of β-stabilization terms (right figures).

Figure 6.8 shows tip displacements for various fibre orientations where the degree of anisotropy is fixed at $p = 10^7$. We recall the same behaviour as stated in Section 4.3, that is, extensional locking for P_1_CG except for the angles 0, where the material is very stiff, and $\pi/2$, where the extensional term is bounded.

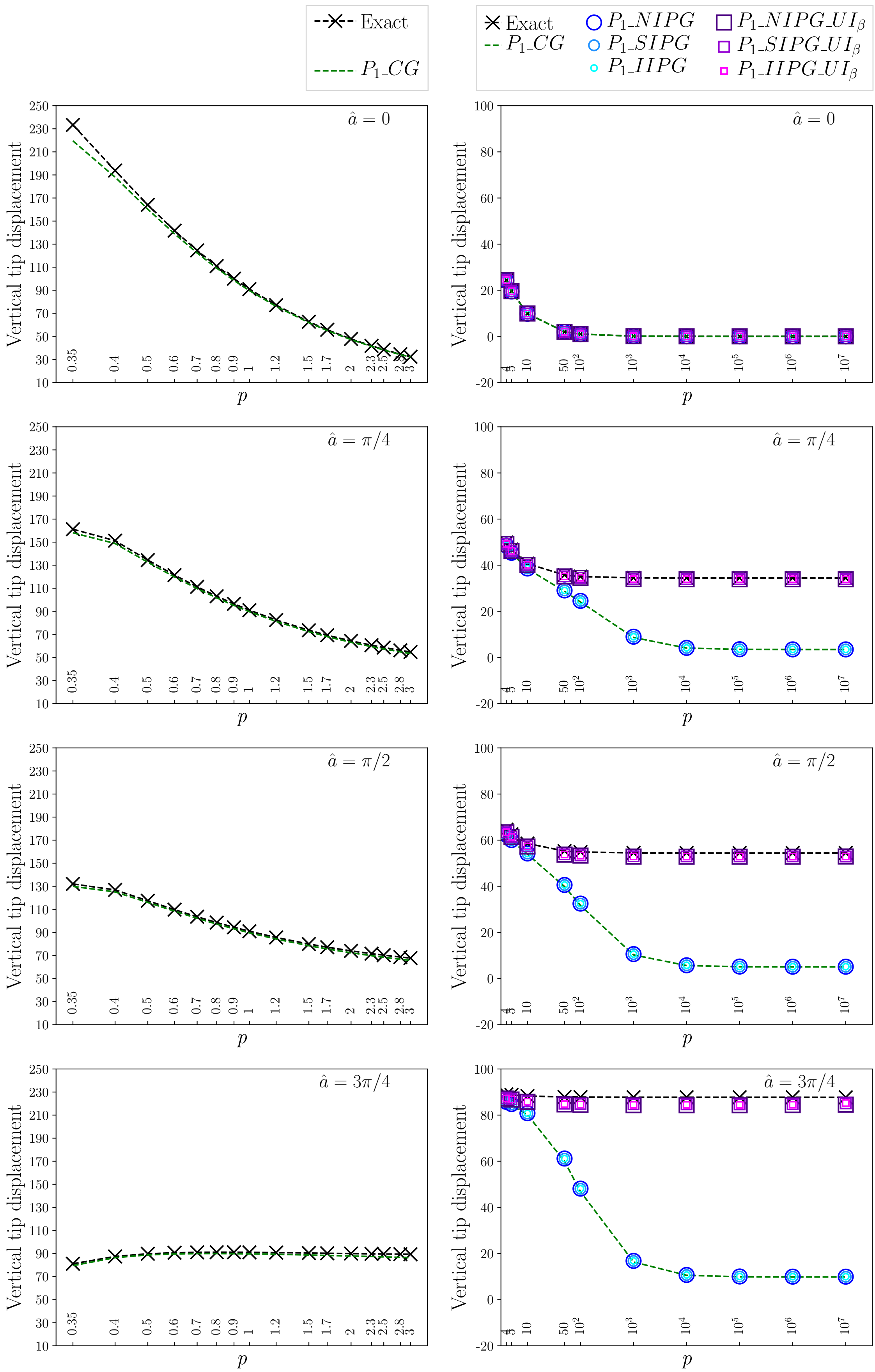

Figure 6.5: Tip displacement vs p for the beam problem, with $\nu = 0.3$, for moderate (left) and high (right) values of p

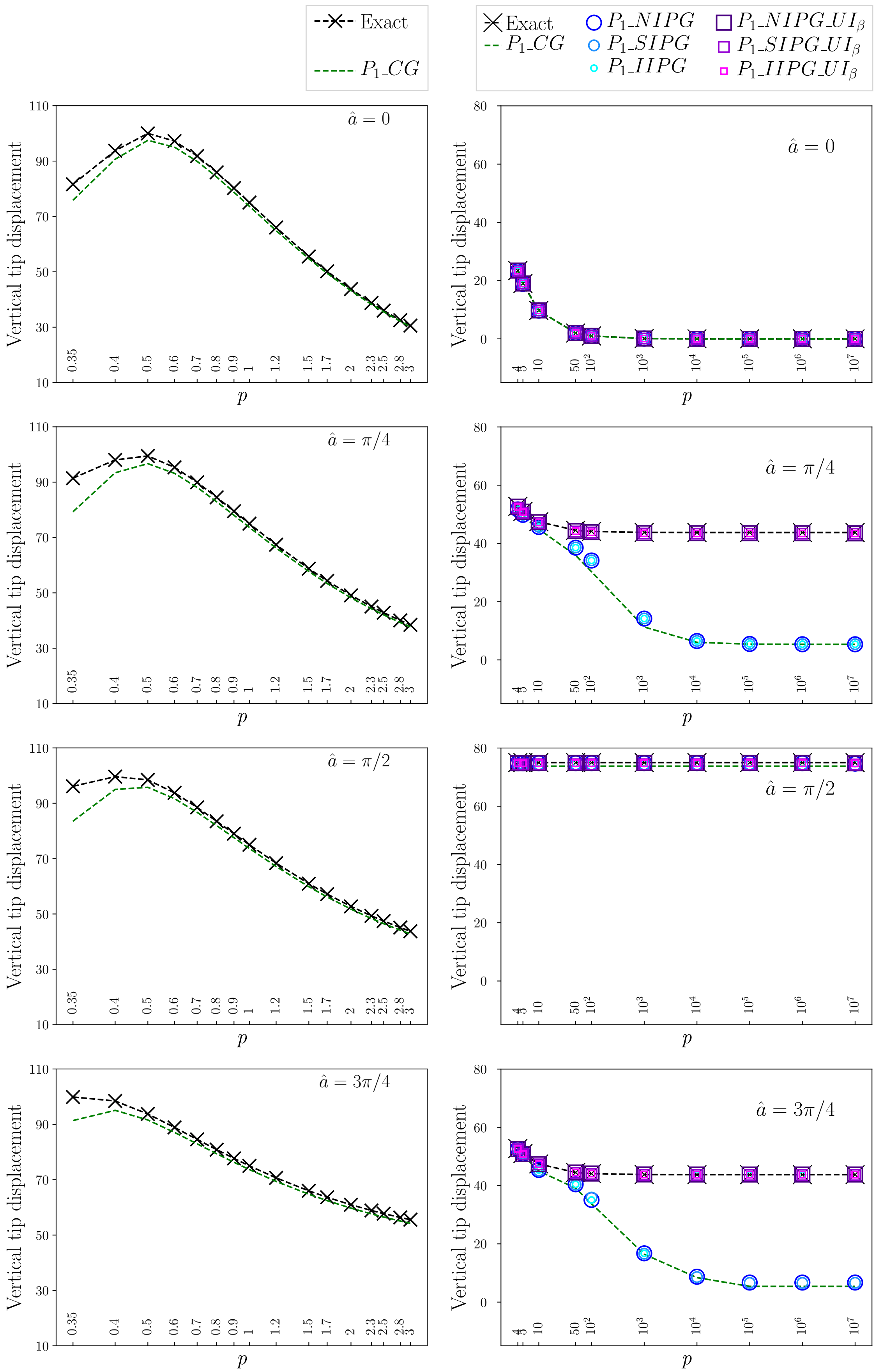

Figure 6.6: Tip displacement vs p for the beam problem, with $\nu = -0.5$, for moderate (left) and high (right) values of p

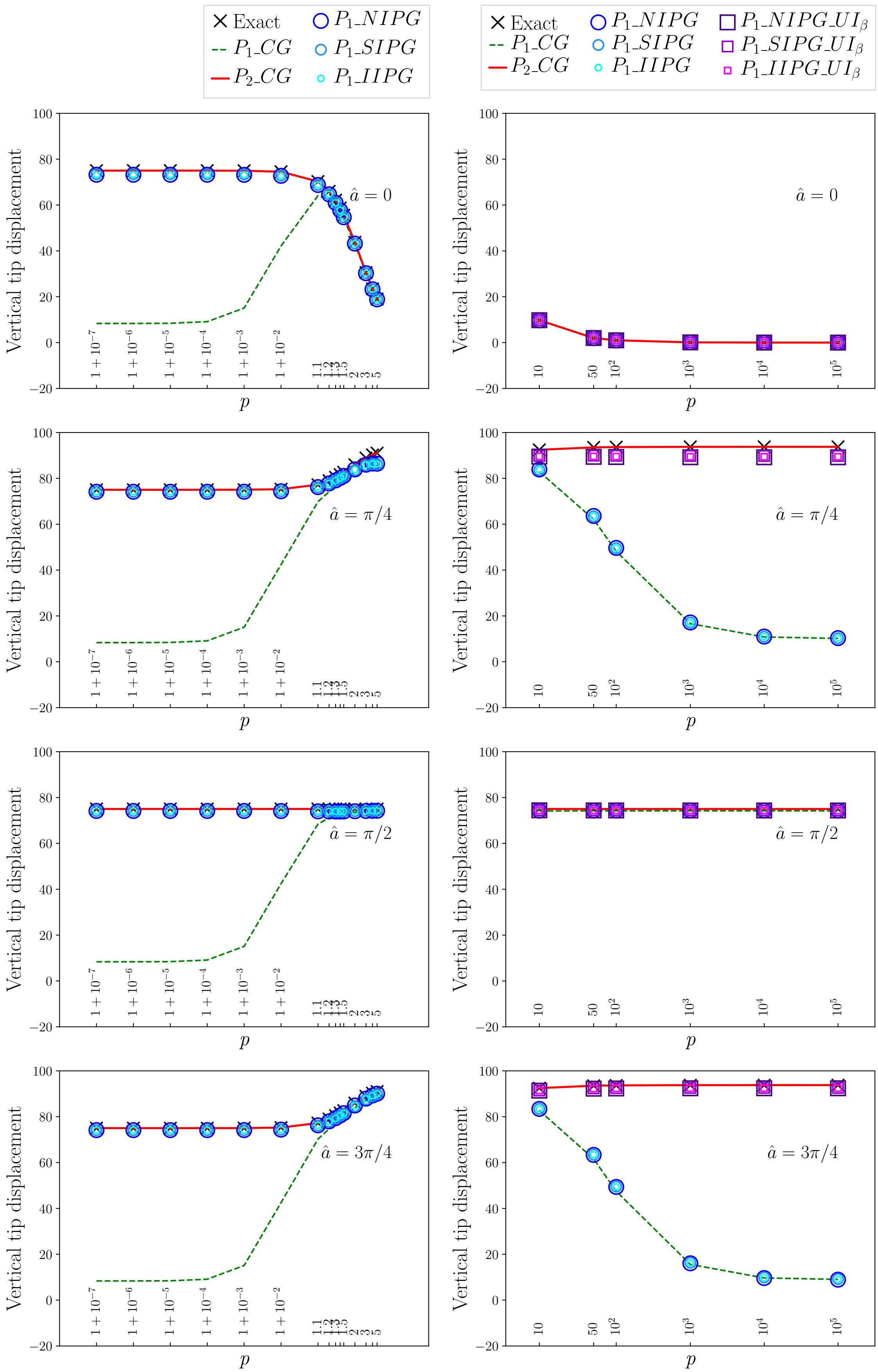

Figure 6.7: Tip displacement vs p for the beam problem, with $\nu = 0.49995$. Moderate (left), and high (right) values of p

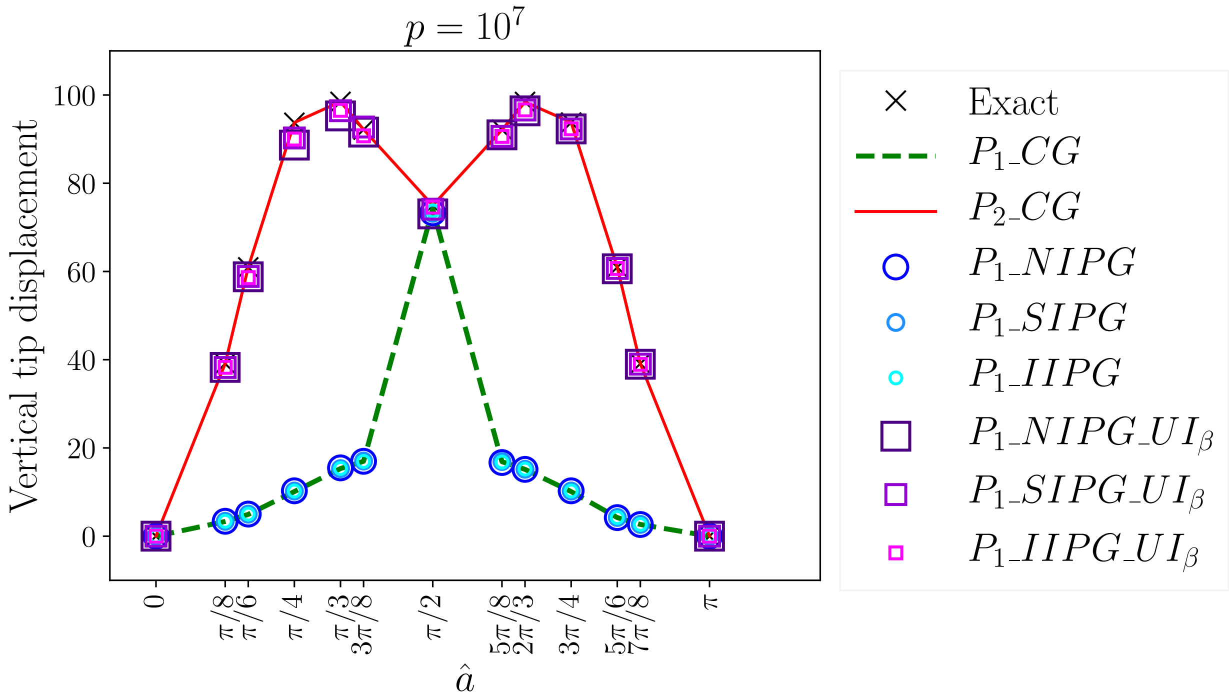

Figure 6.8: Tip displacement for the beam problem measured at different fibre orientations, for $p = 10^7$ and $\nu = 0.49995$

The following set of results, Figure 6.9-6.10, show behaviour for various fibre orientations, and for values of p. The $\mathcal{H}^1$-relative error as defined by (4.1) is mesured.

The left figures show the $\mathcal{H}^1$ relative error convergence plots for all three IPDG formulations and P_1_CG, for $p = 1.0001$. Here all three IPDG formulations show slightly better than optimal (linear) convergence for any fibre direction. P_1_CG shows poor convergence, indicative of volumetric locking.

The middle figures show the $\mathcal{H}^1$ relative error convergence plots for all three IPDG formulations and P_1_CG, for $p = 3$. Here, all formulations at any fibre direction are linearly convergent.

The right figures show the $\mathcal{H}^1$ relative error convergence plots for all three IPDG formulations and P_1_CG, for $p = 10^4$. P_1_CG and the full IPDG methods show poor convergence, indicative of extensional locking. All three IPDG methods with under-integration show convergence at rate 1.6.

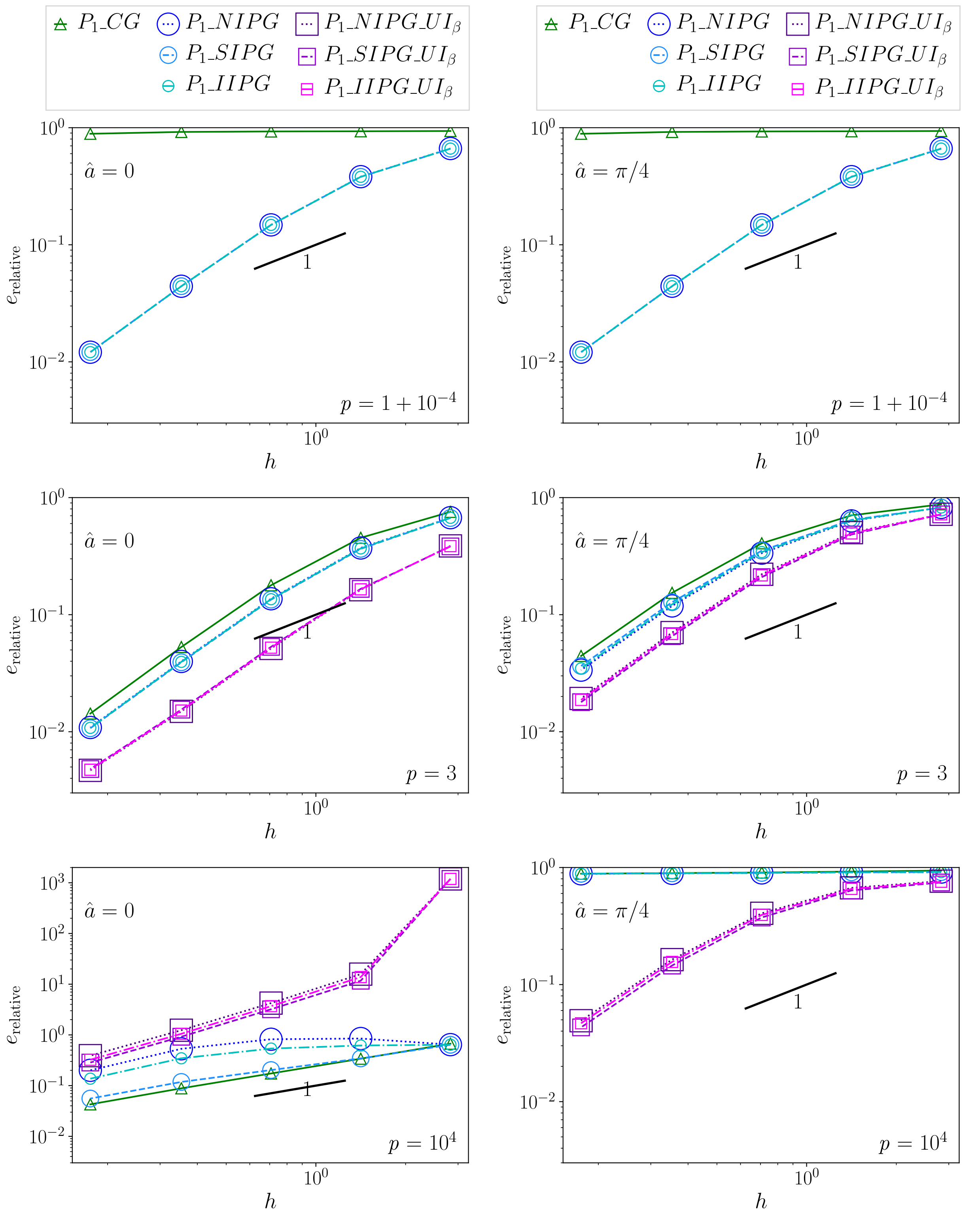

Figure 6.9: Comparison of $\mathcal{H}^1$ errors for conforming and under-integrated elements, for fibre angle 0 (left) and $\pi/4$ (right), with $\nu = 0.49995$. For $p = 1.0001$ (top), $p = 3$ (middle) and $p = 10^4$(bottom)

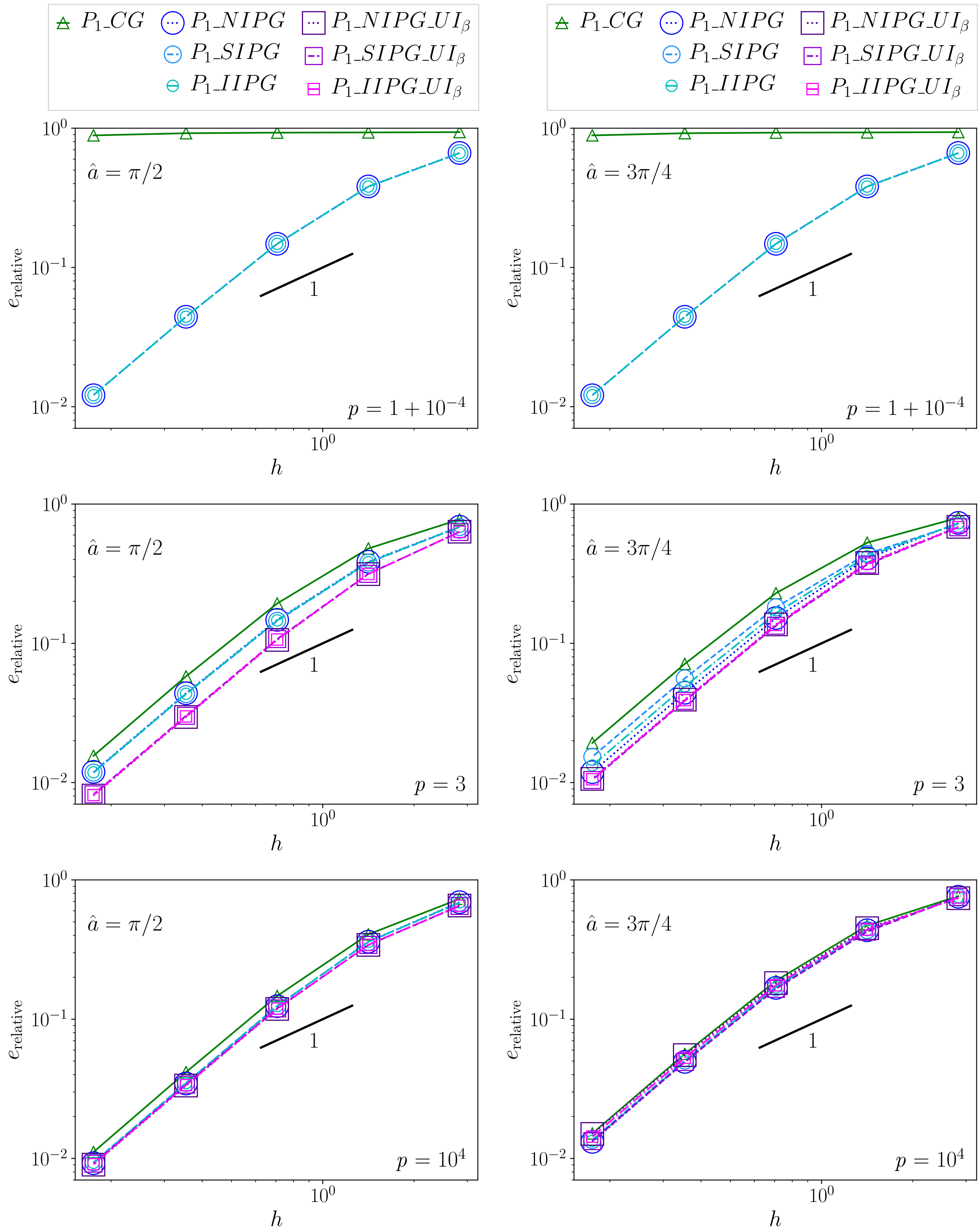

Figure 6.10: Comparison of $\mathcal{H}^1$ errors for conforming and under-integrated elements, for fibre angle $\pi/2$ (left) and $3\pi/4$ (right), with $\nu = 0.49995$. For $p = 1.0001$ (top), $p = 3$ (middle) and $p = 10^4$(bottom)

Chapter 7

Conclusions

This work has been concerned with the development, analysis and implementation of finite element approximations of the boundary value problem for transversely isotropic elastic bodies. Of particular interest have been the conditions under which volumetric and/or extensional locking occur with the use of low-order elements, and the construction of approximations that circumvent locking.

It has first been necessary to undertake a study of the constitutive relations: these have been formulated in terms of five material parameters, beginning with a basic set, and then, a corresponding set of parameters that are largely interpretable physically. Conditions on these parameters for pointwise stability have been established. These conditions have been essential in showing well-posedness of the weak formulation, and of the various discrete formulations considered.

Conforming finite element approximations have been formulated and implemented with the use of low-order (bilinear) quadrilaterals. For moderate values of the parameter that quantifies the degree of anisotropy (that is, the ratio of Young's modulus in the fibre direction to that in the plane of isotropy), behaviour is locking free, as suggested also by an a priori error estimate. As the isotropic limit is approached, the well-known locking behaviour is evident. Locking occurs int the near-inextensible limit. Under-integration of the terms corresponding to volumetric and extensional behaviour leads to locking-free behaviour. The under-integrated formulation is shown to be equivalent to perturbed Lagrangian and mixed formulations. A range of results, for various anisotropy parameters and fibre angles, have been presented to illustrate the behaviour.

The second discrete formulation studied is that of discontinuous Galerkin (DG) approximations. Three interior penalty (IP) approaches: symmetric, nonsymmetric, and incomplete, have been considered. It is well known that, for isotropic materials, behaviour is uniformly convergent in the incompressible limit, with the use of linear triangles. The objective here has been to determine conditions under which locking-free behaviour is achieved for the transversely isotropic case. The volumetric locking-free behaviour of the isotropic case is also evident for the transversely isotropic model. A complete analysis is carried out: the dependence of an error bound on the parameter characterizing high anisotropy suggests locking behaviour, which is indeed observed numerically with the use of standard IP approaches. Under-integration of the edge terms removes this dependence, and computational results for a range of measures of anisotropy and of fibre directions illustrate the locking-free behaviour.

The work presented here has advanced understanding of the mathematical models of transversely isotropic bodies. The extension to the use of a variable fibre direction would bring various challenges, theoretically and numerically. Furthermore, application to other forms of anisotropy, for example to two families of fibres or to orthotropic materials, and extension to the three-dimensional case would also be of high interest, particularly from the computational perspective.

It would be useful to extend the analyses using various formulations. Analyses of the mixed $\mathcal{Q}_1 - \mathcal{P}_0$ (displacement-tension) formulation would complete the numerical approach proposed in Chapter 3. Further investigation on the transversely isotropic problems with other type of mixed formulations, and extension of the DG analyses using lower-order quadrilateral elements would be welcome extension. This work is also intended to be used in exploring theoretically and computationally the large-strain deformation. It is seen in the numerical chapters that the use of P_2- and Q_2- elements might suggest existence of locking in the inextensible limit. Further analytical investigations are required to confirm this.

An a priori estimate analogous to that of Brenner & Sung [8] for the isotropic case was assumed with the DG formulations. The extension to the transversely isotropic case is an open problem.

Finally, when there has been much work on the large-displacement problem, the results in this work present questions that should be posed for large-displacement problems for example, conditions for locking-free behaviour in both displacement-based and mixed formulations.

Appendix A. Closed-form solution for the beam problem

For the beam problem described in Section 4.3, let the exact solution be of the following form

$$\begin{cases} u(x,y) = & A + Bx + Cy + Dxy + Ex^2 + Fy^2, \\ v(x,y) = & G + Hx + Iy + Jxy + Kx^2 + Ly^2. \end{cases}$$

Recall that the boundary conditions are

$$\begin{cases} u(0,y) = g(y), \\ v(0, -\frac{h}{2}) = 0, \end{cases}$$

where

$$g(y) = -\frac{f}{h}\mathbb{S}_{31}\left(y^2 - \frac{h^2}{4}\right),$$

and the linearly varying load $\hat{f}$ with maximum value f is

$$\hat{f}(y) = -\frac{2f}{h}y.$$

Let us first give the expression of each component of the compliance tensor in terms of the components of the elasticity tensor. In Voigt notation, when the fibre direction is aligned with one the axes, we have

$$\mathbb{C} = \begin{pmatrix} \mathbb{C}_{11} & \mathbb{C}_{12} & \mathbb{C}_{13} & 0 & 0 & 0 \\ \mathbb{C}_{12} & \mathbb{C}_{22} & \mathbb{C}_{23} & 0 & 0 & 0 \\ \mathbb{C}_{13} & \mathbb{C}_{23} & \mathbb{C}_{33} & 0 & 0 & 0 \\ 0 & 0 & 0 & \mathbb{C}_{44} & 0 & 0 \\ 0 & 0 & 0 & 0 & \mathbb{C}_{55} & 0 \\ 0 & 0 & 0 & 0 & 0 & \mathbb{C}_{66} \end{pmatrix}$$

Therefore, since $\mathbb{S} = \mathbb{C}^{-1}$

$$
\begin{aligned}
\mathbb{S}_{11} &= \frac{1}{|\mathbb{C}|}(\mathbb{C}_{22}\mathbb{C}_{33} - \mathbb{C}_{23}^2), & \mathbb{S}_{22} &= \frac{1}{|\mathbb{C}|}(\mathbb{C}_{11}\mathbb{C}_{33} - \mathbb{C}_{13}^2), & \mathbb{S}_{44} &= \frac{1}{\mathbb{C}_{44}},\\
\mathbb{S}_{12} &= \frac{1}{|\mathbb{C}|}(\mathbb{C}_{13}\mathbb{C}_{23} - \mathbb{C}_{12}\mathbb{C}_{33}), & \mathbb{S}_{23} &= \frac{1}{|\mathbb{C}|}(\mathbb{C}_{13}\mathbb{C}_{12} - \mathbb{C}_{11}\mathbb{C}_{23}), & \mathbb{S}_{55} &= \frac{1}{\mathbb{C}_{55}},\\
\mathbb{S}_{13} &= \frac{1}{|\mathbb{C}|}(\mathbb{C}_{12}\mathbb{C}_{23} - \mathbb{C}_{13}\mathbb{C}_{22}), & \mathbb{S}_{33} &= \frac{1}{|\mathbb{C}|}(\mathbb{C}_{11}\mathbb{C}_{22} - \mathbb{C}_{12}^2), & S_{66} &= \frac{1}{\mathbb{C}_{66}}.
\end{aligned} \tag{A.1}
$$

with

$$
|\mathbb{C}| = \mathbb{C}_{11}(\mathbb{C}_{22}\mathbb{C}_{33} - \mathbb{C}_{23}^2) - \mathbb{C}_{12}(\mathbb{C}_{12}\mathbb{C}_{33} - \mathbb{C}_{13}\mathbb{C}_{23}) + \mathbb{C}_{13}(\mathbb{C}_{12}\mathbb{C}_{23} - \mathbb{C}_{13}\mathbb{C}_{22}).
$$

From the boundary conditions, we have

$$
u(0, y) = A + Cy + Fy^2 = -\frac{f}{h}\mathbb{S}_{31}\left(y^2 - \frac{h^2}{4}\right).
$$

By identification, we obtain

$$
A = \frac{fh}{4}\mathbb{S}_{31}, \tag{A.2a}
$$

$$
C = 0, \tag{A.2b}
$$

$$
F = -\frac{f}{h}\mathbb{S}_{31}. \tag{A.2c}
$$

We also have

$$
v(0, -\tfrac{h}{2}) = G - I\frac{h}{2} + L\frac{h^2}{4} = 0. \tag{A.3}
$$

The strains and stresses are obtained from

$$
\begin{aligned}
\varepsilon_{11}(x, y) &= \frac{\partial u}{\partial x} = B + Dy + 2Ex,\\
\varepsilon_{22}(x, y) &= \frac{\partial v}{\partial y} = I + Jx + 2Ly,\\
\varepsilon_{12}(x, y) &= \frac{1}{2}\left(\frac{\partial u}{\partial y} + \frac{\partial v}{\partial x}\right) = \frac{1}{2}\big[H + (D + 2K)x + (J + 2F)y\big],
\end{aligned}
$$

and

$$
\begin{aligned}
\sigma_{ij}(x, y) &= \mathbb{C}_{ij11}\varepsilon_{11} + 2\mathbb{C}_{ij12}\varepsilon_{12} + \mathbb{C}_{ij22}\varepsilon_{22}\\
&= \mathbb{C}_{ij11}(B + Dy + 2Ex) + \mathbb{C}_{ij22}(I + Jx + 2Ly) + \mathbb{C}_{ij12}\big[H + (D + 2K)x + (J + 2F)y\big].
\end{aligned}
$$

From the traction boundary conditions, we have

$$\sigma_{11}(l,y) = \mathbb{C}_{11}(B+Dy+2El) + \mathbb{C}_{12}(I+Jl+2Ly) + \mathbb{C}_{13}\big[H+(D+2K)l+(J+2F)y\big] = \hat{f}(y) \quad \text{(A.4)}$$

$$\sigma_{12}(0,y) = \mathbb{C}_{31}(B+Dy) + \mathbb{C}_{32}(I+2Ly) + \mathbb{C}_{33}[H+(J+2F)y] = 0 \quad \text{(A.5)}$$

$$\sigma_{12}(l,y) = \mathbb{C}_{31}(B+Dy+2El) + \mathbb{C}_{32}(I+Jl+2Ly) + \mathbb{C}_{33}\big[H+(D+2K)l+(J+2F)y\big] = 0 \quad \text{(A.6)}$$

$$\sigma_{12}(x,\text{-}\tfrac{h}{2}) = \mathbb{C}_{31}(2B-Dh+4Ex) + 2\mathbb{C}_{32}(I+Jx-Lh) + \mathbb{C}_{33}\big[2H+2(D+2K)x-(J+2F)h\big] = 0 \quad \text{(A.7)}$$

$$\sigma_{12}(x,\tfrac{h}{2}) = \mathbb{C}_{31}(2B+Dh+4Ex) + 2\mathbb{C}_{32}(I+Jx+Lh) + \mathbb{C}_{33}\big[2H+2(D+2K)x+(J+2F)h\big] = 0 \quad \text{(A.8)}$$

$$\sigma_{22}(x,\text{-}\tfrac{h}{2}) = \mathbb{C}_{21}(2B-Dh+4Ex) + 2\mathbb{C}_{22}(I+Jx-Lh) + \mathbb{C}_{23}\big[2H+2(D+2K)x-(J+2F)h\big] = 0 \quad \text{(A.9)}$$

$$\sigma_{22}(x,\tfrac{h}{2}) = \mathbb{C}_{21}(2B+Dh+4Ex) + 2\mathbb{C}_{22}(I+Jx+Lh) + \mathbb{C}_{23}\big[2H+2(D+2K)x+(J+2F)h\big] = 0 \quad \text{(A.10)}$$

The equilibrium equations are:

$$\operatorname{div}\boldsymbol{\sigma} = \begin{pmatrix} \dfrac{\partial\sigma_{11}}{\partial x} + \dfrac{\partial\sigma_{12}}{\partial y} \\ \dfrac{\partial\sigma_{12}}{\partial x} + \dfrac{\partial\sigma_{22}}{\partial y} \end{pmatrix} = \mathbf{0}.$$

We have

$$\begin{aligned} \frac{\partial\sigma_{11}}{\partial x} &= 2\mathbb{C}_{11}E + \mathbb{C}_{12}J + \mathbb{C}_{13}(D+2K), \\ \frac{\partial\sigma_{12}}{\partial y} &= \mathbb{C}_{31}D + 2\mathbb{C}_{32}L + \mathbb{C}_{33}(J+2F), \\ \frac{\partial\sigma_{12}}{\partial x} &= 2\mathbb{C}_{31}E + \mathbb{C}_{32}J + \mathbb{C}_{33}(D+2K), \\ \frac{\partial\sigma_{22}}{\partial y} &= \mathbb{C}_{21}D + 2\mathbb{C}_{22}L + \mathbb{C}_{23}(J+2F), \end{aligned}$$

so that

$$2\mathbb{C}_{11}E + (\mathbb{C}_{12}+\mathbb{C}_{33})J + 2\mathbb{C}_{13}D + 2\mathbb{C}_{13}K + 2\mathbb{C}_{32}L + 2\mathbb{C}_{33}F = 0, \quad \text{(A.11)}$$

$$2\mathbb{C}_{31}E + 2\mathbb{C}_{23}J + (\mathbb{C}_{33}+\mathbb{C}_{21})D + 2\mathbb{C}_{33}K + 2\mathbb{C}_{22}L + 2\mathbb{C}_{23}F = 0. \quad \text{(A.12)}$$

By identification and combination of equations (A.3)-(A.12), we obtain the following system of 10 equations with 9 unknowns:

$$\begin{cases} 4G - 2Ih + Lh^2 = 0, & \text{(A.13a)} \\ \mathbb{C}_{11}B + \mathbb{C}_{13}Dl + 2\mathbb{C}_{11}El + \mathbb{C}_{13}H + \mathbb{C}_{12}I + \mathbb{C}_{12}Jl + 2\mathbb{C}_{13}Kl = 0, & \text{(A.13b)} \\ \mathbb{C}_{11}D + \mathbb{C}_{13}J + 2\mathbb{C}_{12}L = -\dfrac{2f}{h} - 2\mathbb{C}_{13}F, & \text{(A.13c)} \\ \mathbb{C}_{13}B + \mathbb{C}_{33}H + \mathbb{C}_{23}I = 0, & \text{(A.13d)} \\ \mathbb{C}_{13}D + \mathbb{C}_{33}J + 2\mathbb{C}_{23}L = -2\mathbb{C}_{13}F, & \text{(A.13e)} \\ \mathbb{C}_{33}D + 2\mathbb{C}_{13}E + \mathbb{C}_{23}J + 2\mathbb{C}_{33}K = 0, & \text{(A.13f)} \\ \mathbb{C}_{12}D + \mathbb{C}_{23}J + 2\mathbb{C}_{22}L = -2\mathbb{C}_{23}F, & \text{(A.13g)} \\ \mathbb{C}_{12}B + \mathbb{C}_{23}H + \mathbb{C}_{22}I = 0, & \text{(A.13h)} \\ \mathbb{C}_{23}D + 2\mathbb{C}_{12}E + \mathbb{C}_{22}J + 2\mathbb{C}_{23}K = 0, & \text{(A.13i)} \\ \mathbb{C}_{13}D + 2\mathbb{C}_{11}E + \mathbb{C}_{12}J + 2\mathbb{C}_{13}K = 0. & \text{(A.13j)} \end{cases}$$

We start with equations (A.13c), (A.13e), and (A.13g) to determine the value of D, J and L.

$$\begin{cases} \mathbb{C}_{11}D + \mathbb{C}_{13}J + 2\mathbb{C}_{12}L = -\dfrac{2f}{h} - 2\mathbb{C}_{13}F, \\ \mathbb{C}_{13}D + \mathbb{C}_{33}J + 2\mathbb{C}_{23}L = -2\mathbb{C}_{13}F, \\ \mathbb{C}_{12}D + \mathbb{C}_{23}J + 2\mathbb{C}_{22}L = -2\mathbb{C}_{23}F. \end{cases}$$

The last equation gives

$$J = \frac{1}{\mathbb{C}_{23}} \left(-2\mathbb{C}_{23}F - \mathbb{C}_{12}D - 2\mathbb{C}_{22}L \right).$$

The system is then reduced to

$$\begin{cases} \left(\mathbb{C}_{11} - \dfrac{\mathbb{C}_{12}\mathbb{C}_{13}}{\mathbb{C}_{23}} \right) D + 2\left(\mathbb{C}_{12} - \dfrac{\mathbb{C}_{13}\mathbb{C}_{22}}{\mathbb{C}_{23}} \right) L = -\dfrac{2f}{h}, \\ \left(\mathbb{C}_{13} - \dfrac{\mathbb{C}_{12}\mathbb{C}_{33}}{\mathbb{C}_{23}} \right) D + 2\left(\mathbb{C}_{23} - \dfrac{\mathbb{C}_{33}\mathbb{C}_{22}}{\mathbb{C}_{23}} \right) L = 0. \end{cases}$$

We then obtain

$$D = -\frac{2f}{h}\mathbb{S}_{11}, \quad L = -\frac{f}{h}\mathbb{S}_{12} \quad \text{and} \quad J = 0.$$

Next, we use equations (A.13f), (A.13i), and (A.13j) to determine the value of E and K. The system is reduced to

$$\begin{cases} 2\mathbb{C}_{13}E + 2\mathbb{C}_{33}K = -\mathbb{C}_{33}D, \\ 2\mathbb{C}_{12}E + 2\mathbb{C}_{23}K = \mathbb{C}_{23}D, \\ 2\mathbb{C}_{11}E + 2\mathbb{C}_{13}K = \mathbb{C}_{13}D, \end{cases}$$

which gives

$$E = 0, \quad \text{and} \quad K = \frac{f}{h}\mathbb{S}_{11}.$$

Equations (A.13b), (A.13d), and (A.13h) are reduced to

$$\begin{cases} \mathbb{C}_{11}B + \mathbb{C}_{13}H + \mathbb{C}_{12}I = 0, \\ \mathbb{C}_{13}B + \mathbb{C}_{33}H + \mathbb{C}_{23}I = 0, \\ \mathbb{C}_{12}B + \mathbb{C}_{23}H + \mathbb{C}_{22}I = 0. \end{cases}$$

Using the positive definiteness of $\mathbb{C}$, the determinant of the system is strictly positive; thus

$$B = H = I = 0.$$

Finally, with equation (A.13a), we obtain

$$G = \frac{fh}{4}\mathbb{S}_{12}.$$

We conclude that the exact solution of the beam problem stated in Section 4.3 is

$$\begin{cases} u(x, y) = & -\dfrac{2f}{h}\left(\mathbb{S}_{11}xy + \dfrac{1}{2}\mathbb{S}_{31}\left(y^2 - \dfrac{h^2}{4}\right)\right), \\ v(x, y) = & -\dfrac{f}{h}\left(\mathbb{S}_{21}\left(y^2 - \dfrac{h^2}{4}\right) - \mathbb{S}_{11}x^2\right). \end{cases} \tag{A.14}$$

The coefficients $\mathbb{S}_{ij}$ in (A.14) are given below. For plane strain, the strain-stress relationship for a transversely isotropic material, with fibre direction $\boldsymbol{a} = \left(\begin{smallmatrix} a_1 \\ a_2 \end{smallmatrix}\right)$, is

$$\begin{pmatrix} \varepsilon_{11} \\ \varepsilon_{22} \\ 2\varepsilon_{12} \end{pmatrix} = \begin{pmatrix} \mathbb{S}_{11} & \mathbb{S}_{12} & \mathbb{S}_{13} \\ \mathbb{S}_{12} & \mathbb{S}_{22} & \mathbb{S}_{23} \\ \mathbb{S}_{13} & \mathbb{S}_{23} & \mathbb{S}_{33} \end{pmatrix} \begin{pmatrix} \sigma_{11} \\ \sigma_{22} \\ \sigma_{12} \end{pmatrix},$$

where, from (A.1),

$$\mathbb{S}_{11} = \frac{1}{\det\mathbb{C}}\Big[\big(\lambda + 2\mu_t + 2(\gamma+\alpha)a_2^2 + \beta a_2^4\big)\big(\mu_t + \frac{\gamma}{2} + \beta a_1^2 a_2^2\big) - \big((\alpha+\gamma)a_1a_2 + \beta a_1 a_2^3\big)^2\Big]$$
$$\mathbb{S}_{12} = \frac{1}{\det\mathbb{C}}\Big[\big((\alpha+\gamma)a_1a_2 + \beta a_1^3 a_2\big)\big((\alpha+\gamma)a_1a_2 + \beta a_1 a_2^3\big) - \big(\lambda + \alpha + \beta a_1^2 a_2^2\big)\big(\mu_t + \frac{\gamma}{2} + \beta a_1^2 a_2^2\big)\Big]$$
$$\mathbb{S}_{13} = \frac{1}{\det\mathbb{C}}\Big[\big(\lambda + \alpha + \beta a_1^2 a_2^2\big)\big((\alpha+\gamma)a_1a_2 + \beta a_1 a_2^3\big) - \big((\alpha+\gamma)a_1a_2 + \beta a_1^3 a_2\big)\big(\lambda + 2\mu_t + 2(\gamma+\alpha)a_2^2 + \beta a_2^4\big)\Big]$$
$$\mathbb{S}_{22} = \frac{1}{\det\mathbb{C}}\Big[\big(\lambda + 2\mu_t + 2(\gamma+\alpha)a_1^2 + \beta a_1^4\big)\big(\mu_t + \frac{\gamma}{2} + \beta a_1^2 a_2^2\big) - \big((\alpha+\gamma)a_1a_2 + \beta a_1^3 a_2\big)^2\Big]$$
$$\mathbb{S}_{23} = \frac{1}{\det\mathbb{C}}\Big[\big(\lambda + \alpha + \beta a_1^2 a_2^2\big)\big((\alpha+\gamma)a_1a_2 + \beta a_1^3 a_2\big) - \big(\lambda + 2\mu_t + 2(\gamma+\alpha)a_1^2 + \beta a_1^4\big)\big((\alpha+\gamma)a_1a_2 + \beta a_1 a_2^3\big)\Big]$$
$$\mathbb{S}_{33} = \frac{1}{\det\mathbb{C}}\Big[\big(\lambda + 2\mu_t + 2(\gamma+\alpha)a_1^2 + \beta a_1^4\big)\big(\lambda + 2\mu_t + 2(\gamma+\alpha)a_2^2 + \beta a_2^4\big) - \big(\lambda + \alpha + \beta a_1^2 a_2^2\big)^2\Big]$$

with

$$
\begin{aligned}
\frac{1}{\det \mathbb{C}} =& \big(\lambda + 2\mu_t + 2(\gamma+\alpha)a_1^2 + \beta a_1^4\big)\Big[\big(\lambda + 2\mu_t + 2(\gamma+\alpha)a_2^2 + \beta a_2^4\big)\big(\mu_t + \frac{\gamma}{2} + \beta a_1^2 a_2^2\big) \\
&\qquad - \big((\alpha+\gamma)a_1 a_2 + \beta a_1 a_2^3\big)^2\Big] \\
&- \big(\lambda + \alpha + \beta a_1^2 a_2^2\big)\Big[\big(\lambda + \alpha + \beta a_1^2 a_2^2\big)\big(\mu_t + \frac{\gamma}{2} + \beta a_1^2 a_2^2\big) \\
&\qquad - \big((\alpha+\gamma)a_1 a_2 + \beta a_1^3 a_2\big)\big((\alpha+\gamma)a_1 a_2 + \beta a_1 a_2^3\big)\Big] \\
&+ \big((\alpha+\gamma)a_1 a_2 + \beta a_1^3 a_2\big)\Big[\big(\lambda + \alpha + \beta a_1^2 a_2^2\big)\big((\alpha+\gamma)a_1 a_2 + \beta a_1 a_2^3\big) \\
&\qquad - \big((\alpha+\gamma)a_1 a_2 + \beta a_1^3 a_2\big)\big(\lambda + 2\mu_t + 2(\gamma+\alpha)a_2^2 + \beta a_2^4\big)\Big].
\end{aligned}
$$

Appendix B. Properties of the structural tensor M

Let $\boldsymbol{a} \in \mathbb{R}^d$ be a unit vector and set $\boldsymbol{M} = \boldsymbol{a} \otimes \boldsymbol{a}$. For any second order tensor $\boldsymbol{A}$, and any scalar C, the following statements hold:

(i) $\boldsymbol{M}^T = \boldsymbol{M}^2 = \boldsymbol{M}$,

(ii) $\operatorname{tr} \boldsymbol{M} = 1$,

(iii) $\boldsymbol{M} : \boldsymbol{I} = 1$,

(iv) $\boldsymbol{M} : \boldsymbol{M} = 1$,

(v) $\operatorname{tr}(\boldsymbol{A}\boldsymbol{M}) = \operatorname{tr}(\boldsymbol{M}\boldsymbol{A}) = \boldsymbol{M} : \boldsymbol{A}$,

(vi) $\boldsymbol{M} : \boldsymbol{M}\boldsymbol{A} = \boldsymbol{M} : \boldsymbol{A}\boldsymbol{M} = \boldsymbol{M} : \boldsymbol{A}$,

(vii) $\boldsymbol{M}\boldsymbol{A}\boldsymbol{M} = (\boldsymbol{M} : \boldsymbol{A})\boldsymbol{M}$,

(viii) $|C\boldsymbol{M}|^2 \leq |C|^2|\boldsymbol{M}|^2 = |C|^2$,

(ix) $|\boldsymbol{M} : \boldsymbol{A}|^2 \leq d^2|\boldsymbol{A}|^2$,

(x) $|\boldsymbol{A}\boldsymbol{M}|^2 \leq d|\boldsymbol{A}|^2$

Proof. To prove (ix), we have

$$
\begin{aligned}
|\boldsymbol{M} : \boldsymbol{A}|^2 &= (a_i a_j A_{ij})\,(a_k a_l A_{kl}) \\
&\leq \left(\frac{1}{2} A_{ij}(a_i^2 + a_j^2)\right) \left(\frac{1}{2} A_{kl}(a_k^2 + a_l^2)\right) \\
&\leq \sum_{i,j,k,l} A_{ij} A_{kl} \qquad (a_k^2 \leq 1,\ \forall k) \\
&\leq \frac{1}{2} \sum_{i,j,k,l} (A_{ij}^2 + A_{kl}^2) \\
&= \frac{d^2}{2} \left(\sum_{i,j} A_{ij}^2 + \sum_{k,l} A_{kl}^2 \right) \\
&= d^2 \sum_{i,j} A_{ij}^2 \\
&= d^2 |\boldsymbol{A}|^2
\end{aligned}
$$

To prove (x),

$$
\begin{aligned}
|\boldsymbol{AM}|^2 &= (\boldsymbol{AM})_{ij} (\boldsymbol{AM})_{ij} \\
&= (A_{ik} a_k a_j)(A_{il} a_l a_j) \\
&= A_{ik} A_{il} a_k a_l \qquad (\text{since} \sum_j a_j^2 = 1) \\
&\leq \frac{1}{2} A_{ik} A_{il} (a_k^2 + a_l^2) \\
&\leq \sum_{k,l} A_{ik} A_{il} \qquad (a_k^2 \leq 1,\ \forall k) \\
&\leq \frac{1}{2} \sum_{k,l} (A_{ik}^2 + A_{il}^2) \\
&= \frac{d}{2} \left(\sum_k A_{ik}^2 + \sum_l A_{il}^2 \right) \\
&= d \sum_{i,k} A_{ik}^2 \\
&= d |\boldsymbol{A}|^2
\end{aligned}
$$

□

Appendix C. Useful bounds for the DG formulation and analysis

Refer to Chapter 5 for relevant notation.

We have

$$\sum_{\Omega_e \in \mathcal{T}_h} \sum_{E \in \partial\Omega_e^i} \int_E \cdot \, ds = 2 \sum_{E \in \Gamma_i} \int_E \cdot \, ds. \tag{C.1}$$

By definition of standard interpolant error estimate, we have:

$$\|\boldsymbol{u} - \Pi_k \boldsymbol{u}\|_{m,\Omega} \leq C h^{k+1-m} |\boldsymbol{u}|_{k+1,\Omega}. \tag{C.2}$$

For $\boldsymbol{v} \in [\mathcal{H}^1(\Omega_e)]^d$ and $\phi \in [\mathcal{L}^2(\Omega_e)]^d$, we have

$$\|\boldsymbol{v}\|_{0,E} \leq C h_e^{-1/2} \|\boldsymbol{v}\|_{0,\Omega_e}, \tag{C.3a}$$

$$\|\boldsymbol{v}\|_{0,\partial\Omega_e} \leq C \left(h_e^{-1/2} \|\boldsymbol{v}\|_{0,\Omega_e} + h_e^{1/2} |\boldsymbol{v}|_{1,\Omega_e} \right), \tag{C.3b}$$

$$\sum_{E \in \Gamma_{iD}} \frac{1}{h_E} \|\lfloor \boldsymbol{v} \rfloor\|_{0,E}^2 \leq \sum_{\Omega_e \in \mathcal{T}_h} \sum_{E \in \partial\Omega_e^{iD}} \frac{2}{h_E} \|\boldsymbol{v}\|_{0,E}^2, \tag{C.3c}$$

$$\sum_{E \in \Gamma_{iD}} h_E \|\{\phi\}\|_{0,E}^2 \leq C \sum_{\Omega_e \in \mathcal{T}_h} h_e \|\phi\|_{0,\partial\Omega_e^{iD}}^2, \tag{C.3d}$$

$$\sum_{E \in \Gamma_{iD}} \frac{1}{h_E} \|\{\phi\}\|_{0,E}^2 \leq \sum_{\Omega_e \in \mathcal{T}_h} \sum_{E \in \partial\Omega_e^{iD}} \frac{1}{h_E} \|\phi\|_{0,E}^2. \tag{C.3e}$$

Bibliography

[1] H. Altenbach. Modelling of anisotropic behavior in fiber and particle reinforced composites. In T. Sadowski, editor, *Multiscale Modelling of Damage and Fracture Processes in Composite Materials*, pages 1–62. Springer, 2005.

[2] D.N. Arnold, F. Brezzi, B. Cockburn, and L.D. Marini. Unified analysis of Discontinuous Galerkin methods for elliptic problems. *SIAM Journal on Numerical Analysis*, 39:1749–1779, 2002.

[3] D.N. Arnold and R.S. Falk. Well-posedness of the fundamental boundary value problems for constrained anisotropic elastic materials. *Archive for Rational Mechanics and Analysis*, 98(2):143–165, 1987.

[4] F. Auricchio, G. Scalet, and P. Wriggers. Fiber-reinforced materials: finite elements for the treatment of the inextensibility constraint. *Computational Mechanics*, 60(6):905–922, 2017.

[5] I. Babuška. The p and hp versions of the finite element method: The state of the art. In *Finite Elements*, pages 199–239. Springer, 1988.

[6] I. Babuska and M. Suri. Locking effects in the finite element approximation of elasticity problems. *Numerische Mathematik*, 62:439–463, 1992.

[7] I. Babuška and M. Suri. The p and h-p versions of the finite element method, basic principles and properties. *SIAM*, 36(4):578–632, 1994.

[8] S. C. Brenner and L.-Y. Sung. Linear finite element methods for planar linear elasticity. *Mathematics of Computation*, 59(200):321–338, 1992.

[9] F. Brezzi, D. Boffi, L. Demkowicz, R.G. Durán, R.S. Falk, and M. Fortin. *Mixed finite elements, compatibility conditions, and applications.* Springer, 2008.

[10] F. Brezzi and M. Fortin. *Mixed and Hybrid Finite Element Methods*, volume 734. New York: Springer-Verlag, 1991.

[11] P. G. Ciarlet. *The Finite Element Method for Elliptic Problems.* North-Holland, Amsterdam, 1978.

[12] J.A. Cottrell, T.J.R. Hughes, and Y. Bazilevs. *Isogeometric Analysis: Toward Integration of CAD and FEA.* John Wiley & Sons, 2009.

[13] M. Crouzeix and P-A Raviart. Conforming and nonconforming finite element methods for solving the stationary stokes equations I. *ESAIM: Mathematical Modelling and Numerical Analysis-Modélisation Mathématique et Analyse Numérique*, 7(R3):33–75, 1973.

[14] L. B. Da Veiga, F. Brezzi, and L. D. Marini. Virtual elements for linear elasticity problems. *SIAM Journal on Numerical Analysis*, 51(2):794–812, 2013.

[15] M.J.H. Dantas. On the boundary value problems of linear elasticity with constraints. *Journal of Elasticity*, 54(2):93–111, 1999.

[16] J. K. Djoko, B. P. Lamichhane, B. D. Reddy, and B. I. Wohlmuth. Conditions for equivalence between the Hu-Washizu and related formulations, and computational behavior in the incompressible limit. *Computer Methods in Applied Mechanics and Engineering*, 195:4161–4178, 2006.

[17] G.E. Exadaktylos. On the constraints and relations of elastic constants of transversely isotropic geomaterials. *International Journal of Rock Mechanics and Mining Sciences*, 38(7):941–956, 2001.

[18] R.S. Falk. Nonconforming finite element methods for the equations of linear elasticity. *Mathematics of Computation*, 57(196):529–550, 1991.

[19] B.J. Grieshaber, A.T. McBride, and B.D. Reddy. Uniformly convergent interior penalty methods using multilinear approximations for problems in elasticity. *SIAM Journal on Numerical Analysis*, 53(5):2255–2278, 2015.

[20] P. Hansbo and M.G. Larson. Discontinuous Galerkin methods for incompressible and nearly incompressible elasticity by nitsche's method. *Computer Methods in Applied Mechanics and Engineering*, 191(17-18):1895–1908, 2002.

[21] P. Hansbo and M.G. Larson. Discontinuous Galerkin and the Crouzeix–Raviart element: Application to Elasticity. *ESAIM: Mathematical Modelling and Numerical Analysis*, 37(1):63–72, 2003.

[22] Z. Hashin. Theory of composite materials. In Z. Hashin and C.T. Herakovich, editors, *Mechanics of Composite Materials*, pages 201–242. Pergamon Press, 1970.

[23] M. Hayes and C.O. Horgan. On the displacement boundary-value problem for inextensible elastic materials. *Quarterly Journal of Mechanics and Applied Mathematics*, 27(3):287–297, 1974.

[24] M. Hayes and C.O. Horgan. On mixed boundary-value problems for inextensible elastic materials. *Zeitschrift für Angewandte Mathematik und Physik ZAMP*, 26(3):261–272, 1975.

[25] P. Houston, D. Schötzau, and T.P. Wihler. An hp-adaptive mixed Discontinuous Galerkin FEM for nearly incompressible linear elasticity. *Computer Methods in Applied Mechanics and Engineering*, 195(25-28):3224–3246, 2006.

[26] T.J.R. Hughes. *The Finite Element Method: Linear Static and Dynamic Finite Element Analysis*. Prentice-Hall, Inc., 1987.

[27] J. Humphrey. *Cardiovascular Solid Mechanics: Cells, Tissues and Organs*. Springer, New York, 2002.

[28] W.M. Lai, D.H. Rubin, and E. Krempl. *Introduction to Continuum Mechanics*. Butterworth-Heinemann, 2009.

[29] B. P. Lamichhane, B. D. Reddy, and B. I. Wohlmuth. Convergence in the incompressible limit of finite element approximations based on the Hu–Washizu formulation. *Numerische Mathematik*, 104:151–175, 2006.

[30] V. Lubarda and M. Chen. On the elastic moduli and compliances of transversely isotropic and orthotropic materials. *Journal of Mechanics of Materials and Structures*, 3(1):153–171, 2008.

[31] J.E. Marsden and T.J.R. Hughes. *Mathematical Foundations of Elasticity.* Prentice-Hall, Inc, Englewood Cliffs, 1983.

[32] R.W. Ogden. *Non-linear Elastic Deformations.* Ellis Horwood Ltd., Chichester, 1984.

[33] A.C. Pipkin. Stress analysis for fiber-reinforced materials. *Advances in Applied Mechanics*, 19:1–51, 1979.

[34] B.D. Reddy and D. van Huyssteen. A virtual element method for transversely isotropic elasticity. In review. Available at http://arxiv.org/abs/1810.00688.

[35] D. Royer, J.-L. Gennisson, T. Deffieux, and M. Tanter. On the elasticity of transverse isotropic soft tissues (L). *The Journal of the Acoustical Society of America*, 129(5):2757–2760, 2011.

[36] J. Schröder and P. Neff. Invariant formulation of hyperelastic transverse isotropy based on polyconvex free energy functions. *International Journal of Solids and Structures*, 40(2):401–445, 2003.

[37] J. Schröder, P. Neff, and D. Balzani. A variational approach for materially stable anisotropic hyperelasticity. *International Journal of Solids and Structures*, 42(15):4352–4371, 2005.

[38] L. R. Scott and M. Vogelius. Norm estimates for a maximal right inverse of the divergence operator in spaces of piecewise polynomials. *ESAIM: Mathematical Modelling and Numerical Analysis*, 19(1):111–143, 1985.

[39] S. Shahi and S. Mohammadi. A comparative study of transversely isotropic material models for prediction of mechanical behavior of the aortic valve leaflet. *International Journal of Research in engineering and Technology*, 2(4):192–196, 2013.

[40] A.J.M. Spencer. *Deformations of Fibre-reinforced Materials.* Clarendon Press, Oxford, 1972.

[41] A.J.M Spencer. The formulation of constitutive equations for anisotropic solids. In J.P. Boehler, editor, *Mechanical Behavior of Anisotropic Solids/Comportment Méchanique des Solides Anisotropes*, pages 3–26. Springer, Dordrecht, 1982.

[42] T.C. Ting. *Anisotropic Elasticity: Theory and Applications.* Oxford University Press, 1996.

[43] M. Vogelius. An analysis of the p-version of the finite element method for nearly incompressible materials. *Numerische Mathematik*, 41(1):39–53, 1983.

[44] J.A. Weiss, B.N. Maker, and S. Govindjee. Finite element implementation of incompressible, transversely isotropic hyperelasticity. *Computer Methods in Applied Mechanics and Engineering*, 135(1-2):107–128, 1996.

[45] T. P. Wihler. Locking-free DGFEM for elasticity problems in polygons. *IMA Journal of Numerical Analysis*, 24(1):45–75, 2004.

[46] P. Wriggers, J. Schröder, and F. Auricchio. Finite element formulations for large strain anisotropic material with inextensible fibers. *Advanced Modeling and Simulation in Engineering Sciences*, 3(1):25, 2016.

[47] A. Zdunek and W. Rachowicz. A 3-field formulation for strongly transversely isotropic compressible finite hyperelasticity. *Computer Methods in Applied Mechanics and Engineering*, 315:478–500, 2017.

[48] A. Zdunek and W. Rachowicz. A mixed higher order FEM for fully coupled compressible transversely isotropic finite hyperelasticity. *Computers & Mathematics with Applications*, 74(7):1727–1750, 2017.

[49] A. Zdunek, W. Rachowicz, and T. Eriksson. A five-field finite element formulation for nearly inextensible and nearly incompressible finite hyperelasticity. *Computers & Mathematics with Applications*, 72(1):25–47, 2016.